PROCEEDINGS
OF THE
NATIONAL ACADEMY OF SCIENCES

Volume 13 April 15, 1927 Number 4

ON THE EXPANSION OF HARMONIC FUNCTIONS IN TERMS OF HARMONIC POLYNOMIALS

By J. L. Walsh

Department of Mathematics, Harvard University

Communicated March 4, 1927

Fourier's Series is an expansion of an arbitrary function $f(\theta)$ of period 2π in terms of trigonometric functions:

$$f(\theta) = \sum_{k=0}^{\infty} (a_k \cos k\theta + b_k \sin k\theta).$$

If (r, θ) are considered polar coördinates in the plane and (x, y) the corresponding rectangular coördinates, the function $f(\theta)$ may be considered defined on the unit circle $r = 1$, and on that circle expanded in terms of trigonometric functions. But if the series be written in the form

$$f(r, \theta) = \sum_{k=0}^{\infty} r^k(a_k \cos k\theta + b_k \sin k\theta),$$

we have the same expansion for $r = 1$, yet each term of the series is a harmonic function of (x, y), and indeed a harmonic *polynomial* in those variables. Moreover, if the series converges uniformly in θ for $r = 1$, the series converges likewise uniformly in the closed region $r \leqq 1$. The sum of the series is, therefore, harmonic for $r < 1$ and continuous for $r \leqq 1$, although the original function $f(\theta)$ is defined merely *on* the circle $r = 1$.

Little seems to have been done hitherto in the literature in consideration of expansions in terms of harmonic polynomials—expansions of arbitrary functions defined on given curves, or expansions in regions of harmonic functions defined in those regions—beyond the illustration just given.[1] The object of the present note is to give an example of such expansions, generalizations of Fourier's Series, by proving the following theorem:

Theorem 1. *Let C be a simple closed finite analytic curve in the (x, y)-plane. Then there exist harmonic polynomials*

$$p_1(x, y), \quad p_2(x, y), \quad p_3(x, y), \quad \ldots.$$

such that if $f(x, y)$ is defined and continuous on C and on C is of bounded variation,[2] *then $f(x, y)$ can be developed into a series*

$$f(x, y) \equiv a_1 p_1(x, y) + a_2 p_2(x, y) + a_3 p_3(x, y) + \ldots, \qquad (1)$$

where the series (1) *converges uniformly in the closed region consisting of C and its interior. The series* (1) *thus represents a function harmonic interior to C, continuous in the corresponding closed region, and having the value $f(x, y)$ on C. There exist continuous functions $q_n(x, y)$, $n = 1, 2, 3, \ldots$, defined on C, such that the coefficients of* (1) *are given by the formulas*

$$a_n = \int_C f(x, y) q_n(x, y) ds, \quad n = 1, 2, 3, \ldots;$$

the functions $q_n(x, y)$ depend on C but not on $f(x, y)$.

Theorem 1 is an almost direct application of the following theorem.[3]

THEOREM 2. *Suppose that $\{\bar{u}_n(\varphi)\}$ is a set of uniformly bounded continuous normal orthogonal functions in the interval $0 \leqq \varphi \leqq 2\pi$, and that in this interval $\{u_n(\varphi)\}$ is a set of uniformly bounded continuous functions each of which can be developed into a series*

$$u_n(\varphi) = \bar{u}_n(\varphi) + \sum_{k=1}^{\infty} c_{nk} \bar{u}_k(\varphi), \qquad n = 1, 2, \ldots, \qquad (2)$$

where the coefficients have the values

$$c_{nk} = \int_0^{2\pi} [u_n(\varphi) - \bar{u}_n(\varphi)] \bar{u}_k(\varphi) d\varphi. \qquad (3)$$

Suppose further that the three series

$$\sum_{n,k=1}^{\infty} c_{nk}^2 \quad , \quad \sum_{n=1}^{\infty} \left(\sum_{k=1}^{\infty} c_{nk}^2 \right)^{\frac{1}{2}} \quad , \quad \sum_{k=1}^{\infty} \left(\sum_{n=1}^{\infty} c_{nk}^2 \right)^{\frac{1}{2}}, \qquad (4)$$

converge and that the sum of the first is less than unity.

Then there exists a set of continuous functions $\{v_n(\varphi)\}$ such that $\{u_n(\varphi)\}$ and $\{v_n(\varphi)\}$ are biorthogonal sets:

$$\int_0^{2\pi} u_n(\varphi) v_k(\varphi) d\varphi = \begin{cases} 1, & n = k, \\ 0, & n \neq k. \end{cases}$$

Furthermore, if $f(\varphi)$ is any function integrable and with an integrable square (in the sense of Lebesgue) on the interval $0 \leqq \varphi \leqq 2\pi$, then the two series

$$f(\varphi) \sim \sum_{n=1}^{\infty} a_n u_n(\varphi) \quad , \quad a_n = \int_0^{2\pi} f(\varphi) v_n(\varphi) d\varphi,$$

$$f(\varphi) \sim \sum_{n=1}^{\infty} b_n \bar{u}_n \varphi \; , \; b_n = \int_0^{2\pi} f(\varphi) \bar{u}_n(\varphi) d\varphi,$$

have essentially the same convergence properties, in the sense that their term-by-term difference converges uniformly and absolutely to the sum zero on the interval $0 \leqq \varphi \leqq 2\pi$.

Theorem 2 will be shown to yield the following result:[4]

THEOREM 3. *Let the functions*

$$p_1'(x', y'), \quad p_2'(x', y'), \quad p_3'(x', y'), \quad \ldots .$$

be harmonic for $\rho \leqq 1 + \epsilon$, $\epsilon > 0$, *where* (x', y') *are rectangular coördinates in the plane and* (ρ, φ) *the corresponding polar coördinates, and suppose we have on and within the circle* γ': $\rho = 1 + \epsilon$, *the following inequalities:*

$$\begin{aligned}
&\left| p_1'(x', y') - \frac{1}{\sqrt{2\pi}} \right| \leqq \epsilon_1 , \\
&\left| p_{2n}'(x', y') - \frac{1}{\sqrt{\pi}} \rho^n \cos n\varphi \right| \leqq \epsilon_{2n} , \qquad (5) \\
&\qquad\qquad\qquad\qquad\qquad\qquad n = 1, 2, 3, \ldots . \\
&\left| p_{2n+1}'(x', y') - \frac{1}{\sqrt{\pi}} \rho^n \sin n\varphi \right| \leqq \epsilon_{2n+1} ,
\end{aligned}$$

where the series $\sum_{n=1}^{\infty} \epsilon_n^2$ *converges and its sum is less than* $\frac{1}{2\pi}$ *and where the series* $\sum_{n=1}^{\infty} \epsilon_n$ *converges. Then any function* $f'(x', y')$ *which is continuous and of bounded variation on the circle* γ: $\rho = 1$, *can be developed into a series*

$$f'(x', y') = a_1' p_1'(x', y') + a_2' p_2'(x', y') + \ldots ,$$

where the series converges uniformly for $\rho \leqq 1$; *the sum of the series is thus harmonic for* $\rho < 1$ *and continuous for* $\rho \leqq 1$. *There exists a set of functions* $q_n'(x', y')$, *defined and continuous on* γ, *such that the coefficients* a_n' *are given by the formulas*

$$a_n' = \int_\gamma f'(x', y') q_n'(x', y') d\varphi ;$$

the functions $q_n'(x', y')$ *do not depend on the function* $f'(x', y')$, *but merely on the functions* $p_n'(x', y')$.

Theorem 3 is proved from Theorem 2 by setting on γ, $0 \leqq \varphi \leqq 2\pi$,

$$u_n(\varphi) = p_n'(x', y'), \qquad n = 1, 2, 3, \ldots ,$$

$$\bar{u}_1(\varphi) = \frac{1}{\sqrt{2\pi}}, \ \bar{u}_{2n}(\varphi) = \frac{1}{\sqrt{\pi}} \cos n\varphi, \ \bar{u}_{2n+1}(\varphi) = \frac{1}{\sqrt{\pi}} \sin n\varphi, \ n = 1, 2, 3, \ldots .$$

The sets of functions $\{\bar{u}_n\}$ and $\{u_n\}$ are obviously uniformly bounded, and the set $\{u_n\}$ can be developed into series (2) in terms of the functions

$\{\bar{u}_n\}$, for the functions $p'_n(x', y')$ are harmonic and hence *analytic* functions of the real variables x' and y' (and of the variable φ) for $\rho \leqq 1 + \epsilon$. It remains merely to consider the series (4).

In order to compute the coefficients c_{nk}, we find it convenient to expand $p'_n(x', y')$ into a Fourier Series on the circle γ':[5]

$$p'_n(x', y') - \rho^m \bar{u}_n(\varphi) = \frac{c_{n1}}{\sqrt{2\pi}} + \frac{\rho}{\sqrt{\pi}}(c_{n2}\cos\varphi + c_{n3}\sin\varphi) + \frac{\rho^2}{\sqrt{\pi}}(c_{n4}\cos 2\varphi + c_{n5}\sin 2\varphi) + \ldots., \qquad m = \begin{cases} \frac{n}{2}, & n \text{ even}, \\ \frac{n-1}{2}, & n \text{ odd}, \end{cases} \tag{6}$$

$$\rho^k c_{n2k} = \int_0^{2\pi} [p'_n(x', y') - \rho^m \bar{u}_n(\varphi)]\bar{u}_{2k}(\varphi)d\varphi, \quad k = 1, 2, 3, \ldots.,$$

$$\rho^k c_{n2k+1} = \int_0^{2\pi} [p'_n(x', y') - \rho^m \bar{u}_n(\varphi)]\bar{u}_{2k+1}(\varphi)d\varphi, \quad k = 0, 1, 2, \ldots.,$$

the development being valid for $\rho = 1 + \epsilon$ and hence likewise for all values of ρ less than $1 + \epsilon$, in particular valid for $\rho = 1$.

Bessel's Inequality as derived from (6) for $\rho = 1$ is

$$\sum_{k=1}^{\infty} c_{nk}^2 \leqq \int_0^{2\pi} [u_n(\varphi) - \bar{u}_n(\varphi)]^2 d\varphi.$$

This integral is not greater than $2\pi\,\epsilon_n^2$. Hence the first of the series (4) converges to a sum less than unity, and the second of those series converges.

From (6) for $\rho = 1 + \epsilon$ and from the inequalities (5) we derive

$$|\, c_{n1}\,| \leqq \sqrt{2\pi}\,\epsilon_n, \; |\, c_{n2k}\,| \leqq \frac{2\sqrt{\pi}\,\epsilon_n}{(1+\epsilon)^k}, \; |\, c_{n2k+1}\,| \leqq \frac{2\sqrt{\pi}\,\epsilon_n}{(1+\epsilon)^k},$$

$$n, k = 1, 2, 3, \ldots.$$

The series $\sum_{n=1}^{\infty} c_{n\,2k}^2$ and $\sum_{n=1}^{\infty} c_{n\,2k+1}^2$ are both dominated by the series

$$\sum_{n=1}^{\infty} \frac{4\pi\epsilon_n^2}{(1+\epsilon)^{2k}},$$

whose sum is less than $\frac{4\pi}{(1+\epsilon)^{2k}}$. Hence the series

$$\sum_{k=1}^{\infty} \left(\sum_{n=1}^{\infty} c_{nk}^2 \right)^{\frac{1}{2}}$$

converges and Theorem 3 is completely established.

We are now in a position to prove Theorem 1. The interior of C can be mapped one-to-one and conformally on the interior of γ, and the mapping will be conformal and smooth in larger regions containing C and γ,

respectively, in their interiors.[6] We choose a circle γ' within the latter region but exterior to γ and concentric with it; the transform of γ' is a simple analytic closed curve C'. The transforms of the functions

$$\frac{1}{\sqrt{2\pi}}, \frac{1}{\sqrt{\pi}}\rho\cos\varphi, \frac{1}{\sqrt{\pi}}\rho\sin\varphi, \frac{1}{\sqrt{\pi}}\rho^2\cos 2\varphi, \frac{1}{\sqrt{\pi}}\rho^2\sin 2\varphi, \ldots \quad (7)$$

are harmonic in (x, y) in and on C', hence in the corresponding closed region can be uniformly approximated as closely as desired by harmonic polynomials in (x, y).[7] These approximating polynomials are defined to be the polynomials

$$p_1(x,y), p_2(x,y), p_3(x, y), \ldots,$$

respectively, and approximation is to be so close that for a suitable (that is, satisfying the requirements of theorem 3) set $\{\epsilon_n\}$, inequalities (5) are satisfied in the (x', y')-plane; the transforms of the polynomials $p_n(x, y)$ are, of course, to be identified with the harmonic functions $p_n'(x',y')$ of Theorem 3.

The functions $q_n'(x, y)$ are to be defined on C in terms of the functions $q_n'(x', y')$ of Theorem 3 by the equation

$$q_n(x, y) = \frac{d\varphi}{ds} q_n'(x', y'),$$

where the equation refers to points of C and γ which correspond under the conformal map already used, and where s is arc length on C.

If $f(x, y)$ is continuous and of bounded variation on C, its transform in the (x',y')-plane is likewise continuous and of bounded variation. Any continuous function of bounded variation can be uniformly expanded on γ in terms of the Fourier functions (7), hence on γ in terms of the functions $p_n'(x', y')$, that is, on C in terms of the polynomials $p_n(x, y)$. The series of polynomials converges uniformly on C, hence uniformly in the closed region consisting of C and its interior. Series (1) thus furnishes a solution of the Dirichlet Problem for the boundary values $f(x, y)$ in the region bounded by C, if $f(x, y)$ is continuous and of bounded variation on C. If $f(x, y)$ is merely known to be *continuous* on C, the sequence of first Cesàro means for (1) converges uniformly in and on C, and thus furnishes a solution of the Dirichlet Problem for these boundary values.

The writer hopes to study further properties of the expansions (1) and of analogous expansions of functions in harmonic polynomials, including orthogonal harmonic polynomials.

[1] The present writer has studied the question from the standpoint of uniform approximation (or of uniformly convergent developments), deriving extensions of Weierstrass's theorems on approximation of a continuous or harmonic function, rather than extensions of Fourier's Series.

See a forthcoming paper in Crelle's Journal.

Compare also Bergmann, S., *Math. Annalen*, **86** (1922), 238–271, who considers, in general, developments of harmonic functions which can be obtained from developments of analytic functions.

[3] It is likewise sufficient if $f(x, y)$ satisfies a Lipschitz Condition,

$$|f(x_1, y_1) - f(x_2, y_2)| \leqq M\sqrt{(x_1 - x_2)^2 + (y_1 - y_2)^2},$$

where M is constant and (x_1, y_1) and (x_2, y_2) are arbitrary points of C.

[3] Walsh, J. L., *Trans. Amer. Math. Soc.*, **22** (1921), 230–239, Theorem 1.

[4] Theorem 3 is analogous to a theorem proved by means of Theorem 2, for analytic instead of harmonic functions. See Walsh, *Trans. Amer. Math. Soc.*, **26** (1924), 155–170. That theorem for analytic functions is essentially a modification of a result due to Birkhoff, Paris, *Comptes Rendus*, **164** (1917), 942–945.

[5] The same development is, of course, obtained by expanding $p'_n(x', y')$ on γ instead of on γ'; the coefficients c_{nk} may be obtained by integration on either γ or γ'.

[6] See, e.g., Picard, *Traité d'Analyse*, t. II (Paris, 1893), pp. 272, 276; Bieberbach, *Einführung in die konforme Abbildung* (Sammlung Göschen, Berlin u. Leipzig, 1915), p. 120.

[7] This result may be easily proved from Runge's classical theorem on the expansion of an analytic function in terms of polynomials. A proof is given in the paper referred to under 1.

ON THE CORRECTION TO SAHA'S FORMULA FOR SMALL DEVIATIONS FROM THERMODYNAMIC EQUILIBRIUM

By B. P. Gerasimovič

Harvard College Observatory, Cambridge, Massachusetts

Communicated March 4, 1927

All applications of the ionization theory to solar and stellar physics are based on an implicit supposition that the layers of the star where spectral lines arise are in a state of thermodynamic equilibrium, which is determined by the effective temperature of a celestial body. In fact, the use of Planck's law of radiation and the "principle of detailed equilibrium" of quantum processes alone allow us to deduce Saha's formula—the basis of the modern theory of stellar spectra. This hypothesis is, of course, quite justifiable if we have in view only a first approximation—some rough explanation of the variation of spectra with temperature. But as soon as we want to deepen the theory there arises the necessity for some revision of the above-mentioned fundamental hypothesis.

It is theoretically quite clear that the upper photospheric layer and the adjacent thin reversing layer cannot be exactly in thermodynamic equilibrium, because their temperature is lower than that of the radiation penetrating them from below by a factor of $\sqrt[4]{2}$, according to Schwarz-

schild. The difference is great enough to influence the ionization and, in fact, Russell explains the well-known anomaly of the Ba^+ atoms in the solar spectrum by the influence of intensive radiation from below. It is easy to see that this influence must be much more important for stars having extended atmospheres; for these we may expect large deviations from Saha's formula. It, therefore, seems interesting to determine the correction to the known ionization formula for small deviations from thermodynamic equilibrium, and to calculate its amount for the important and well-studied case of the solar spectrum.

The Equations of Statistical and Radiative Equilibrium.—We shall suppose that the upper photospheric layer or, what is practically the same, the lower part of the reversing layer, deviates from thermodynamic equilibrium so slightly that it is possible to characterize its proper radiation as isotropic. Consider the gaseous layer; from above it is stimulated by isotropic radiation of its own temperature, T_0, and from below by the radiation from the lower layers, with spectral distribution corresponding to the effective temperature of the star ($T > T_0$); its intensity is expressed by Planck's law corrected by some factor A. If the gaseous layer is situated at some distance from the star, A would characterize the "dilution" of radiation.

In the case of immediate fitting of the layer under consideration to the radiating layer of the star the radiation cannot be exactly isotropic, and its density is not exactly equal to the density of black body radiation of the same effective temperature, because the radiation is contributed from different layers of the star.

In the following I shall restrict myself to the simplest case where the gaseous layer is composed of one element only, whose atoms have only one quantum state. If our system is in thermodynamic equilibrium the spectral distribution of the energy radiated must necessarily be the same as that of the absorbed energy; i.e., the radiative equilibrium must hold for all frequencies, ν, in every element $d\nu$ of a spectrum. Therefore, for a given ν, $d\nu$ and the corresponding velocity v of an electron (connected by relation $\frac{mv^2}{2} = h\nu - \chi_0$, where χ_0 is ionization potential) the number of ν-radiations is equal to the number of ν-absorptions, or more precisely the number of ν-captures = the number of corresponding ionizations. We see, therefore, that in thermodynamic equilibrium statistical equilibrium coincides with radiative equilibrium. In the general case this is no longer true. For a steady state (if such a state can exist) these two kinds of equilibrium are expressed by two different equations. We can only assert that in this case the total number of captures (for all values of ν and v) is equal to the total number of different ionizations, and that the total energy absorbed is equal to the total energy radiated. The first

expresses the statistical equilibrium, the second the radiative equilibrium; in thermodynamic equilibrium these conditions flow together, each giving the well-known Saha formula.[1]

Let $\psi(\nu)I(\nu)d\nu$ be the probability of ionization under the influence of radiation $I(\nu)d\nu$, and $F(v)$ the probability of capture after collision of an electron having velocity v. For these functions the formulae of Milne[2] and Kramers[3] will be valid, because they express atomic properties:

$$\psi(\nu) = \frac{4\pi^2 m^2 c^2 v^2 F(v)}{h^3 \nu^3}; \qquad F(v) = \frac{\text{const.}}{v^2 \nu}$$

where m is the mass of an electron, c the velocity of light and h Planck's constant. Let N be the number of atoms, x the percentage of atoms ionized and k the Boltzmann constant. Since $N(1-x)$ is the number of neutral atoms, the number of ν ionizations in time dt is $N(1-x)\psi(\nu)I(\nu)d\nu dt$. Neglecting for the sake of simplicity the captures stimulated by radiation, we find that the number of recombinations with v electrons will be

$$8\pi^2 x^2 N^2 \left(\frac{m}{2\pi k T_0}\right)^{3/2} e^{-\frac{mv^2}{2kT_0}} v^3 F(v) dv dt.$$

We, therefore, obtain the following equation of statistical equilibrium, which expresses the fact that the total number of captures is equal to the total number of ionizations. This equation ensures the constancy of ionization x.

$$N(1-x)\int_{\nu_0}^{\infty} \psi(\nu)I(\nu)d\nu = 8\pi^2 x^2 N^2 \left(\frac{m}{2\pi k T_0}\right)^{3/2} \int_0^{\infty} e^{-\frac{mv^2}{2kT_0}} v^3 F(v) dv. \quad (1)$$

The velocity, v, is connected with the frequency, ν, by the formula

$$\frac{mv^2}{2} = h\nu - h\nu_0 = h\nu - \chi_0$$

where χ_0 is the ionization potential. Similarly we obtain the equation

$$N(1-x)\int_{\nu_0}^{\infty} \nu\psi(\nu)I(\nu)d\nu = 8\pi^2 x^2 N^2 \left(\frac{m}{2\pi k T_0}\right)^{3/2} \int_0^{\infty} \nu e^{-\frac{mv^2}{2kT_0}} v^3 F(v) dv. \quad (2)$$

This equation of radiative equilibrium insures the constancy of the macroscopic characteristics of the gas. The intensity of ionizing radiation, according to our supposition, will be

$$I(\nu) = A.\frac{2h\nu^3}{c^2}\frac{1}{e^{\frac{h\nu}{kT}}-1} + \frac{h\nu^3}{c^2}\frac{1}{e^{\frac{h\nu}{kT_0}}-1}.$$

The radiation of the layer itself acts only from "above;" from "below" it is drowned in the flux of radiation of temperature T. In the case of thermodynamic equilibrium $T_0 \longrightarrow T$ and $A \longrightarrow 1/2$. Substituting this expression for I in (1) and (2) we get the final equations of equilibrium. The integration of the first equation leads to the series of integral logarithmic functions $E(-t)$. Considering only sufficiently large values of $\frac{h\nu_0}{kT}$ and $\frac{h\nu_0}{kT_0}$ (since only such values have astrophysical interest) we may employ the useful development of integral logarithms, converging rapidly for big values of t:

$$E(-t) = \int_{-\infty}^{-t} \frac{e^z dz}{z} = -e^{-t}\left[\frac{1}{t} - \frac{1!}{t^2} + \frac{2!}{t^3} - \ldots\ldots\right].$$

If, according to the law of an ideal gas, we introduce $N = P/(1+x)kT_0$ (where P is hydrostatic pressure) our equations take the following form (neglecting exponentials of the third order)

$$ATe^{-\frac{h\nu_0}{kT}}\left[\left(1 - \frac{kT}{h\nu_0}\right) + \frac{1}{2}e^{-\frac{h\nu_0}{kT}}\left(1 - \frac{kT}{2h\nu_0}\right)\right] + \frac{1}{2}T_0 e^{-\frac{h\nu_0}{kT_0}}\left[\left(1 - \frac{kT_0}{h\nu_0}\right) + \frac{1}{2}e^{-\frac{h\nu_0}{kT_0}}\left(1 - \frac{kT_0}{2h\nu_0}\right)\right] = \frac{x^2}{1-x^2}\frac{Ph^3}{(2\pi kmT_0)^{3/2}}\left(1 - \frac{kT_0}{h\nu_0}\right) \quad (1.1)$$

$$ATe^{-\frac{h\nu_0}{kT}}\left(1 + \frac{1}{2}e^{-\frac{h\nu_0}{kT}}\right) + \frac{T_0}{2}e^{-\frac{h\nu_0}{kT_0}}\left(1 + \frac{1}{2}e^{-\frac{h\nu_0}{kT_0}}\right) = \frac{x^2}{1-x^2}\frac{Ph^3}{(2\pi mkT_0)^{3/2}}. \quad (2.1)$$

When $T_0 \longrightarrow T$ and $A \longrightarrow 1/2$ these equations flow together and give Saha's formula if we take stimulated captures into account. In our case each of them gives an ionization formula, and their combination determines A as a function of T_0:

$$A(T-T_0)Te^{-\frac{h\nu_0}{kT}} - \frac{A(2T_0-T)}{4}Te^{-\frac{2h\nu_0}{kT}} - \frac{T_0^2}{8}e^{-\frac{2h\nu_0}{kT_0}} = 0.$$

Or, for big values of $\frac{h\nu_0}{kT}$ and $\frac{h\nu_0}{kT_0}$,

$$A = e^{\frac{h\nu_0}{kT}\left(1-\frac{2}{z}\right)}\frac{z^2}{8(1-z)} \qquad \text{where } z = \frac{T_0}{T}. \quad (3)$$

We see that in a steady state the temperature is determined by the external radiation and the properties of the gas: it must be greater for larger

ionization potentials; if the different elements are mixed, the temperature must be the same for all components, and equalization is reached by the behavior of higher quantum states and higher ionization stages.

The Ionization Formula and Schwarzschild's Value for the Boundary Temperature.—The value of A must be very near to $^1/_2$ for the sun; otherwise the temperatures of the sun as determined by the applications of Planck's law (T_1) and by using the solar constant (T_2) would be different. If the higher layers of the Sun's atmosphere were transparent $2A$ would be equal to $(T_2/T_1)^4$—in reality $2A \geqslant (T_2/T_1)^4$. We know that the effective temperatures of the sun T_1 and T_2 deviate systematically from each other so that $T_2 < T_1$. Having in view H. H. Plaskett's[4] new determinations based on the spectrophotometry of some regions free of visible absorption lines, we may consider that the discrepancy, though real, is less than was supposed some years ago. According to Plaskett T_1 is between 6700° and 7000°, and using Abbot's data $T_2 = 6200°$. We consequently establish the following inequality, $1 > 2A > 0.7$. In reality A must be very near to $^1/_2$.

We see now from (3) that for all reasonable χ_0 for the sun T_0 is very near to T, i.e., the "boundary temperature" of the sun practically does not differ from its effective temperature, as determined spectrophotometrically. It seems that we are in contradiction with well-known result of the theory of radiative equilibrium $T_0 = (^1/_2)^{1/4} T$ which indicates a sufficiently large deviation of T_0 from T. But this contradiction between "macroscopic" and "microscopic" theories is very simply explained. Schwarzschild's theory supposes that the photospheric gas is "gray," i.e., that its coefficient of absorption (k) is the same for all wave-lengths; the "microscopic" theory stated above is free from this supposition; it leads to $k \propto \nu^{-3}$ (for $\nu < \nu_0$, k is zero) and the gas is not "gray." The general "macroscopic" theory would lead to a result consistent with the above theory. Milne[5] has, in fact, established that for the gas absorbing only in the far ultra-violet T_0 tends asymptotically to T for radiative equilibrium.

It would be interesting to apply our formula to the upper layers of the solar atmosphere and corona. But we must remember our fundamental supposition that the radiation of the gas may be expressed by the black body law. This hypothesis is applicable only to the layers which are adjacent to the photosphere—the layers to which we must apply the laws of luminescent radiation lie higher up; it is impossible to determine where the "stellar" region degenerates into the "nebulous" one.

Let us consider only the thin "stellar" layer and neglect some variations of opacity and density; if we denote by r the height above the photosphere, our equation (3) shows that the temperature falls off as r^{-1}. For "gray" material the macroscopic theory of radiative equilibrium shows that the temperature diminishes as r^{-2}, and for absorption in the far ultra-violet there is a state of complete isothermal equilibrium according to Milne.[5]

The Correction to the Saha Formula.—Comparing our ionization formula with Saha's it is easy to find that the correcting factor for the latter is

$$A\,\frac{T}{T_0}\,e^{-\frac{h\nu_0}{kT}+\frac{h\nu_0}{kT_0}}\left[1-\frac{k(T-T_0)}{h\nu_0}\right]+\frac{1}{2}.$$

In thermodynamic equilibrium this factor is naturally unity, and we have seen that for the sun it is very near to unity because $T_0 = T$. It, therefore, seems impossible to explain in this way certain anomalies in the solar spectrum such as the behavior of Ba^+, which is to be explained rather by some atomic property (perhaps the "steric factor" introduced by Saha,[6] or by the existence of a metastable D state).

For the stars, especially for giants and early type stars which show emission lines, this correcting factor may be of some importance, but in view of the lack of precision of the available data on spectral line photometry it seems premature at present to discuss this question further.

[1] Gerasimovič, *Zeit. Phys.*, **39**, 1926 (361).
[2] *Phil. Mag.*, **47**, 1924 (224).
[3] *Phil. Mag.*, **46**, 1923 (843).
[4] *Pub. Dom. Ap. Obs.*, **2**, 1923 (213).
[5] *M. N. R. A. S.*, **82**, 1922 (368).
[6] *Phil. Mag.*, **40**, 1920 (472).

CHEMICAL CONSTANTS AND ABSOLUTE ENTROPY

BY WORTH H. RODEBUSH

UNIVERSITY OF ILLINOIS

Communicated March 2, 1927

Recent calculations of the chemical constants for sodium and potassium[1,2,3,4,5] have not been particularly concordant but in several cases new data have been contributed which reduce the uncertainty in the calculations. Thus Simon and Zeidler[3] have obtained specific heat data at low temperatures for potassium and sodium which is in substantial agreement with that of Eastman and Rodebush.[6] Egerton has confirmed the data obtained in this laboratory[1,2] on the vapor pressures of these metal at low pressures. Finally Dr. A. L. Dixon has obtained in this laboratory satisfactory data on the specific heats of the liquid metals so that for the first time it is possible to calculate the entropies of the vapors of sodium and potassium with complete and seemingly reliable data.

The only part of the calculation that requires elaboration is the fitting of an equation to the vapor pressure data. Dr. Dixon finds that C_p for molten potassium is nearly constant and equal to 7.80 in the temperature

range immediately above the boiling point. This would indicate that the vapor pressure equation should contain a term 1.40 log T. When we plot the data of Egerton and Fiock and Rodebush[2] on a log p_1 $\frac{1}{T}$ diagram we find excellent agreement between the two sets of data but it is impossible to fit the data with any equation except a simple linear form which does not allow for variation of ΔH with the temperature. On the other hand if we disregard the boiling point we may fit all the other data surprisingly well with the equation:

$$\log_{10} p_{\text{mm.}} = -\frac{4780}{T} - 1.40 \log T + 11.670.$$

The justification for the above procedure is the assumption that the vapor at the boiling point can no longer be treated as a perfect gas. On the other hand we are of course assuming that the vapor at pressures below 30 to 40 mm. may be treated as a perfect gas.

A similar situation is found in the case of sodium. The boiling point is disregarded as are the data of Rodebush and DeVries at intermediate pressures. These latter data were obtained by the same method as those of Fiock and Rodebush on potassium but the apparatus had not been developed to a satisfactory degree and the results are probably high. The equation

$$\log_{10} p_{\text{mm.}} = -\frac{5730}{T} - 1.25 \log T + 11.580$$

fits the data of Egerton and Rodebush and DeVries,[1] at low pressures, in an entirely satisfactory manner and incidentally the data of Haber and Zisch[7] at intermediate pressures. The entropies of the vapors at 298° K. and 1 atmosphere are tabulated below. The value for potassium is in substantial agreement with that calculated by Fiock and Rodebush. The value for sodium is higher than the probable range estimated by Rodebush and DeVries because of an error made by them in the calculation of the entropy of fusion. The value for sodium is lower than that obtained by Simon[3] and it appears difficult to justify Simon's vapor-pressure equation. For comparison the entropies of lead and mercury are included. The entropy of lead vapor is as calculated by Rodebush and Dixon[8] while the value for mercury is taken from the paper by Fogler and Rodebush[6] with a correction for the specific heat data at low temperatures obtained since by Simon.[9]

In the second column of table 1 are given the values predicted by the Tetrode equation. It will be noted that values for sodium and potassium are high by 1.3 units which is near the value $R\ln 2$ predicted by Schottky,[10] Fowler[11] and others for atoms whose lowest quantum state has an a priori

probability of 2. Taylor[12] has shown that sodium and potassium possess two possible orientations in a magnetic field and Van Vleck[5] has suggested that the entropies of sodium and potassium should show this effect.

ENTROPIES OF THE VAPORS AT 298°K. AND 1 ATMOSPHERE

	OBSERVED	PREDICTED
Potassium	38.2	36.9
Sodium	36.7	35.4
Mercury	41.7	41.8
Lead	42.9	41.9

This seemingly excellent confirmation of the theory of thermodynamic probability justifies one or two observations from a theoretical standpoint. It is assumed in the case of potassium that only a single orientation is possible to an atom in the metallic crystal lattice. If more than one orientation were possible for a given atom in the solid then the entropy of the solid would presumably be greater than zero at absolute zero. Since the magnetic moment is usually considered to be due to moving charges this hypothetical deviation from the third law could be explained as due to the existence of kinetic energy in the solid at 0°K. It is interesting to speculate as to whether all exceptions to the Third Law can be explained as due to the presence of kinetic energy in the condensed phase at absolute zero. Pauling and Tolman[13] have apparently proved that random orientation of molecules is sufficient to cause a positive deviation from the Third Law but their demonstration makes use of the vapor phase which in turn presupposes that the molecules possess kinetic energy to some extent even in the condensed phase.

Another point which may be mentioned in this connection is that Ehrenfest and Trkal[14] and Fowler[15] take the position, that there is no such thing as absolute thermodynamic probability or absolute entropy. Ehrenfest applies the quantum conditions in a way that apparently leaves the thermodynamic probability of the vapor phase purely a relative number depending on the units used. It will be noted, however, that the mathematical expression obtained by Ehrenfest differs from that obtained by Tetrode chiefly in that Planck's constant h appears in the numerator with a negative exponent rather than in the denominator with a positive exponent. In order to obtain the expression for equilibrium between the vapor and the solid phase it is necessary to introduce the quantum constant of "action" with a definite value. This would certainly suggest that the thermodynamic probability of a system is a definite number and hence justify the concept of absolute entropy.

[1] Rodebush and De Vries, *J. Amer. Chem. Soc.*, **47**, 2488 (1925).
[2] Fiock and Rodebush, *Ibid.*, **48**, 2522 (1926).
[3] Simon and Zeidler, *Zeit. physik. Chem.*, **123**, 383 (1926).
[4] Edmondson and Egerton, *Proc. Roy. Soc.*, **113A**, 520 (1927).

[6] Van Vleck, *Physic. Rev.*, **28**, 980 (1926).
[7] Eastman and Rodebush, *J. Amer. Chem. Soc.*, **40**, 489 (1918).
[8] Haber and Zisch, *Zeit. Physik*, **9**, 325 (1922).
[9] Rodebush and Dixon, *Physic. Rev.*, **26**, 851 (1925); Fogler and Rodebush, *J. Amer. Chem. Soc.*, **40**, 2080 (1923).
[10] Simon, *Ann. Physik*, **68**, 241 (1922).
[11] Schottky, *Physik. Zeit.*, **22**, 1 (1921).
[12] Fowler, *Phil. Mag.*, **45**, 32 (1923).
[13] Taylor, *Physic. Rev.*, **28**, 576 (1926).
[14] Pauling and Tolman, *J. Amer. Chem. Soc.*, **47**, 2148 (1925).
[15] Ehrenfest and Trkal, *Proc. Amsterdam Akad.*, **23**, 162 (1920).
[16] Fowler, *Phil. Mag.*, **44**, 823 (1922).

ON CHEMICAL ACTIVATION BY COLLISIONS

BY RICHARD C. TOLMAN, DON M. YOST AND ROSCOE G. DICKINSON

GATES CHEMICAL LABORATORY, CALIFORNIA INSTITUTE OF TECHNOLOGY

Communicated March 3, 1927

1. *Introduction.*—In the case of first order unimolecular gas reactions, such as the decomposition of nitrogen pentoxide, there is a well-known, theoretical difficulty[1] in discovering any process of activation rapid enough to maintain the full Maxwell-Boltzmann quota of activated molecules and thus to assure a first order course to the reaction. This problem has recently been treated anew by Fowler and Rideal,[2] who consider, in a somewhat new light, the possibility of activation by molecular collisions. By assuming that activation occurs as the result of practically every collision in which the sum of the internal energies ϵ_1 and ϵ_2 carried by the two molecules and their relative kinetic energy η is greater than the energy necessary for activation ϵ_1, Fowler and Rideal find it possible, even using kinetic theory diameters, to obtain rates of activation considerably greater than known rates of reaction. The purpose of the present note is to emphasize, rather more strongly than has been done by Fowler and Rideal, the difficulties involved in making the assumption that activation occurs at every collision where the energy available is sufficient for the purpose.

2. *General Plausibility of the Assumption.*—The first difficulty concerns itself with the general plausibility of the assumption. Since the expression for the fraction of all collisions, in which the total energy available is greater than any value ϵ, is mainly determined by an exponential factor of the form $e^{-\epsilon/kT}$ it is evident, with the large values of the energy of activation actually encountered, that in the great majority of activating collisions the total energy available would only be slightly greater than that necessary for activation, and hence practically all the energy would have to flow into one of the two molecules.

This seems, however, a somewhat surprising conclusion, since, on the rather uncertain grounds of ordinary physical intuition, we should expect in the case of collisions between two similar structures with equal capacities for holding energy, that there would be a strong tendency towards equalization in the energy contents of the two structures rather than an absolute necessity for practically all the energy to accumulate in one of the structures.

It is, of course, doubtful how far we should trust old-fashioned physical intuition in the case of quantum phenomena. Nevertheless, there is one case in which we can feel sure that the energy would not all accumulate in one of two colliding molecules, namely, when we have a symmetrical collision between molecules in the same quantum state, since in such a collision neither molecule could be regarded as having a greater power than the other of drawing energy from their common total supply. Such symmetrical collisions would perhaps form only an infinitesimal fraction of all collisions, nevertheless the consideration helps to illustrate the point.

3. *Calculation of Deactivational Diameters.*—The other difficulties which we wish to consider have to do with the large deactivational diameters necessitated by their assumption. For this purpose it will be desirable to obtain what may be regarded as an average value for the deactivational diameter in the following manner. Consider a gas containing N molecules per cubic centimeter, each molecule having s variables (coördinates or momenta) which contribute classical quadratic terms to the internal energy of the molecule. Then, as shown by Fowler and Rideal, the number of molecules at equilibrium having energy greater than that necessary for activation, ϵ_0, would be

$$N_{act.} = N \frac{1}{\Gamma(1/2 s)} \left(\frac{\epsilon_0}{kT}\right)^{1/2 s - 1} e^{-\frac{\epsilon_0}{kT}}. \qquad (1)$$

If we assume now that the process of activation is collisional, then in accordance with the principle of microscopic reversibility this quota of activated molecules would be maintained constant under equilibrium conditions by an equality in the number of activational and deactivational collisions. The maximum possible rate of deactivation by collisions with unactivated molecules of reactant can be taken, however, equal to the *total* number of collisions made per second as predicted by the ordinary kinetic theory formula, giving us,

$$Z_{deact.} = 4N N_{act.} \sigma^{*2} \sqrt{\pi kT/m} \qquad (2)$$

where N may be taken without appreciable error as the total number of molecules of reactant per cubic centimeter and σ^* is, on the average, the mean diameter for a deactivational collision. Substituting (1) in (2) and making use of the equality between rates of activation and deactiva-

tion, we then obtain for the maximum possible rate of activation by collisions with unactivated molecules of reactant,

$$Z_{\text{act.}} = 4N^2\sigma^{*2}\sqrt{\pi kT/m}\,\frac{1}{\Gamma(1/2\,s)}\left(\frac{\epsilon_0}{kT}\right)^{1/2s-1} e^{-\frac{\epsilon_0}{kT}}. \qquad (3)$$

This expression has been derived, of course, for the case of equilibrium, but since we should not expect important variations in the specific rate of activation during the course of the reaction, we may assume it to hold under the actual conditions of the rate measurements, and use it to obtain information as to σ^*. The mode of treatment has advantages for our present purposes over that of Fowler and Rideal, since it will give us actual numerical values for what may be regarded as an average value of σ^* for all deactivational collisions, rather than merely a functional relation connecting the deactivational and activational diameters for each particular kind of collision.

4. *Comparison with Data on the Decomposition of N_2O_5.*—We may now compare the results of equation (3) with the rate of decomposition of N_2O_5 using the same assumptions as Fowler and Rideal. For s we shall take their value

$$s = 14 \qquad (4)$$

which seems reasonable since it would give nitrogen pentoxide a heat capacity per mol of about 17 cal. per degree. And for ϵ_0 we shall use *their* relation (24)

$$\epsilon_0 = q + (1/2s - 1)kT \qquad (5)$$

connecting it with the quantity q in the Arrhenius expression for temperature coefficient of specific reaction rate

$$\frac{d \log k_1}{dT} = \frac{q}{kT^2} \qquad (6)$$

and derived by Fowler and Rideal on the assumption that all molecules of internal energy greater than ϵ_0 have the same chance of decomposition.

Substituting (4) and (5) in (3), we obtain

$$Z_{\text{act.}} = 6.52 \times 10^5\sigma^{*2}N^2e^{-\frac{q}{kT}} \qquad (7)$$

which is to be compared with the experimental rate of decomposition

$$Z_{\text{react.}} = 2.53 \times 10^{14}N\,e^{-\frac{q}{kT}} \qquad (8)$$

which is taken by Fowler and Rideal as representing the results of Hirst and Rideal[3] at pressures of N_2O_5 as low as of 0.05 mm. of Hg.

Taking now the number of molecules per cc. at 0.05 mm. of Hg as being[4] 1.775×10^{15}, and using, as did Fowler and Rideal, a rate of activation one

hundred times greater than the rate of decomposition, we obtain for σ^* the very large value

$$\sigma^* = 4.7 \times 10^{-3} \text{ cm.}$$

and even assuming the case, which is impossible for a first order reaction, of equality of the two rates we obtain the large value,

$$\sigma^* = 4.7 \times 10^{-4} \text{ cm.}$$

5. *Difficulties with Large Diameters.*—There are perhaps no certain theoretical obstacles to such large diameters for activated molecules, and molecular diameters for activated molecules somewhat larger than the ordinary kinetic theory values have certainly been found by Stuart[5] from experiments on the deactivation of excited mercury atoms. Nevertheless, three remarks concerning the extremely large diameters occurring in the theory of Fowler and Rideal must be made.

In the first place, if we have to invent a mechanism involving the transfer of large quantities of energy which is brought about by the approach of the centers of gravity of two molecules to a distance of 4.7×10^{-3} cm. it might be better perhaps to resort to a radiational than a collisional process, since certainly the major portion of the mass of the two molecules is concentrated within distances of the order of 10^{-7} cm. of their centers of gravity.

In the second place, with a total concentration of 1.775×10^{15} molecules per cc. an activated molecule having a diameter of the order of 4.7×10^{-3} cm. would occupy a volume large enough to contain in the neighborhood of 10^8 ordinary molecules. This surprising conclusion is very bothersome. If we assume that other molecules have to stay outside this volume, then we become fearful of the underlying assumptions of the Fowler and Rideal calculations, since as is well known we could not then use the Maxwell-Boltzmann distribution law in its *simple form* to calculate the number of molecules in the activated states. On the other hand, if we assume that other molecules are permitted within this volume, we are surprised that they do not produce the same deactivation that will result from molecules which only reach the boundary of this volume.

Finally there is a difficulty in connection with the use of different diameters σ and σ^* for activational and deactivational collisions. In accordance with the principle of dynamical reversibility, there corresponds to each type of deactivational collision an activational collision which can be obtained from the former solely by a time reversal. The deactivational collision is initiated, however, by the approach of two molecules to the distance σ^* and the activational collisions by their approach to the very much smaller distance σ. Hence we must conclude from the reversibility of the two processes, that in the deactivational collisions molecules that come within

the very large distance σ^* will be mysteriously drawn together to the very much smaller distance σ and will then fly apart in deactivated states.

We have called attention to the foregoing difficulties, recognizing that Fowler and Rideal have themselves been cognizant of difficulties, and not in any way to disparage the useful and beautiful theoretical work which they have done.

[1] See, for example, Tolman, *J. Amer. Chem. Soc.*, **47**, 1524 (1925), where references to other work will be found.

[2] Fowler and Rideal, *Proc. Roy. Soc.*, **A, 113,** 570 (1927).

[3] Hirst and Rideal, *Ibid.*, **A, 109,** 526 (1925).

[4] This figure is used in order to agree with the calculations of Fowler and Rideal. It is, however, apparently the number of molecules at 273°K. rather than that at 300° K. which was approximately the actual temperature of the experiments of Hirst and Rideal.

[5] Stuart, *Zts. Phys.*, **32,** 262 (1925).

A CASE OF NEGATIVE CATALYSIS IN A HOMOGENEOUS SYSTEM

BY ALFRED C. ROBERTSON[1]

GATES CHEMICAL LABORATORY, CALIFORNIA INSTITUTE OF TECHNOLOGY

Communicated March 8, 1927

Introduction.—The purpose of a series of studies[2] made recently has been to elucidate the mechanism of the so-called promoter action on reactions taking place in homogeneous systems. The reactions chosen for this purpose were the catalytic decompositions of hydrogen peroxide as effected by various salts. Hydrogen peroxide was selected because its decomposition products, oxygen and water, have no effect upon the reaction, and because the mechanism of some of its catalytic decompositions are well enough known to admit of the study of the anomalous effects observed when two or more catalysts are present at once. Sometimes the effect of mixed catalysts is the sum of their separate effects, as when hydrogen peroxide is decomposed by sols of platinum and gold.[3] However, in many cases, the total effect is much greater than the sum of the individual effects; one of the catalysts being then said to exert a promoter action. In other cases, the resultant effect is less than the sum of the individual effects, and one of the substances is then said to produce negative catalysis.

These effects are well illustrated by the reactions involving hydrogen peroxide. The catalytic decomposition of this substance usually involves two interdependent simultaneous reactions, by one of which an intermediate compound is formed, and by the other of which it is decomposed.

Thus Bray and Livingston[4] have shown that when hydrogen peroxide is decomposed by hydrobromic acid the two following reactions take place simultaneously:

$$H_2O_2 + 2Br^- + 2H^+ \longrightarrow Br_2 + 2H_2O; \text{ and}$$
$$Br_2 + H_2O_2 \longrightarrow O_2 + 2Br^- + 2H^+.$$

These two reactions soon come to a steady state in which the reactions producing and decomposing the intermediate substance, bromine, proceed with equal rates.

Promoter action has been shown to be due to the formation of a second intermediate compound which is more rapidly acted upon by the hydrogen peroxide, with the evolution of oxygen, than is the first intermediate compound, so that the observed rate of the reaction is increased thereby. Thus it was shown[5] that cupric salts, which promoted the catalytic decomposition of hydrogen peroxide by ferric salts, were converted into cupric acid, and that the subsequent rapid reaction between this substance and hydrogen peroxide accounted for the observed increase in rate.

It is evident that the converse effect, that of negative catalysis, might exist in the case where there is the possibility of the formation of a second intermediate substance which is more slowly acted upon by the hydrogen peroxide than the first intermediate. It has been found that the decomposition of hydrogen peroxide under the joint influence of potassium dichromate and vanadic acid is a reaction of this kind; and it is the purpose of this paper to present briefly the results of its investigation.

Method of Reaction-Rate Measurements.—The reaction rates were measured by the gasometric method, in an improved form of apparatus based upon the original design of Walton.[6] An auxiliary buret, with a flask containing no reactants, has been added to make it possible to apply without computation a correction for any change in the barometric pressure occurring during the course of a slow reaction.

The vanadic acid used was prepared by adding acetic acid to a solution of ammonium vanadate since vanadium pentoxide is difficult to prepare in the pure state and shows a distressing tendency to form sols upon dissolving in water. The ammonium acetate formed thereby, being neutral in reaction, does not change the hydrogen-ion concentration of the solution; its neutral salt effect is doubtless small. Vanadic acid, as shown by the yellow color produced upon acidification, seems to be so weak an acid as to be nearly quantitatively displaced by acetic acid.

Experimental Results.—The rate $-dc/dt$ of the decomposition of the peroxide in all mixtures was found to be only approximately proportional to its concentration, c; however, the data give fairly good constants when calculated according to the expression $K_R = 0.4343(10^4/t)(\log c_0/c)$. The data plotted in figure 1 show the effect upon the values of K_R of

changing the initial concentration of hydrogen peroxide. Because of this effect the initial concentrations were kept as nearly constant as possible and a small correction was applied to the values of reaction rates to reduce them to an arbitrary initial concentration of 187 millimols per liter of hydrogen peroxide when they differed from this value.

The reaction rate K_R at 30° (time expressed in minutes) was found to be 105–108 when the peroxide solution contained 0.5 mM./l. (millimols per liter) of potassium dichromate, as it did in all the experiments with mixed catalysts here considered. It was found to have the small value 7 or 5

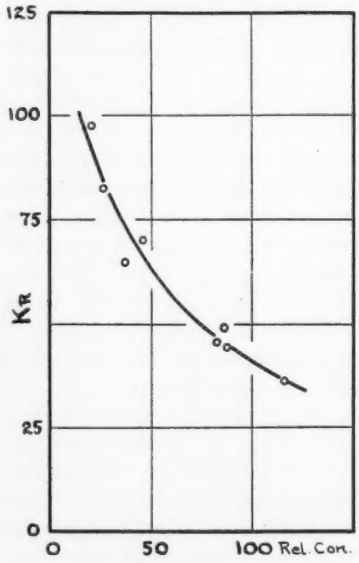

FIGURE 1

Variation of reaction rate with hydrogen peroxide concentration. Dichromate, 0.5 mM./l.; vanadic acid, 5 mM./l.

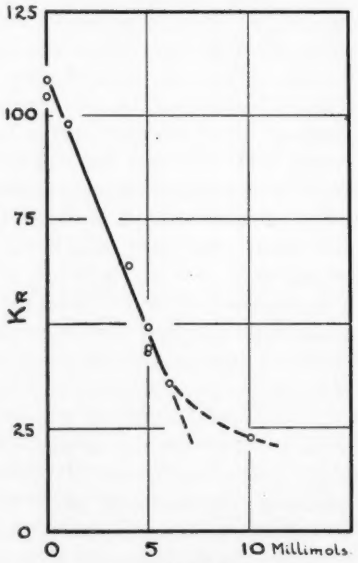

FIGURE 2

Effect of acetic acid upon a mixture containing dichromate (0.5 mM./l.) and ammonium vanadate (5 mM./l.)

when the solution contained no dichromate, but 20 mM./l. of ammonium vanadate or of vanadic acid, respectively. This is a larger quantity of ammonium vanadate than was ever present in the experiments with mixed catalysts.

An experiment with a mixture containing 0.5 mM./l. of dichromate and 20 mM./l. of neutral ammonium vanadate gave a reaction rate substantially identical with that produced by the dichromate alone. This showed that vanadate when neutral has no promoter action; in other words, that it does not influence the catalytic effect of the dichromate.

Experiments were then made with solutions all of which contained the dichromate at 0.5 and the vanadate at 5 mM./l,. but which contained varying concentrations of acetic acid. The results are shown in figure 2. It is seen that the decrease in rate is almost proportional to the amount of acid added. When more than equivalent amounts of acetic acid were added, the straight-line relationship no longer held. This arose from the fact that reduction then took place, as was shown by the changed color of the solution after the peroxide had been decomposed.

Experiments with solutions containing 0.5 mM./l. of dichromate and 1 mM./l. of vanadic acid, but with varying amounts of ammonium vanadate gave the following results:

Ammonium vanadate in mM./1.	0	5	10	20
Reaction rate K_R	97	98	$96^1/_2$	107

These experiments show that increase in vanadate has little effect unless accompanied by an increase in the acid concentration. The following results, which correspond to the data plotted in figures 2 and 3, also show this to be true.

$NH_4VO_3 = 5$	CH_3COOH	1	2	4	5
	K_R	98	(85)	64	45
$NH_4VO_3 = 0$	HVO_3	1	2	4	5
	K_R	94	70	(52)	45

The results indicate, therefore, that only free vanadic acid molecules affect the rate of decomposition; and they show further that acetic acid displaces nearly equivalent quantities of the vanadic acid from its salt.

A series of experiments was made with solutions containing the usual amount of dichromate and varying quantities of vanadic acid. These gave the results shown in figure 3. In this figure the abscissae represent the number of millimols of vanadic acid per liter on two scales (shown at the foot of the figure) corresponding to the upper and lower curves, respectively. It will be seen that the first very minute amounts of vanadic acid increase the rate from its normal value of about 108 to above 120, but that even at 0.80 millimolar the rate has fallen to below 100 and that at 25 millimolar it has dropped to about 35, after which it decreases further only very slowly with increasing amounts of added vanadic acid. The principal effect of the vanadic acid cannot be to remove the hydrogen peroxide from the reaction, since the amount of vanadic acid which halves the reaction rate can react with only about 1.5% of the hydrogen peroxide originally present.

The optical properties of perchromic and pervanadic acids are so similar that it was not possible to obtain even semi-quantitative values as to the extent to which the perchromic acid reacts with the vanadic acid to form pervanadic acid. However, examination at a suitable concentration of

reactants showed that much more pervanadic acid was formed by hydrogen peroxide in the presence of potassium dichromate than in its absence. Werther[7] found, moreover, that a blue ethereal solution of perchromic acid after shaking with an aqueous vanadic acid solution, was decolorized with the simultaneous formation of pervanadic acid; it seems probable that the red perchromic acid reacts in an analogous manner.

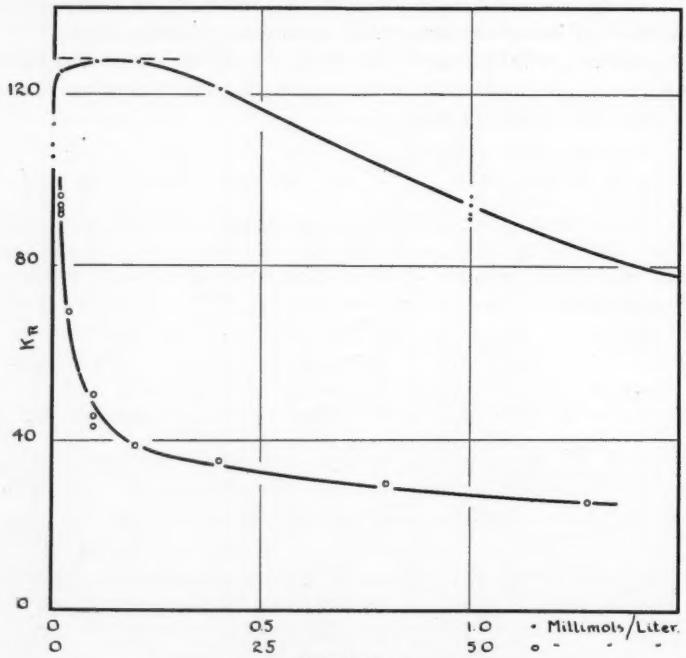

FIGURE 3
Reaction rate for added vanadic acid.

Theoretical Discussion of the Results.—The phenomenon of negative catalysis may be explained, in the same manner as promoter action, by the conception of a change in the path of the catalytic reactions.[8] In this case the explanation is as follows: The catalytic decomposition of hydrogen peroxide by dichromate is doubtless due to the following reactions:

$$K_2Cr_2O_7 + H_2O_2 \longrightarrow 2KCrO_4 + H_2O \qquad (1)$$

$$2KCrO_4 + H_2O_2 \longrightarrow K_2Cr_2O_7 + H_2O + O_2. \qquad (2)$$

The compound formed in these reactions is no doubt K_3CrO_8, but the formula $KCrO_4$ is used for the sake of convenience.

Reaction (1) proceeds rapidly at first and then reaction (2) becomes ef-

fective, and a steady state of catalysis is attained with a certain concentration of $KCrO_4$ present.

With vanadic acid the two corresponding reactions take place, as expressed by the following equations:

$$HVO_3 + H_2O_2 \longrightarrow HVO_4 + H_2O \quad (3)$$
$$HVO_4 + H_2O_2 \longrightarrow HVO_3 + O_2. \quad (4)$$

Reaction (4), however, takes place much more slowly than reaction (2) in conformity with the fact that the reactivity of pervanadic acid and hydrogen peroxide is much less than that of perchromic acid and hydrogen peroxide. However, when these two agents are simultaneously present with hydrogen peroxide, reaction (2) is in large measure replaced by reaction (4), because the following rapid reaction takes place to a large extent:

$$2KCrO_4 + HVO_3 \longrightarrow K_2Cr_2O_7 + HVO_4. \quad (5)$$

The result of this reaction is to diminish the proportion of the more reactive perchromic acid present, and thus to retard greatly the peroxide decomposition. This retarding effect should evidently increase as the concentration of vanadic acid is increased, and should approach a limiting value, as has been shown to be the case when most of the perchromic acid is converted by the rapid reaction (5) into pervanadic acid and but little of it is decomposed according to reaction (2).

A quantitative investigation of the shape of the curve, which should be analogous to a promotion curve,[9] is rendered impracticable because of the complications caused by the slight acidity introduced by the negative catalyst.

Summary.—It has been shown in this investigation that vanadic acid greatly diminishes the rate of the catalytic decomposition of hydrogen peroxide by potassium dichromate. The "negative catalysis" is explained upon the basis of a change in the path of the reaction: the intermediate perchromic acid is converted into the less reactive pervanadic acid, whereby the total rate is decreased very largely. Another system is being sought where there are no complications which will interfere with the study of the shape of the curve.

[1] NATIONAL RESEARCH FELLOW IN CHEMISTRY.

[2] Bohnson and Robertson, *J. Am. Chem. Soc.*, **45**, 2512 (1923); Robertson, *Ibid.*, **47**, 1299 (1925); *Ibid.*, **48**, 2073 (1926).

[3] Henri, *Compt. rend. soc. biol.*, **55**, 864 (1903).

[4] Bray and Livingston, *J. Am. Chem. Soc.*, **45**, 1251 (1923).

[5] Robertson, *J. Am. Chem. Soc.*, **47**, 1304 (1925).

[6] Walton, *Z. phys. Chem.*, **47**, 188 (1904).

[7] Werther, *J. prakt. Chem.*, **83**, 195 (1861).

[8] Robertson, *J. Am. Chem. Soc.*, **48**, 2078 (1926).

[9] Robertson, *Ibid.*, **48**, 2076 (1926).

ON THE DETERMINATION OF THE APPARENT DIAMETERS OF THE IONS IN THE DEBYE-HÜCKEL THEORY OF STRONG ELECTROLYTES

BY T. H. GRONWALL

DEPARTMENT OF CHEMISTRY, COLUMBIA UNIVERSITY

Communicated March 12, 1927

In the Debye-Hückel theory,[1] the average of the apparent diameters a_1 and a_2 of the ions of a symmetrical salt of valence type $(z, -z)$ is proportional to the coefficient of the second term in the expansion, in powers of the square root of the ionic strength, of the osmotic coefficient or of the logarithm of the activity coefficient of either salt or solvent. Consider, for instance, the latter, and let V be the volume of the solution, containing n_0 mols of solvent and n mols of salt, D_0 the dielectric constant of the pure solvent and D that of the solution (D may depend on the concentration as well as on the absolute temperature T), R the gas constant, N the Avogadro number and ϵ the unit electric charge. Writing

$$C^2 = \frac{4\pi N^2\epsilon^2 \times 10^{-19}}{RD_0T} \tag{1}$$

and

$$g^2 = \frac{2 \times 10^3 nz^2}{V}, \tag{2}$$

so that g^2 is twice the ionic strength, the expansion of $\log f_0$ (the *natural* logarithm of the *mol fraction* activity coefficient of the solvent) becomes

$$G = \frac{8\pi N \times 10^{-24} \log f_0}{g^3 \partial V/\partial n_0} = \frac{1}{3} C^3 - \frac{1}{2} C^4 \cdot \frac{10^8 a_1 + 10^8 a_2}{2} g + \ldots \tag{3}$$

Plotting G against g and measuring the slope $-\alpha$ of the curve at $g = 0$, we obtain from (3)

$$\frac{1}{2}(10^8 a_1 + 10^8 a_2) = \frac{2}{C^4} \cdot \alpha, \tag{4}$$

(a_1 and a_2 in centimeters). All apparent ion diameters which have been calculated were obtained by methods essentially equivalent to this, and the gravest objection that has been raised against the Debye-Hückel theory is that, in some cases, the diameters are unreasonably small (KNO_3, KIO_3)[1,2] or even negative (TlCl in $TlNO_3$).[3] To remedy this defect, Bjerrum has recently developed formulas based on the hypothesis of ion association.[2]

It is the purpose of the present note to show that satisfactory values of the apparent diameters result from the Debye-Hückel theory, without

any additional hypothesis, by returning to the unabridged form of the Debye-Hückel fundamental equation

$$\frac{1}{r^2}\frac{d}{dr}\left(r^2\frac{d\psi_i}{dr}\right) = \frac{8\pi N\epsilon z n}{DV}\,\mathrm{sh}\left(\frac{N\epsilon z}{RT}\psi_i\right). \tag{5}$$

Together with the boundary conditions

$$\psi_i \longrightarrow 0 \text{ as } r \longrightarrow \infty,$$

$$\frac{d\psi_i}{dr} = -\frac{\epsilon z_i}{D}\cdot\frac{1}{a_i^2} \text{ at } r = a_i (i = 1, 2; z_1 = z, z_2 = -z), \tag{6}$$

(4) determines the potential $\psi_i(a_i)$ at an ion of the ith kind. Writing

$$\kappa^2 = \frac{8\pi N^2\epsilon^2 z^2 n}{RDTV}, \tag{7}$$

$$\rho = \kappa r, \qquad x_i = \kappa a_i \tag{8}$$

and expanding the hyperbolic sine to the right in (5) in powers of ψ_i, we obtain

$$\frac{d}{d\rho}\left(\rho^2\frac{d\psi_i}{d\rho}\right) - \rho^2\psi_i = \rho^2\Phi(\psi_i) = \rho^2\sum_{n=1}^{\infty}\frac{1}{(2n+1)!}\left(\frac{N\epsilon z}{RT}\right)^{2n}\psi_i^{2n+1}. \tag{9}$$

Forming Green's function for the differential operator to the left with the boundary conditions (6), it is readily shown that (5) and (6) are equivalent to the integral equation

$$\psi_i(\rho) = \frac{\epsilon z_i x_i}{D(1+x_i)}\frac{e^{x_i-\rho}}{a_i\rho} - \frac{1}{2\rho}\int_{x_i}^{\infty}\left(e^{-|u-\rho|} + \frac{x_i-1}{x_i+1}e^{2x_i-u-\rho}\right)\Phi(\psi_i(u))u\,du. \tag{10}$$

The Debye-Hückel approximation to ψ_i, which leads to (3), consists of the first term to the right in (10) and evidently results from (9) upon replacing the right-hand member by zero. We now expand ψ_i in powers of $1/D$; since Φ contains only odd powers of ψ_i, this expansion takes the form

$$\psi_i(\rho) = \sum_{n=0}^{\infty}\frac{\psi_{i,\,2n+1}(\rho)}{D^{2n+1}}, \tag{11}$$

and substitution in (10) yields the following recurrent determination of $\psi_{i,1}, \psi_{i,3}, \psi_{i,5}, \ldots$:

$$\begin{aligned}\psi_{i,1}(\rho) &= \frac{\epsilon z_i x_i}{1+x_i}\frac{e^{x_i-\rho}}{a_i\rho},\\ \psi_{i,\,2n+1}(\rho) &= -\frac{1}{2\rho}\int_{x_i}^{\infty}\left(e^{-|u-\rho|} + \frac{x_i-1}{x_i+1}e^{2x_i-u-\rho}\right)\Phi_{i,\,2n+1}(u)u\,du,\end{aligned} \tag{12}$$

where

$$\Phi_{i,3}(\rho) = \frac{1}{3!}\left(\frac{N\epsilon z}{RT}\right)^2 \psi_{i,1}(\rho)^3,$$

$$\Phi_{i,5}(\rho) = \frac{3}{3!}\left(\frac{N\epsilon z}{RT}\right)^2 \psi_{i,1}^2\,\psi_{i,3} + \frac{1}{5!}\left(\frac{N\epsilon z}{RT}\right)^4 \psi_{i,1}^5, \tag{13}$$

$$\Phi_{i,7}(\rho) = \frac{9}{3!}\left(\frac{N\epsilon z}{RT}\right)^2 (\psi_{i,1}\,\psi_{i,3}^2 + \psi_{i,1}^2\,\psi_{i,5}) + \frac{5}{5!}\left(\frac{N\epsilon z}{RT}\right)^4 \psi_{i,1}^4\,\psi_{i,3} + \frac{1}{7!}\left(\frac{N\epsilon z}{RT}\right)^6 \psi_{i,1}^7.$$

.....

It is now shown by mathematical induction that for sufficiently small values of x_i and ρ, the contribution of the term containing $\psi_{i,1}^{2n+1}$ in the expression (13) for $\Phi_{i,2n+1}$ to the value of $\psi_{i,2n+1}$ given by (12) is of a lower degree of smallness than the contribution of any of the other terms, so that (11) gives for $\rho = x_i$

$$\psi_i(x_i) = \frac{\epsilon z_i}{Da_i}(1 - x_i + x_i^2) - x_i^2 \sum_{n=1}^{\infty} \frac{1}{(2n-1).(2n+1)!}\left(\frac{N\epsilon z_i}{RT}\right)^{2n}\left(\frac{\epsilon z_i}{Da_i}\right)^{2n+1} + \ldots, \tag{14}$$

the neglected terms being of the order of $x_i^3 \log x_i$. In (14), D may be replaced by D_0, since $1/D = 1/D_0 + \text{const.}\ x_i^2 + \ldots$, which relation follows from the experimentally well-established fact[4] that the curve obtained by plotting D against g^2 (or the concentration) has a finite slope at $g = 0$. The electrostatic potential energy U_e of the ions is now calculated from $\psi_1(x_1)$ and $\psi_2(x_2)$ in the usual manner,[1] and the excess free energy F_e of the solution is given by

$$F_e = T\int_T^{\infty} \frac{U_e}{T^2}\,dT,$$

where the integration is to be performed *as if V and D were independent of T*;[5] moreover, $RT \log f_0 = \partial F_e/\partial n_0$. Performing these calculations with the aid of (14), we get the following final result connecting the slope $-\alpha$ of the G, g curve at $g = 0$ (G being defined by (3)) with the apparent diameters a_1 and a_2:

$$\frac{1}{2}\left[f\left(\frac{\beta.10^8 a_1}{z^2}\right) + f\left(\frac{\beta.10^8 a_2}{z^2}\right)\right] = \frac{\beta}{z^2}\cdot\frac{2\alpha}{C^4}, \tag{15}$$

where

$$\beta = \frac{4\pi N}{10^{27}C^2}, \tag{16}$$

and the function f is defined by

$$f(\xi) = \xi - \sum_{n=1}^{\infty} \frac{2}{(2n-1).(2n+2)!} \cdot \frac{1}{\xi^{2n-1}} . \qquad (17)$$

In particular, assuming $a_1 = a_2 = a$, and denoting the a value calculated from (4) by a_0, (15) becomes

$$f\left(\frac{\beta.10^8 a}{z^2}\right) = \frac{\beta.10^8 a_0}{z^2} . \qquad (18)$$

This, therefore, is the relation between the average apparent diameter a_0 calculated by neglecting terms of higher order than the first in the expansion of the hyperbolic sine in (5), and the average apparent diameter a obtained by retaining all the higher order terms. Since $f'(\xi) > 0$ by (17), it follows that as a_0 increases from $-\infty$ to $+\infty$, a increases monotonely from 0 to $+\infty$.

Thus negative diameters can no longer occur, and very small positive ones are likewise excluded, as appears from the following table:

SOLVENT	SOLUTE	$10^8 a_0$	$10^8 a$ BJERRUM[3]	$10^8 a$ EQ. (18)
$TlNO_3$ in H_2O	TlCl	-0.9[3]	..	1.77
H_2O	KIO_3	0.0[3]	1.33	2.12
H_2O	KNO_3	0.43[1,2]	1.57	2.30

In the general case, where the salt need no longer be symmetrical, but is composed of ν_1 ions of valence z_1 and ν_2 ions of valence z_2 (so that $\nu_1 : \nu_2 = -z_2 : z_1$), the expansion corresponding to (11) contains both odd and even powers of $1/D$, and from the term containing $1/D^2$ there arises a term in G of the order of magnitude of $g \log g$. Defining α by

$$\alpha = \lim_{g \to 0} \left\{ \frac{{}^1/_3 C^3 - G}{g} + \frac{C^4}{6\beta} \left(\frac{\nu_2 z_1 + \nu_1 z_2}{\nu_1 + \nu_2} \right)^2 \left[\log g + \log 3C + \gamma + \frac{1}{3} \right] \right\}, \qquad (19)$$

where γ is Euler's constant, the relation between a_1, a_2 and α becomes

$$\nu_2^2 z_1^2 \varphi\left(\frac{\beta.10^8 a_1}{z_1^2}\right) + \nu_1 \nu_2 z_1 z_2 \left[\varphi\left(\frac{\beta.10^8 a_1}{z_1 z_2}\right) + \varphi\left(\frac{\beta.10^8 a_2}{z_1 z_2}\right) \right]$$
$$+ \nu_1^2 z_2^2 \varphi\left(\frac{\beta.10^8 a_2}{z_2^2}\right) = (\nu_1 + \nu_2)^2 \beta \cdot \frac{2\alpha}{C^4} - \frac{1}{3} (\nu_2 z_1 + \nu_1 z_2)^2 \log \beta$$
$$+ \frac{2}{3} (\nu_2 z_1 + \nu_1 z_2)[\nu_2 z_1 \log z_1 + \nu_1 z_2 \log (-z_2)], \qquad (20)$$

where.

$$\varphi(\xi) = \xi - \frac{1}{3} \log |\xi| + \sum_{n=1}^{\infty} \frac{2(-1)^n}{n.(n+3)!} \cdot \frac{1}{\xi^n} . \qquad (21)$$

In the symmetrical case, $\nu_1 = \nu_2 = 1$, $z_1 = z$, $z_2 = -z$, and (20) reduces to (15) on account of the relation $2f(\xi) = \varphi(\xi) - \varphi(-\xi)$.

[1] Debye, P., and Hückel, E., *Physik. Zs.*, **24**, 185, 1923.

[2] Bjerrum, N., *Danske Vidensk. Selsk.*, **7**, No. 9, 1926.

[3] Schärer, O., *Physik. Zs.*, **25**, 145, 1924. Regarding negative values of the apparent diameter, see also p. 373 of LaMer, V. K., King, C. V., and Mason, C. F., *J. Amer. Chem. Soc.*, **49**, 363, 1927, and LaMer, V. K., and Mason, C. F., *Ibid.*, **49**, 410, 1927.

[4] Walden, P., Ulich, H., and Werner, O., *Z. Phys. Chem.*, **116**, 261, 1925.

[5] Gross, Ph., and Halpern, O., *Physik. Zs.*, **26**, 403, 1925.

[Contribution of the Department of Chemistry, Columbia University, No. 538.]

NEW INFRA-RED ABSORPTION BANDS OF METHANE

BY JOSEPH W. ELLIS

DEPARTMENT OF PHYSICS, UNIVERSITY OF CALIFORNIA AT LOS ANGELES

Cooley[1] has recently examined with grating spectrometers the three infra-red absorption maxima of methane observed by Coblentz[2] with a rock-salt prism spectroscope. The two bands of longest wave-lengths, under the high resolving power of the echelette gratings, appeared triple with intense unresolved zero branches at 7.67μ and 3.33μ, respectively, and with positive and negative branches each exhibiting a structure of approximately equally spaced rotational components. The region of 2.35μ, although possessing a certain structure, displayed no regularity.

Dennison[3] has attempted to coördinate Cooley's observations with the results of his own theoretical study of the methane molecule. He predicted four fundamental modes of vibration of the CH_4 molecule, which should give rise to four bands in its absorption spectrum. He established the 7.67μ, 3.33μ and the 2.37μ component of the 2.35μ region, and a hypothetical band at 6.58μ as these four fundamental bands. Other components of the 2.35μ region he associated with combinations of the three longest wave-length fundamental bands.

The present investigation was undertaken to examine the absorption spectrum of methane between the visible spectrum and 2.8μ by means of a self-registering quartz spectrograph which has been described previously.[4] It was thought that absorption maxima, representing overtones and combination bands, should be observable in this region if a cell of sufficient length were used.

The methane gas was generated by heating in pyrex test tubes a mixture of freshly fused sodium acetate and dry soda lime. A water displacement method was used to store the gas in a large bottle. The absorption cell was a thick-walled vulcanized fibre tube, 87.5 cm. long and 3.7 cm. inside

diameter, with glass end plates sealed on with red wax. The cell was evacuated and methane allowed to bubble over into it slowly through tubes of sulphuric acid. In the record of figure 1*B*, 600 cc. of gas were bubbled through five wash bottles of concentrated sulphuric acid, the whole process

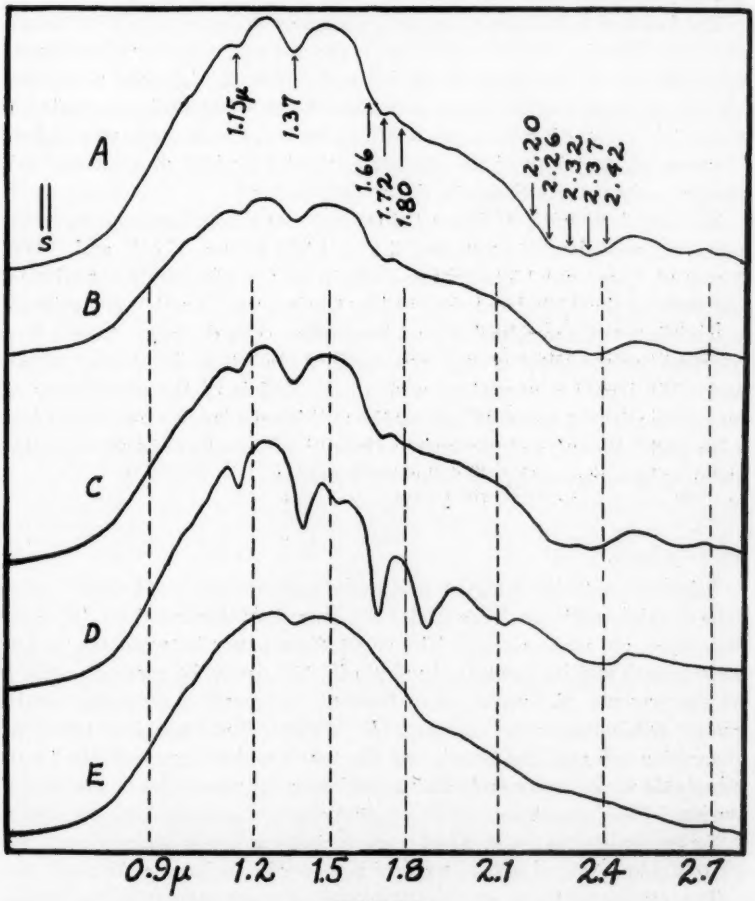

FIGURE 1

consuming 13 minutes. There was a leakage of air during the process sufficient to bring the 950 cc. volume of the absorption tube to atmospheric pressure. Figure 1*A* represents a record repeated under similar circumstances but with a slight adjustment of the source of light to give greater galvanometer deflections. In obtaining the record of figure 1*C*, 750 cc.

of gas were passed for 20 minutes through two 12-inch U-tubes containing glass beads and fuming sulphuric acid, and through two U-tubes of potassium hydroxide. This final precaution of using fuming sulphuric acid was taken to remove all possibility of any ethylene, which might have been generated, passing into the cell.

The beam of light from a tungsten lamp was rendered parallel by means of a glass lens before passing through the cell and afterwards converged upon the slit of the spectroscope by a second lens. The slit width was $^1/_2$ mm. and the portion of the record which this subtended is indicated in figure 1*A*. Since, however, the width of the thermo-elements was slightly in excess of the width of the slit image, the total width of a spectral line would be about three times the slit image indicated.

Records *A*, *B* and *C* of figure 1 show five new absorption maxima at the following wave-length positions: 1.15μ, 1.37μ [1.66μ, 172μ], and 1.80μ. Those at 1.66μ and 1.72μ are assumed to be the partially resolved first harmonic of the 3.33μ band observed by Cooley, while the 1.15μ maximum is doubtless the unresolved second harmonic. The deviation from a true harmonic relationship among the 3.33μ, 1.69μ (that is, 1.66μ, 1.72μ), and 1.15μ bands is consistent with theory and is of the same order of magnitude as that observed among the well-known bands of HCl at 3.46μ, 1.76μ and 1.19μ. The frequencies in mm.$^{-1}$ of these three bands of methane may be expressed by the following formula:

$$\nu_n = 307n - 5.5n^2 \qquad (1)$$

where $n = 1, 2, 3$.

Using the notation adopted by Cooley and Dennison and explained in table 1, the bands at 1.37μ and 1.80μ may be interpreted as $(\nu_4 + \nu_3')$ and $(\nu_4 + \nu_1)$, respectively. The slight discrepancy between the former wave-length and its theoretical value of 1.385μ may be caused partially by the presence of a water vapor band at that position, as shown in the energy distribution curve of figure 1*E*. Record *E* was obtained when the absorption cell was evacuated, and the bands which occur are due to atmospheric water vapor and carbon dioxide in the remainder of the optical system.

No bands are observed which may be interpreted as harmonics of the 7.67μ fundamental.

The region of 2.35μ shows the following components: 2.20μ, 2.26μ, 2.32μ, 2.37μ and 2.42μ. The interpretation by Cooley and Dennison of the significance of these maxima is accepted here with the following additions. The 2.26μ band, not recorded by Cooley, agrees with the value calculated for a combination of the positive branches of ν_4 and ν_3 $(\nu_4^+ + \nu_3^+)$. A corresponding combination of negative branches would coincide with the value of ν_1 at 2.37μ.

The discovery by Schaefer and Philipps[5] of difference combinations in the spectrum of CO_2 has led the author to search for similar bands in the spectrum of methane. A distinct but weak band at 5.8μ in the record given by Coblentz[2] checks well with the 5.88μ value calculated for $(\nu_3-\nu_4)$. A slight dip at 2.16μ, most observable in figure $1C$, may be considered doubtful although in exact agreement with the calculated value for $(\nu_3'-\nu_4)$.

In table 1 are assembled the data of the observations by Cooley and by the author, together with the identification of the bands in terms of four fundamental frequencies.

TABLE 1

IDENTIFICATION	CALCULATED λ	OBSERVED λ COOLEY	OBSERVED λ ELLIS
ν_4	..	7.67μ	..
ν_2	6.58μ	..	..
ν_3	..	3.33	..
ν_1	..	2.37	2.37μ
$*\nu_4'$	3.84	3.84	..
$*\nu_3'$	**1.69	..	1.69
$*\nu_3''$	**1.15	..	1.15
$\nu_4+\nu_2$	3.54	3.54	..
$\nu_4^-+\nu_3^-$	2.38	?	2.37
$\nu_4^0+\nu_3^0$	2.32	2.32	2.32
$\nu_4^++\nu_3^+$	2.26	..	2.26
$\nu_4+\nu_1$	1.80	..	1.80
$\nu_4+\nu_3'$	1.38	..	1.37
$\nu_2+\nu_4'$	2.42	2.42	2.42
$\nu_2+\nu_3$	2.20	2.20	2.20
$\nu_3-\nu_4$	5.88	..	***5.8
$\nu_3-\nu_4'$	2.16	..	(2.16?)

* ν' and ν'' signify first and second harmonics, respectively.
** Calculated from equation (1).
*** From Coblentz's curve.

The examination of the spectrum of methane presented in this paper represents a portion of a larger study of infra-red absorption which has been in progress for the last five years. As the results of other investigators have been published from time to time it has been noticed that, in spite of considerable variations among these, the writer's published values have consistently deviated from their average values in certain regions of the spectrum. In particular, his values at 1.20μ, 1.40μ and 1.70μ have appeared to be 0.01μ, 0.02μ and 0.03μ too low; while at 2.40μ they have been 0.03μ too high. Consequently, a check was made upon certain bands which have been accurately measured with grating spectrometers, namely, the 1.37μ, 1.76μ and 2.73μ bands of water vapor, HCl and CO_2,

respectively. The values of the components of the 2.35μ region of the CH_4 spectrum, although consistent among themselves, were slightly high and were arbitrarily made to agree with those of Cooley's grating measurements. As a result of these checks a correction curve is given in figure 2, the ordinates indicating the amounts to be added to all data previously published by the writer.

The present study of the methane spectrum has thrown new light upon these previous investigations by the writer.[6] Although the structures of the 3.33μ and 7.67μ bands indicate that the methane molecule, as a whole, takes part in the absorption process, it must be observed that the higher liquid members of the paraffin series, as well as other organic compounds, exhibit regions of absorption corresponding to the 1.15μ, 1.37μ, 1.69μ, 2.32μ, 3.33μ and 7.67μ bands. Since the only characteristic common to

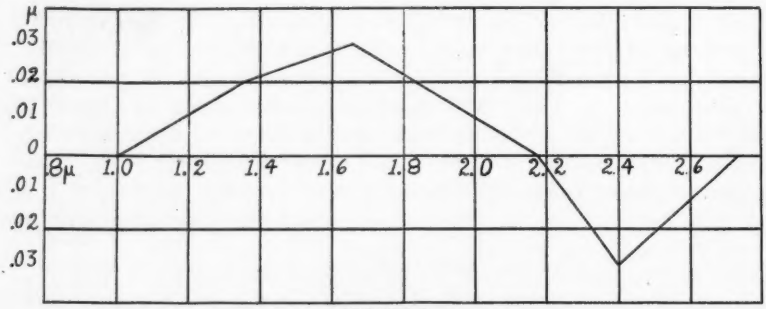

FIGURE 2
Wave-length corrections to previous values.

all of these compounds is the C-H linkage it still seems that these bands must be intimately associated with the atomic pair. But contrary to the hypothesis previously advanced that these bands constitute a single parabolic series, it now seems that such a series starts near 3.3μ (at 3.45μ for paraffin compounds and at 3.25μ for benzene and phenyl compounds), and that the band near 6.8μ represents a second independent fundamental mode of vibration. The bands below 3μ which alternate with the overtones of the 3.3μ band then seem to be combinations of the 6.8μ maximum with that at 3.3μ and its overtones. This overcomes the difficulty previously mentioned that the longest wave-length band could never be made to fit the formula derived from higher members of the series. Furthermore, such a hypothesis would account for the low intensities of alternate bands below 3μ. Although the data for any one substance are incomplete, the observations in the visible region by Russell and Lapraik[7] seem to constitute a part of this system of bands. This subject will probably be pursued further elsewhere.

Figure 1*D* is a record of the absorption by a 15 mm. cell of liquid chloroform, $CHCl_3$, included for comparative purposes. The bands at 1.15μ, 1.40μ and 1.69μ have their analogues in the spectrum of methane. Dreisch[8] has shown that the spectrum of chloroform vapor is practically identical with that of the liquid, thus justifying this comparison.

[1] J. P. Cooley, *Astroph. J.*, **62**, 73 (1925).
[2] W. W. Coblentz, Carnegie Institution Publication No. **35** (1905).
[3] D. M. Dennison, *Astroph. J.*, **62**, 84 (1925).
[4] J. W. Ellis, *J. O. S. A. and R. S. I.*, **11**, 647 (1925).
[5] Schaefer and Philipps, *Zs. Physik*, **36**, 641 (1926).
[6] J. W. Ellis, *Physic. Rev.*, **23**, 48 (1924); **27**, 298 (1926).
[7] Russell and Lapraik, *Chem. Soc. London Trans.*, **39**, 169 (1881).
[8] Th. Dresich, *Zs. Physik*, **30**, 200 (1924).

ON THE NATURE OF LIGHT

BY ERNEST O. LAWRENCE* AND J. W. BEAMS*

YALE UNIVERSITY

Communicated February 5, 1927

Introduction.—There exists in the quantum theory a most unusual circumstance, for the structure of the very thing concerned in the theory, i.e., radiation remains entirely obscure. Various developments of the theory have largely confined themselves to describing the experimentally known quantum transfers of energy, the physical mechanism of the transfers of energy, the physical mechanism of the transfers and the nature of quanta being only vaguely indicated. An interesting exception is the recent suggestion as to the structure of light put forward by Sir J. J. Thomson.[1] This peculiar theoretical situation has arisen, partly at least, because of the fact that there has been no direct experimental evidence to support a detailed view of the nature of radiation and its interaction with matter. For instance, there is no definite information on the length of time elapsing during the process of absorption of a quantum of energy photo-electrically by an electron, and the so-called length of a light quantum—if such a concept has meaning—is equally unknown experimentally. Clearly, experimental evidence concerning these two quantities would be of great assistance in formulating our ideas of the structure of radiation. This communication deals with an experiment which has established very low upper limits to their possible magnitudes.

The Experiment.—The experiment consisted in producing very short segments of light by passing a light beam through a very rapidly operating shutter and observing the photoelectric currents produced in a potassium photo-cell by these light pulses as a function of their length.

The short light segments were produced by a refinement of a previously described method[2] indicated in figure 1. A sixty cycle transformer, T, charged a condenser, C, to a potential difference of about 10,000 volts at which voltage it discharged across a zinc spark gap, the charging and discharging occurring, of course, 120 times per second. Light from the spark was collimated by a lens, L, and on passing through a Nicol prism, N_1, was plane polarized where with suitable diaphragming it passed between two sets of parallel brass plates, K_1 and K_2, immersed in carbon bisulphide and oriented at right angles to each other and 45° with respect to the electric vector of the polarized light. Emerging from this "double Kerr cell" the light passed to a second Nicol N_2 crossed with respect to the first. Light emerging from N_2 entered a very sensitive potassium photo-cell, PC. Both sets of plates, K_1 and K_2, were connected across the spark gap with wires of variable length (a trolley system, T_1T_2, was arranged so that

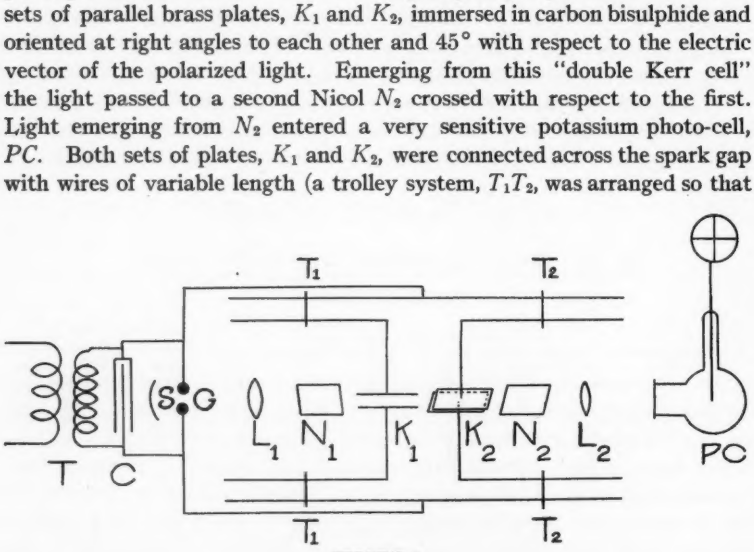

FIGURE 1

the wire paths from the spark gap to either set of plates could be varied conveniently and quickly from 4 meters to 40 meters in steps as small as desired) and, therefore, they assumed potential differences existing across the terminals of the spark gap at a previous time equal to the time required for the propagation of the electrical effects along the wires.

Now during the charging of the condenser the potential differences across both sets of plates are very nearly the same though the wire paths connecting them to the spark gap may be unequal. This is true because the 60 cycle increase of the voltage is very slow in comparison to the rapidity of propagation of the electrical effects along the wires to the Kerr cells. The discharge of the condenser through the spark gap gives rise to a quite different situation, however, because the voltage across the gap drops from a high value to practically zero in an exceedingly short time. The change in voltage is propagated to the Kerr cell plates and they lose their charge at a time subsequent to the spark discharge about equal to the

wire path divided by the velocity of light. Thus, it is evident that if the wire paths to the two sets of plates are not the same one pair of plates comes to zero difference of potential before the other pair and there is a short time when an electric field exists between one set and not between the other.

Plane polarized light from the first Nicol N_1 when passing between the first pair of plates K_1 is elliptically polarized if the plates are at a difference of potential. On passing through the second pair K_2 the ellipticity is compensated and light emerges from the combination plane polarized as before and unable to pass through N_2. Only when the electric field between one pair of plates is greater than between the other is there a resultant ellipticity of the light. In this case light passes through the second Nicol N_2 and impinges on the photo-cell PC. Thus, during the charging of the condenser no light passes because the field between K_1 and K_2 are very nearly the same and light emerges from N_2 only during the short interval of time after the discharge of the spark when one pair of plates is charged and the other is not. In other words, light emerges from the system of Nicols and Kerr cells for the very short interval of time equal to the wire path difference from SG to K_1 and K_2, divided by the velocity of propagation of the electrical effects along the wires (approximately the velocity of light). Thereby short segments of light of various lengths were produced by changing the wire path to one pair of plates, keeping the wire path to the other constant. In this way photo-electric effects produced by these short pulses entering the photo-cell were studied as a function of their length.

Results.—The data exhibited in figure 2 typify the results obtained when one of the trolleys was held constant and the other moved from a position of shorter wire path through the position of equality to longer wire path positions. The abscissas thus show the wire path differences in cm. and the ordinates represent the corresponding observed photo-electric currents. It is seen as the trolley is moved from a position of shorter wire path (abscissa = -100 cm.) to equality with the other (abscissa = 0) the photo-current rapidly decreases to zero and equally rapidly rises again as the trolley is moved to longer wire distances (abscissa = $+100$ cm.). It may be remarked at this point that the curve does not exhibit perfect symmetry about the minimum because the spark is not uniformly intense in time and the coming in or decay of the luminosity produced changes in the slopes of the curve. By taking data over various time intervals after the spark discharge it was shown that sharp changes in slope were due to this cause.

If the light source were uniformly intense and the photo-electric effect per unit light intensity were independent of the length of the light pulses, one would expect that the photo-electric effect would decrease linearly to zero as the wire path difference was diminished and again increase linearly as the path difference were increased. On the other hand, if

the length of a light quantum were of the same order of magnitude as the length of the segments, presumably fractional quanta would be produced which would not have enough energy to eject an electron photo-electrically and the photo-current would be abnormally small. Also, in case the time required for an electron to absorb sufficient energy to be ejected were greater than the time it takes for the segment of light to pass over it, i.e., its length divided by the velocity of light, the pulse would not be able to eject the electron and the photo-current for such short segments would be zero. It is clear, therefore, that if either of these quantities were sufficiently large our plot of photo-electric effect versus length of light segment would not show the very sharp minimum of figure 2 but would exhibit a region over which the photo-currents were zero. The sharpness of the minimum of the series of experimental points (circles of figure 2) wherein the smallest light pulses were 10 cm. (similar data have also been obtained with segments as short as 5 cm.), therefore, leads to the conclusion that *if light quanta are of the commonly understood wave nature, they are less than 3 cm. in length and an electron absorbs a light quantum photo-electrically in less than* 10^{-10} *sec.*

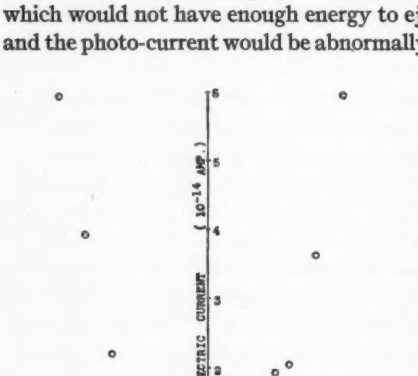

FIGURE 2

Discussion of the Experiment.—One is impressed with the apparent rapidity of action of the combination of Kerr cells and Nicols constituting the light shutter. The production of the short segments is understandable providing that the time of breakdown of the resistance of the spark gap is exceedingly small. Unfortunately, there exists no experimental data on the rapidity of beginning of a spark of this sort—the fastest oscillographs being unable to detect a time of breakdown at all. However, theoretical estimates indicate that the time is very short—less than 10^{-9} sec. It is even more difficult to gain knowledge of the way the voltage decreases during the first stage of the discharge. It seems probable, however, that at the beginning the voltage drops very rapidly. Since the Kerr effect varies as the square of the voltage the ellipticity of the light would change much more rapidly than the voltage. On the basis of these considerations it seems plausible that the Kerr cells were acting with great speed. Per-

haps the best experimental evidence that the Kerr effects in the present experiments switched from large to small values in periods of time of the order of magnitude of 10^{-10} sec. is the experiment itself, for it is difficult to account for so sharp a minimum in the observed curves if this were not the case.

On computation of the time it takes an array of molecules producing a Kerr effect to assume random positions by thermal agitation alone, it is found that it is approximately 10^{-12} sec. One of the writers has shown the existence of a lag in the Kerr effect[2] (which, of course, is compensated out in the two Kerr cells of the present experiments). It is, therefore, not inconceivable that the molecules of the carbon bisulphide persist in the condition producing the Kerr effect for a considerable time after the relaxing of the electric field and then in a very short time (10^{-12} sec.) assume random positions after the breakdown starts. Such a phenomenon would readily account for the quick action of the Kerr cells though the time of discharge of the spark were quite considerable.

In making estimates of the lengths of the light segments in terms of wire path differences it has been assumed that the changes in electrical potential were propagated along the wires with the velocity of light. This assumption has the strongest support of many experiments performed years ago. R. Blondlot[3] observed the propagation of discharges along wires concluding that the surges travel practically with the velocity of light and Saunders[4] and Trowbridge and Duane[5] arrived at similar conclusions using standing waves. It is interesting to point out that in the present experiment photo-electric effects have been observed by light flashes occurring 120 times per second, each flash lasting roughly 10^{-10} sec. In other words, photo-currents produced by light shining only one one-hundred millionth of the time were measured. In order to do this a photo-cell of greatest sensitivity was required. The greatest factor, however, in the success of the experiment was the fact that the light from the spark is enormously intense when shining, as compared to its average intensity over a long interval of time.

Discussion of the Results.—As pointed out in the introduction, it is difficult to estimate on the basis of current theories the magnitude of the two quantities—the length of radiation quanta and the time of photo-electric action. It is often suggested that since it is possible to get interference over path differences of about one meter light quanta must be of even greater length. Such an argument, however, is of little force because such a mode of reasoning would imply also that quanta are "split" at the half-silvered mirror of a Michelson interferometer. A more acceptable estimate is the calculation of the length of light quanta made by G. P. Thomson[6] on the basis of the finite breadth of spectral lines. Thomson concluded that quanta were longer than 8 cm. To test the matter he looked for a

decrease in the breadth of a doppler shifted line, observed in a spectroscope in line with two narrow slits placed 45° with a column of rapidly moving atoms emitting light, as the slits were narrowed. Finding no such effect he concluded that quanta were shorter than about 3 cm. in agreement with the results here presented.

There is an even smaller basis for an estimate of the time interval during which an electron absorbs the energy of a quantum. Since the electron acquires a finite amount of energy it is probable that a finite time is involved in the process. In the case of excitation of atoms by radiation it is quite well established now that there is a "dark time" during which an atom remains excited—usually of the order of magnitude of 10^{-8} sec.—but the time interval during which it passes from the normal to the excited state is unknown. There is reason to believe that this latter period is much smaller than the former and one would expect this period of time to be of the same order of magnitude as the time interval associated with photo-electric ejection of an electron. The results here presented clearly support such a view.

This experiment leads to the conclusion that quanta as bundles of energy of considerable dimensions do not exist and suggest that the effects of radiation on atoms are independent of the length of the pulses to the extent that the effects would be independent on the classical theory. This conclusion harmonizes well with a theory advanced by Professor W. F. G. Swann[7] in which he developed the consequences of the postulate that quanta of negligible dimensions follow the Poynting flux of the classical theory. A similar idea is incorporated in the more recent theory of the structure of light put forward by Sir J. J. Thomson.[1] In this theory light has a dual structure consisting of quanta in the form of rings of electric lines of force (dimensions of the order of magnitude of the wave-length) and Maxwellian waves which are the pathfinders determining where the quanta may go—again along the Poynting flux. Both theories are supported by the present experiment.

It is a very pleasant duty to record our indebtedness to Professor W. F. G. Swann for his interest in this work. We wish also to thank Mr. Donald Cooksey for the loan of a pair of very fine Nicol prisms.

* NATIONAL RESEARCH FELLOW.

[1] Thomson, *Phil. Mag.*, **50**, 1181 (1925).
[2] Beams, *J. O. S. A. and R. S. I.*, **13**, 597 (1926).
[3] Blondlot, R., *Comptes Rendus*, **117**, 543 (1893).
[4] Saunders, *Phys. Rev.*, **4**, 81 (1896).
[5] Trowbridge and Duane, *Amer. J. Sci.*, **49**, 297 (1895).
[6] Thomson, *Proc. Roy. Soc.*, **A104**, 115 (1923).
[7] Swann, *Science*, **425**, Apr. 24 and **452**, May 1 (1925).

BANDS IN THE EXTREME ULTRA-VIOLET SPECTRUM OF A HELIUM DISCHARGE

BY L. A. SOMMER

JEFFERSON PHYSICAL LABORATORY, HARVARD UNIVERSITY

Communicated March 5, 1927

Lyman[1] has found in photographs taken in helium with a vaccum spectrograph (one meter concave grating) an intense and persistent "line" at λ 600.3 $\pm$ 0.6, which has a diffuse character and shows under certain conditions an apparently continuous broadening toward longer wavelengths, extending to λ 618. As Lyman stresses, it almost coincides with the transition 1^1S-2^1S (λ calc. 601.44) of the helium spectrum (forbidden under ordinary conditions of excitation).

Dorgelo and Abbink[2] find in their helium photographs a similar, rather strong line at λ 600.03 and do not consider it improbable that it may be the neon-line $1p-4s_2$ (in the old notation), λ 600.03 which might be excited by impacts of the second kind with metastable 2^3S states of helium.

In Lyman's observations it is very remarkable that the relative intensity of this "line" compared with the lines of the helium series 1^1S-m^1P ($\lambda\lambda$ 584.40, 537.12, 522.21, etc.) does not change appreciably, if the "purity" of the helium in the discharge tube is increased. Besides, it appears on the plate in *uncondensed* discharges simultaneously with the intense line λ 537.12. These observations seem to indicate that the persistent radiation (λ 600 Å) must indeed be ascribed to helium, but not as the atomic line 1^1S-2^1S. The term scheme of helium gives no other possibility for the interpretation of this "line" as an atomic line.

It, therefore, suggests itself to inquire if one is not concerned here with radiation of the helium molecule or, better, if there may not exist a fundamental state in the He molecule spectrum corresponding to the fundamental state ^1S (= 198,298 cm.$^{-1}$) of the atom.

In fact, there is found a far-reaching analogy between the location of the electronic levels of the He-atom and the He-molecule. It is well known that Fowler[3] succeeded in arranging the electron levels of the He-band spectrum so as to obey a Rydberg formula. This analogy is illustrated by the following table, which contains a comparison of the observed effective quantum numbers of the electron levels in the He-molecule and the He-atom, respectively.[4]

We shall endeavor to compute the position of a band[5] 1^1S-2^1S and extrapolate for this purpose from the (effective) quantum number n^* = 1.853 of the 2^1S term in the molecule in analogy to the course of the corresponding quantum numbers (1.850, 0.744) in the atom to the value n^* = 0.744 for the 1^1S term in the molecule. This value for n^* is reason-

able because the difference of the n^* values for the S terms (same principal quantum number) in the molecule and atom, respectively, becomes smaller and smaller as one passes from the S terms of higher to those of lower principal quantum number (comp. Table 1). If we calculate with $n^* = 0.744$ the combination 1^1S-2^1S, we find from the term values ν 198,300 and ν 31,970 a value λ 601 Å; in other words just at the place in the spectrum where the intense diffuse "line" is observed.

TABLE 1

OBSERVED EFFECTIVE QUANTUM NUMBERS OF ELECTRONIC STATES IN HELIUM

TOTAL QU. NO.	TRIPLET-SYSTEM						SINGLET-SYSTEM				
	MOLECULE			ATOM			MOLECULE		ATOM		
	S	P	D	S	P	D	S	P	S	P	D
1							**0.744**		0.744		
2	1.788	(1.928)*		1.689	1.937		1.853	...	1.850	2.009	
3	2.810	2.928	3.013	2.697	2.933	2.997	...	2.964	2.857	3.011	2.998
4	3.818	3.928	...	3.700	3.932	3.997	...	3.965	3.858	4.011	3.998
5	...	4.928	...	4.701	4.932	4.997	...	4.996	Etc.		
6	...	5.927		Etc.				5.964			
		Etc.									

* Calculated.

This consideration led to a closer investigation of the structure of the "line" λ 600.3 ± 0.6. Luckily a large number of plates taken in helium were available, which Lyman had obtained in order to study on the one hand the principal series 1^1S-m^1P of atomic helium and, on the other hand, the problem of further advance into the extreme ultra-violet (below 200 Å). The plates were taken over a period of several years with five different concave gratings (0.5 and 1 m radius), under various conditions of excitation and with different samples of helium. These plates were subjected to careful scrutiny. It was found that the "line" λ 600.3 ± 0.6, as well as the series 1^1S-m^1P, appears with considerable intensity in *uncondensed discharges* rectified by means of kenotrons, and becomes weaker as one increases the discharge energy in the tube. In strong spark discharges (spark gap about 12 mm., capacity about 0.034 m.f.) all these lines vanish entirely excepting perhaps a trace of the resonance line 1^1S-2^1P, λ 584.40, while new lines appear. This supports our view that the "line" cannot be a transition between atomic levels 1^1S-2^1S caused by the presence of the electric field. Besides the observed wave-length differs from the computed one by at least 0.5 Å.

The diffuse character and the apparently continuous broadening of the "line" toward longer wave-lengths lead, hence, to the suggestion that this He-radiation at λ 600.3 ± 0.6 is in reality a band. In fact, on long-exposure plates (3–4 hours) *a band* shaded toward the red could indeed be discerned in the place of the diffuse line. The computation of the position of such a band as given above, as well as the conditions of excitation, make it probable that we are dealing here with a helium band which arises from a

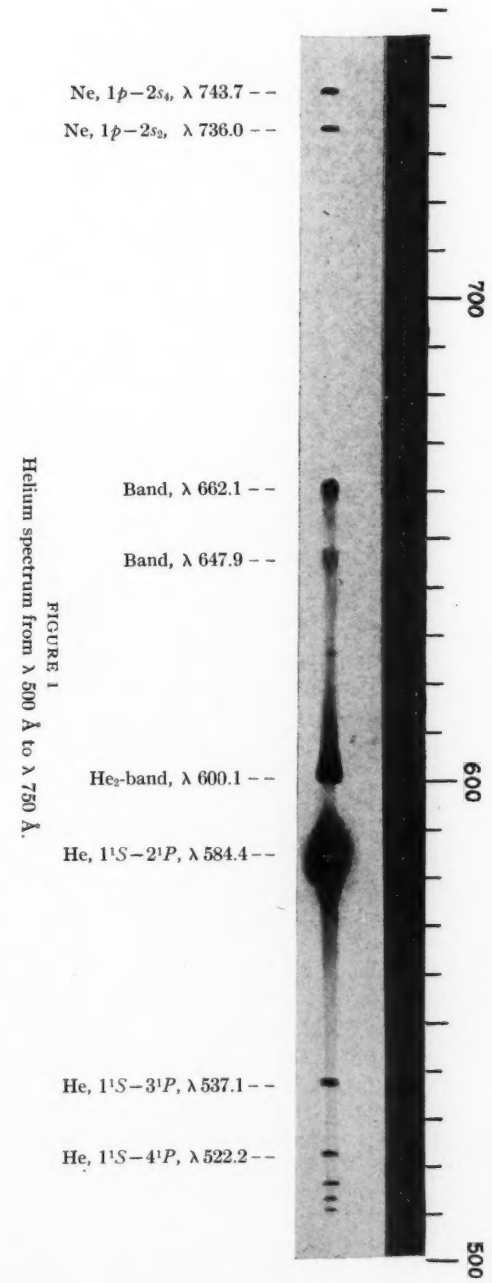

FIGURE 1
Helium spectrum from λ 500 Å to λ 750 Å.

low-lying term in the He-molecule spectrum corresponding to the fundamental term ^1S in the He-atom spectrum and having almost the same term value.

Figure 1 shows an enlargement of a long-exposure plate obtained with direct current in almost pure helium; the wave-length scale is also given, and a drawing of the spectrum without the general dark background. On the right can be seen the above-mentioned principal series of He, 1^1S-m^1P, with its strongly over-exposed first member at λ 584.44, which has suffered self-reversal. On the left at λ 600 the band shaded toward the red appears. The maximum of intensity lies at λ 600.13; the rotational structure is not resolved in the first or second order of a one-meter concave grating.

It is to be noted that besides the band at λ 600.13 two (possibly even four) weaker bands appear whose rotational structure is unresolved in the first order. One of these bands (shaded toward the violet) lies at λ 662.10, a less intense one (also shaded toward the violet) at λ 647.90. The continuous background appears somewhat strengthened at λ 638.5 and λ 653.6 on the original plates. Whether this is due to two additional bands (comp. figure) cannot be decided. Interpretation of these bands has been obtained.

In case our suggestion that a transition 1^1S-2^1S in the He-molecule accompanied by rotations is responsible for the band at λ 600 should be confirmed, then we must conclude that this electron jump takes place without oscillatory transition, since the corresponding bands are missing. In the visible He-bands, too, no oscillation quanta and only low rotational quanta have been observed, evidently on account of the small stability of the He-molecule. On the other hand, if the band 1^1S-2^1S exists, one should at least expect the band 1^1S-2^1P at λ 589 (calc.; comp. Table 1). It is not improbable that this band is present but cannot be identified on account of the great intensity of the line 1^1S-2^1P at λ 584.40.

As regards the explanation of Dorgelo and Abbink[2] for the radiation at λ 600, the figure shows at the left end the resonance lines of neon $1p-2s_4$ (λ 743.7) and $1p-2s_2$ (736.0), since the helium could not be freed from the last traces of neon. A comparison of intensities makes it immediately evident that the band at λ 600.13 cannot be regarded as a higher series member ($1p-4s_2$) of the neon series $1p-ms_2$, the fundamental member $1p-2s$ of which lies at λ 736.0.

I am indebted to Professor Lyman for his kind permission to scrutinize his photographic plates and to Dr. Mulliken for the suggestion, arising from a discussion, that a search for a low-lying term in the He-band spectrum might be desirable. I also wish to express my obligations to the International Education Board for furnishing the stipend which made this investigation possible.

[1] Th. Lyman, *Astrophys. J.*, **60**, No. 1, July, 1924.

[2] H. B. Dorgelo and T. H. Abbink, *Zeitschr. Physik*, **37**, 667, 1926.

[3] A. Fowler, *Proc. Roy. Soc.*, **A91**, 208, 1915; W. E. Curtis and R. G. Long, *Proc. Roy. Soc.*, **A108**, 513, 1925.

[4] R. S. Mulliken, *Proc. Nat. Acad. Sci.*, **12**, No. 3, 158, March, 1926.

[5] The electron jumps in the CuH-spectrum show, for instance, that in a molecule transitions $^1S-{}^1S$ are possible under ordinary conditions. Although such transitions are unknown in the visible He_2 spectrum, it cannot be concluded that the transition 1^1S-2^1S is also absent. For it may be (comp. R. S. Mulliken, *Phys. Rev.*, **28**, No. 6, Dec., 1926, p. 1208, etc.) that in the lowest state 1^1S the levels $j = 1/2, 2^1/2, 4^1/2$, etc., are not missing, but are present with partial, or even full "weight," and that in the state 2^1S they also appear with small "weight."

WHITE-LIGHT INTERFERENCE FRINGES WITH A THICK GLASS PLATE IN ONE PATH. PART II

BY W. N. BIRCHBY

NORMAN BRIDGE LABORATORY OF PHYSICS, CALIFORNIA INSTITUTE OF TECHNOLOGY

Communicated March 7, 1927

In Part I of this paper[1] the writer developed a theory of the white-light fringes observed in the Michelson interferometer when a thick plate of glass, or other refractive substance, is placed in one of the paths. Part I treated of the axial beam, whose composition determines the color of the central spot in the fringe pattern. An explanation was given of the very great number of colored fringes, running up to several thousand, which is observed under these conditions. In this part we discuss certain phenomena which depend for their explanation upon the analysis of a beam oblique to the optical axis. To observe these phenomena we obtain, as described in Part I, circular fringes in sodium light, insert the thick plate in one of the paths, shorten that path until in the neighborhood of the most brilliant sodium maximum, in which position colored fringes will be seen with white light. If we observe these fringes through a spectroscope with the slit placed across the center of the system, the slit being long enough to cut across the whole field, the spectrum is seen to be crossed by a system of concentric dark rings, looking very much like a shadow of the fringe system itself. If now one of the paths is slowly shortened or lengthened, these dark rings expand or contract, as the case may be, just as in the fringe system. In addition, the center of the system on the spectrum travels very slowly from one end of the spectrum to the other. These phenomena may be observed easily and distinctly if a rather wide slit, cut in a card, is placed in the path of the light before it enters the interferometer, and the fringes are then viewed through a direct-vision spectroscope, without slit.

Derivation of the Fundamental Equation.—We shall proceed to derive an expression for the phase-difference on re-uniting of the two beams into which an oblique beam is split by the interferometer, in terms of the wave-length, the angle made with the optical axis and other factors. The source is supposed to give a set of beams of plane wave-front coming from all directions. The course of one of these beams, inclined at an angle i to the optical axis, the angle lying in the base plane of the instrument, is drawn in figure 4. Although the derivation is limited to beams whose angles of inclination lie in the base-plane the result would be the same, on account of the symmetry about the optical axis, if the angle lay in any other plane. In the diagram M_1 and M_2 are the interferometer mirrors, OQ is the half-silvered surface. The thick plate is placed in contact with M_2 for convenience in making the derivation, though this is, of course, not essential. P_2 gives the direction of the optical axis before reflection from the half-silvered surface, P_1 the direction after reflection. The compensating plate and the half-silvered plate itself, excepting the surface OQ, are omitted, as the portions of the paths through them cancel out in every case, and have no influence on the result. Only two rays of the beam are drawn, a pair that will meet at the same point on the half-silvered surface on leaving the instrument. It should be kept in mind that the beam drawn in the diagram forms only one point of the fringe pattern, the whole pattern being formed by beams coming from an infinite number of directions. The part of the path marked GHJ is in the thick plate, and the angle between the optical axis and the beam in this part of the path is r. P_1 and P_2 are the distances from B, on the half-silvered surface, to M_1 and M_2, respectively. As the difference only, P_1-P_2, appears in the result, it does not matter what point on the half-silvered surface is used in defining them. The thickness and the index of refraction of the plate are denoted by t and μ, respectively. The wave-length of the light in air is λ, and the difference of phase of the two parts of the beam on re-uniting is ϕ.

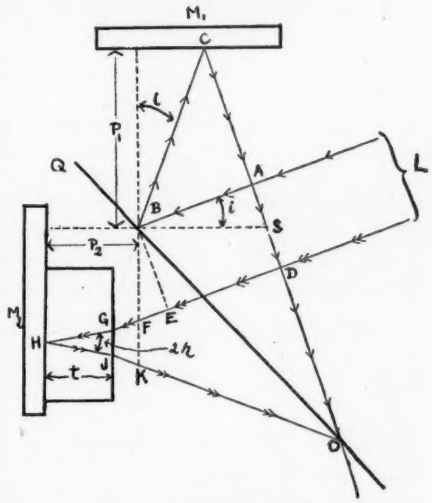

FIGURE 4

We wish to form an expression for $\phi/(2\pi)$, the difference of the numbers

of light waves in the two paths. The paths may be considered to start from any two simultaneous points on the wave-front, such as A and D in the diagram. Then the paths of the two rays are $ABCSO$ and $DEFGHJKO$, respectively. In forming the difference, SO cancels KO, and AB cancels DE, leaving $2BC$ for one path, and $EF + 2FG + 2GH$ for the other. $BC = P_1 \sec i$; $FG = (P_2 - t) \sec i$; $GH = t \sec r$. To find the number of light waves in each part, divide the length of path by λ, multiplying the length of the path through glass by μ before doing so. In this way we get

$$\phi/(2\pi) = \frac{1}{\lambda}(2BC - 2FG - 2\mu GH - EF)$$

or

$$\phi/(2\pi) = \frac{1}{\lambda}[2P_1 \sec i - 2(P_2 - t) \sec i - 2\mu t \sec r - EF].$$

To find EF, we have $BK = BS = 2P_1 \tan i$; $FK = 2t \tan r + 2(P_2 - t) \tan i$. Therefore, $BF = 2(P_1 - P_2) \tan i + 2t(\tan i - \tan r)$ and $EF = BF \sin i = 2(P_1 - P_2) \sin^2 i \sec i + 2t(\sin^2 i \sec i - \tan r \sin i)$ since $\sin i = \mu \sin r$, this becomes

$$EF = 2(P_1 - P_2) \sin^2 i \sec i + 2t \sin^2 i \sec i - 2\mu t \sin^2 r \sec r.$$

Hence

$$\frac{\phi\lambda}{(4\pi)} = (P_1 - P_2) \sec i(1 - \sin^2 i) + t \sec i(1 - \sin^2 i) - \mu t \sec r(1 - \sin^2 r).$$

Finally, putting $P_1 - P_2 = D$, we get the desired expression:

$$\frac{\phi\lambda}{(4\pi)} = (D + t) \cos i - \mu t \cos r \quad \ldots\ldots\ldots\ldots\ldots\ldots\ldots\ldots \quad (12)$$

Discussion of the Equation.—Equation (12) can be used to explain the spectrum rings in the following way: On the two-dimensional field into which the image of the slit is drawn out by the spectroscope, the direction down the length of the spectrum represents λ, the direction across the width of the spectrum gives i, with $i = 0$ down the middle line of the width. On account of the small range of i which is used, not more than from $-3°$ to $+ 3°$, $\sin i$, $\tan i$ and i itself in radian measure, may be considered interchangeable in drawing a diagram. If we think of i and λ as the coördinates, and plot the curvé represented by equation (12), holding the other quantities constant, we shall have a curve at every point of which the phase-difference has the same value, or in other words, one of the

spectrum rings. Repeating the process, changing ϕ by multiples of 2π we can draw the whole system.

Wave-Length and Phase-Difference at the Center of the Spectrum Rings.—If we put $i = 0$, and consequently $r = 0$, in (12) we shall be restricted to the line of zero inclination, down the middle of the spectrum diagram. Assigning a value to ϕ, and solving the resulting equation for λ, we shall find the points at which a particular spectrum ring crosses the middle line. This work cannot be carried out without assuming some form for the relation between μ and λ. If we use Cauchy's formula, $\mu = A + B/\lambda^2$, in (12), after putting $i = 0$, we get the following cubic in λ:

$$\left(\frac{\phi}{(2\pi)}\right)\lambda^3 - 2(D + t - At)\lambda^2 + 2Bt = 0. \quad \ldots\ldots\ldots\ldots\ldots\ldots \quad (13)$$

It can be shown that this equation has either two or no real positive roots. It always has one negative root, with which we are not concerned. If there are two positive roots we have a real ring crossing the zero axis at the two points indicated. If the two roots coincide, we have the value of λ for the central spot of the spectrum ring system. The condition for equal roots, obtained by putting the minimum value of the left-hand side of (13) equal to zero, is

$$\frac{\phi_c}{(2\pi)} = \frac{4}{3}\sqrt{\frac{(D + t - At)^3}{3Bt}} \quad \ldots\ldots\ldots\ldots\ldots\ldots\ldots\ldots \quad (14)$$

This equation gives the phase-difference at the central spot, and shows that it increases with D. Placing this value of ϕ in (13), and solving for λ, we obtain

$$\lambda_c = \sqrt{\frac{3Bt}{D + t - At}}, \quad \ldots\ldots\ldots\ldots\ldots\ldots\ldots\ldots\ldots \quad (15)$$

the wave-length of the central spot. As this expression decreases when D is increased, it gives the explanation of the observed fact that the center of the system of rings moves down the spectrum as the position of the moveable mirror is changed. If we place in this equation in succession the values of λ at the extremes of the visible spectrum, λ_1 and λ_2, and the corresponding values, D_1 and D_2, of the path-difference, and subtract after solving each equation for D, we get

$$D_2 - D_1 = 3Bt\left(\frac{1}{\lambda_2^2} - \frac{1}{\lambda_1^2}\right) \quad \ldots\ldots\ldots\ldots\ldots\ldots\ldots\ldots \quad (16)$$

which is the same as equation (10) of the previous paper, thus showing that the range of D for white-light fringes is the same as the range during which the central spot is traveling through the spectrum. The phase-difference at the central spot is evidently the greatest or least phase-difference for all the spectrum-rings. That it is the greatest follows from figure 2 of the previous paper. Since ϕ decreases as we go outward from the center, and ϕ_c increases with D, it follows that the rings expand as the center moves toward the blue end, and *vice versa*. These conclusions agree with the observed facts.

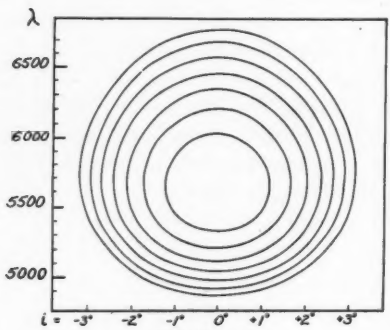

FIGURE 5

To find the wave-lengths at which the successive rings cross the line of zero inclination, down the spectrum, we use (13), putting $\frac{\phi}{(2\pi)} = \frac{\phi_c}{(2\pi)} - n$, and using the value for $\frac{\phi_c}{(2\pi)}$ given by (14). This gives

$$\left(\frac{4}{3}\sqrt{\frac{(D+t-At)^3}{3Bt}} - n\right)\lambda^3 - 2(D+t-At)\lambda^2 + 2Bt = 0 \ldots\ldots \quad (17)$$

With $n = 0$, this equation has a double root whose value is given by (15). Putting $n = 1, 2, 3 \ldots$ in succession, and solving for the two positive roots, we get the wave-lengths at which the successive rings cross the spectrum.

Simplified Form of Equation (12)² for Small Values of i.—In order to graph the spectrum fringes we shall make some approximations in equation (12) which are justifiable for small values of i. It is permissible to take $\cos i = \sqrt{1 - \sin^2 i}$ as approximately $1 - \frac{i^2}{2}$, and $\cos r = \sqrt{1 - \frac{\sin^2 i}{\mu^2}}$ as $1 - \frac{i^2}{(2\mu^2)}$. Making these substitutions in (12) and collecting the coefficient of i^2 gives

$$\frac{\phi\lambda}{(4\pi)} = (D + t - \mu t) - \frac{i^2}{2}\left(D + t - \frac{t}{\mu}\right).$$

Placing $\mu = A + B/\lambda^2$ gives

$$\frac{\phi\lambda}{(4\pi)} = \left(D + t - At - \frac{Bt}{\lambda^2}\right) - \frac{i^2}{2}\left(D + t - \frac{t\lambda^2}{(A\lambda^2 + B)}\right).$$

Since B is only about 2% of the denominator in the last term, we may neglect it, giving

$$\frac{\phi\lambda}{(2\pi)} = 2(D + t - At) - i^2\left(D + t - \frac{t}{A}\right) - \frac{2Bt}{\lambda^2} \quad \ldots\ldots\ldots \quad (18)$$

or

$$\left(D + t - \frac{t}{A}\right)i^2 = 2(D + t - At) - \left(\frac{\phi}{(2\pi)}\right)\lambda - \frac{2Bt}{\lambda^2} \quad \ldots\ldots \quad (19)$$

From this equation, by assigning the proper value to $\frac{\phi}{(2\pi)}$, any spectrum ring may be graphed. When $i = 0$, (18) reduces to (13).

Numerical Illustration.—By assuming a set of values of the various constants, a graph of the spectrum rings, figure 5, was made. The following values were taken: $D = 1.65$; $t = 3$; $\mu = A + B/\lambda^2$; $A = 1.5$; $B = 53 \times 10^{-10}$. With these values (14) gives $\frac{\phi_c}{(2\pi)} = 354.66$; (15) gives $\lambda_c = 0.0005639$. Equation (17) becomes

$$(354.66 - n)\lambda^3 - 0.30\lambda^2 + 318 \times 10^{-10} = 0.$$

From this equation the following table of the points where the first 13 rings cross the zero line was made:

n	1	2	3	4	5	6	7	8	9	10	11	12	13
$\lambda_1 \times 10^7$	5406	5316	5249	5195	5147	5106	5068	5033	5002	4972	4944	4918	4893
$\lambda_2 \times 10^7$	5897	6012	6104	6183	6256	6323	6386	6447	6505	6560	6615	6667	6719

Equation (19) becomes

$$i^2 = 0.11321 - 0.37736\left(\frac{\phi}{(2\pi)}\right)\lambda - 120.00 \times 10^{-10}\left(\frac{1}{\lambda^2}\right).$$

Assigning to $\phi/(2\pi)$ the values 353.66, 352.66, etc., in succession, the successive rings were graphed. For the sake of clearness, the even-numbered rings only are drawn in the diagram.

The writer again takes great pleasure in acknowledging the helpful and constructive interest of Dr. Paul S. Epstein during the preparation of this paper.

[1] *Proc. Nat. Acad. Sci.*, **10**, No. 11, pp. 452–457, November, 1924.

[2] This modification of equation (12) is due to Dr. Epstein.

MOLECULAR SPACE ARRAY IN LIQUID PRIMARY NORMAL ALCOHOLS: THE CYBOTACTIC STATE

By G. W. Stewart and Roger M. Morrow

Physical Laboratory, University of Iowa

Communicated March 15, 1927

For more than a decade[1] the X-ray circular diffraction halo in liquids has been known. Doubtless numerous times the suggestion has been made[2] that there is in the liquid a spacial arrangement of molecules, probably as fragmentary crystals. But definite evidence of such a structure has been lacking. The authors, with the assistance of Mr. Wm. D. Crozier, have investigated by means of $M_0K\alpha$ X-radiation the liquid primary normal alcohols from ethyl to lauryl and have obtained the following:

1. There are two significant distances determined by diffraction intensity peaks.

2. One of these distances remains fairly constant varying from 4.6 Å with lauryl, $C_{11}H_{23}(OH)$, to 4.4 Å with butyl, $C_4H_9(OH)$, and then decreasing more rapidly to methyl, $CH_3(OH)$, 3.8 Å.

3. The other distance varies linearly with the content of CH_2 in the molecule, the variation for each such addition being approximately 1.54 Å. The distance for lauryl is about 22 Å.

4. The evidence leads to the conclusion that the latter distance is occasioned by the length of the chain molecule and the former by the distance of separation of molecules perpendicular to the chain.

5. From computation of density and from the polarity of the compound, one finds that two OH polar groups appear to unite, making a chain two molecules in length, and that the planes containing these groups are not perpendicular to the chains.

6. The addition of each CH_2 lengthens the molecule by approximately 1.3 Å, which is the same order as crystalline C distances, and is in agreement with the similar experiments of Müller and Saville[3] and earlier observers on solid long chain hydrocarbons. The above interpretation of separation of chains and relative positions of heads, is in agreement (within the error of our experiment) with the calculations of Adam,[4] who found the area of cross-section occupied by each saturated fatty acid chain on the surface of water was 21.0×10^{-16} cm.^{2}, and this is equal to $(4.58 \times 10^{-8})^2$ cm.^{2}

In the experiments the peak width was over 3° whereas the width for the same radiation diffracted from a crystal was about 0.4°.

The experiments indicate clearly a definite space array. Comparisons of peaks in liquid and solid state at approximately the same temperatures show that the computed spacings are not the same. The space array in

the liquid is not crystalline, but is one in which molecular mobility is permitted and the resulting peaks represent the most probable spacings. A name is proposed for this non-crystalline, space-array state. The noun is *cybotaxis* and the adjective *cybotactic*.

This conception of the liquid state gives a description of a "solution" and contributes to various theories in connection with liquids. The experiments and discussion will soon be published in full.

[1] Debye and Scherrer, *Nachr. Gesell. Göttingen* (1916), p. 6.
[2] Vide Hewlett, *Phys. Rev.*, **20** (1922), p. 688 and others.
[3] Müller and Saville, *Journal Chem. Soc.*, **127** (1925), p. 599.
[4] Adam, *Proc. of Roy. Soc.* (1921), (1922), (1923).

---

*PINHOLE PROBE MEASUREMENTS WITH MASSIVE CYLINDRICAL AIR COLUMNS**

BY CARL BARUS

DEPARTMENT OF PHYSICS, BROWN UNIVERSITY

Communicated March 8, 1927

1. *Introductory.*—After completing the work with the broad horn of my last paper,[1] similar experiments were made with a long slender horn (40 cm. long) and with cylindrical tubes (28 cm. long, 2.8 cm. diam.). The results in the former case are too complicated to be given here. In the latter (tube), the nodal pressure-capacity (s, C) graphs of the transformer (electric oscillation) consisted of a group of nearly straight and parallel lines, running close together, so long as the pinhole lay below the middle (d = 14 cm.) of the tube. After this (d = 15 cm. to 0) the slopes decreased rapidly. There were no marked crests, but rather noise increasing continuously with the capacity, C, or falling pitch. The break circuit (electric siren) graphs, however, showed the usual cuspidal crests (here at a', e'', a'') with long intervals of relative silence between. As far as the middle of the pipe, the crests were about of the same nodal intensity, s. Hence these data accentuate the results already described for the horn. In the s-d graphs, the a' and a'' crests lay at about d = 7 cm. and near the bottom, while the e'' crest was marked near the middle d = 15 cm. of the pipe. From this it appears both the a' and a'' of the motor break (siren) evoke the first overtone a'' of the d' closed organ pipe; whereas in the case of the e'', the pipe with a telephone plate at one end vibrates as an open organ pipe with a node near the middle.

2. *Extensible Pipe.*—Since there are three vibrating systems in the transformer method, two of them should be made adjustable if the third is given, to obtain the largest acoustic pressure values (s). An extension

was, therefore, added to the pipe (insert, figure 1) so that its length could be increased continuously, from $d = 28$ to 35 cm. By setting this for the maximum s at any capacity, C, the remainder of the curve was then worked out. A remarkable result presented itself, with an important bearing on the pinhole probe, inasmuch as the graphs now consisted of right line elements, between breaks.

In figure 1 the largest s was first found for the pipe depth near $d = 30$ cm. by tuning (the probe being at the bottom of the tube as usual). The graph obtained for varying C (0 to 1.1 m.f.) starts with a linear sweep as far as $C = 0.3$ m.f. (a'), then bends abruptly to a second linear sweep

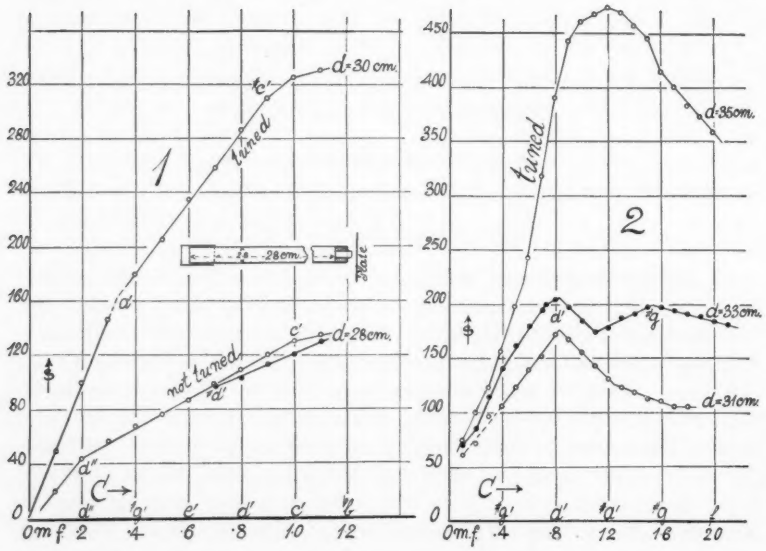

as far as $C = 0.9$ m.f., after which the course is curved to the crest beyond the figure. It would seem that each of these lines corresponds to a given kind of vibration; i.e., to a given overtone which breaks abruptly into the next available.

The behavior of the untuned pipe ($d = 28$ cm.) for the given spring tension is shown in the lower curve. There is a break at $C = 0.2$ (d'') and at $C = 1.0$ (c') m.f. In the repetition (black dots) the break at $C = 0.7$ (# d') is probably an accidental small change in the tension of the electrical spring break. Between these points the graph is strikingly linear.

After the tube was further elongated to the pipe depth, $d = 35$ cm., now adequately in resonance with the spring break, a second and much

stronger maximum, figure 2, appeared. The rectilinear progress between $C = 0.1$ to 0.3, 0.4 to 0.5, 0.6 to 0.8, 1.0 to 1.2, 1.3 to 1.5, 1.6 to 2.0 m.f., is marked throughout. Even near the crest $C = 1.2$ the tendency is still observable. This relatively enormous crest ($s = 475$) is in keeping with the near resonance of break, pipe and electric oscillation.

It seemed worthwhile to test the case further with untuned lengths between $d = 28$ cm. and $d = 34$ cm., and throughout large C ranges (0 to 2 m.f.). Examples of the graphs are given in figure 2 for an altered transformer spring tension. Broken rectilinear paths are the rule particularly for $d = 31, 33$, where the roof-like crests are striking.

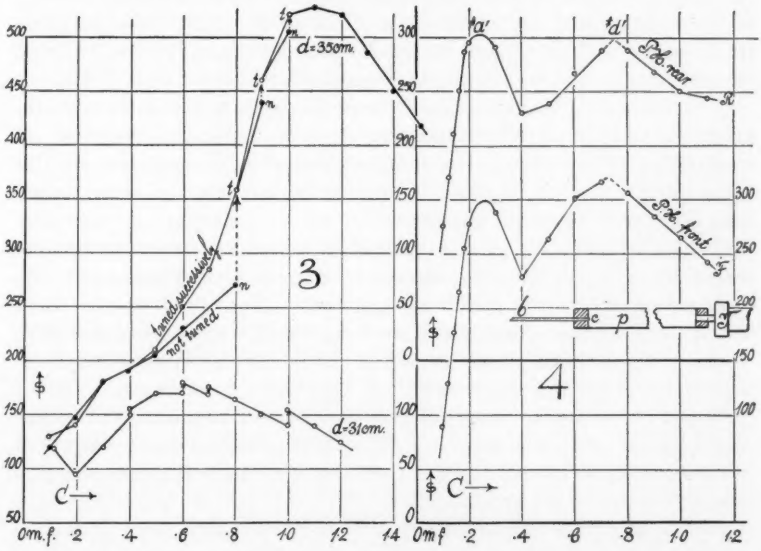

Finally in figure 3 for the optimum $d = 35$, the successively tuned pipe (open circles) is compared with the untuned pipe (black circles). Below $C = 0.5$ the divergence is not large, both starting under tuned conditions. Thereafter the divergence rapidly increases, the tuned pipe naturally being in excess. From $C = 0.8$ on, passage of the untuned (n) condition to the tuned condition (t) is indicated by arrows. To get the maximum s-values it is thus necessary to re-tune the pipe at all pitches. The successive tuning (resonance throughout) has raised the crest to nearly $s = 550$, an acoustic pressure of over 0.4 mm. of Hg.

The same figure shows the corresponding behavior at the smaller maximum at $d = 31$. Linear progress is interrupted by the tuning indicated by the arrows.

3. *Closed Organ Pipe.*—The open-mouthed organ pipe is very noisy, so that in this respect the doubly closed organ pipe shown in the insert, figure 4, is preferable. Here p is the pipe 27 cm. long in the clear, T the attached activating telephone and bc the pinhole probe. The point c may either be thrust to the rear, near the telephone, or (as in figure) the pinhole c may be near the front of the tube. This should make no difference in the acoustic pressure, s, other things being equal. The telephone, T, was activated by the transformer method, as the specific results of this method are particularly in question.

The graphs R and F (the former raised for clearness), for the same tense spring break adjustment left unchanged, but with the pinhole, respectively, in the rear (bottom) and in the front of the doubly closed tube, are practically identical. They again consist of linear parts (as above) with abrupt breaks. Each exhibits two crests, respectively, above a' and $\#\ d'$.

4. *Alternating Current.*—The attempt to energize the primary of the induction coil by an alternating current proved unsatisfactory for the reason that while the induction is relatively feeble as compared with the break circuit methods used heretofore, the heating effect of these continuous currents is out of all proportion.

5. *Remarks.*—In my work heretofore, I have associated the fringe displacement, s, i.e., the nodal intensity or acoustic pressure with the usual energy (E per unit of volume) equation. If n is the frequency and a the amplitude of the sound wave, we may, therefore, write $E = p + \rho v^2/2 = Ks + (\rho/2)(2\pi an)^2$. At the mouth of the tube s is zero and a the maximum; at the bottom or node a is zero and s a maximum. The expectation that a similar equation could also be used to interpret the fringe displacement at a given point for different frequencies is not warranted. For if we put $4\pi^2n^2 = 1/LC, p = Ks$ and assume E to be constant along the linear elements of the graphs, the result is $-(s-s') = (\rho/2KL)(A^2/C - A'^2/C')$ whereas the graphs suggest $\Delta s \propto \Delta C$ simply, along each element.

The view that the oscillation frequency (n) of the organ pipe is impressed on the oscillation frequency (n') of the secondary actuating the telephone plate is also unsatisfactory. For if Y is the amplitude of the electric circuit under a harmonic electromotive force $E \cos \omega t$

$$Y = E/\sqrt{(\omega'^2-\omega^2)^2 + K^2\omega^2}$$

where $\omega = 2\omega n$ and $\omega' = 2\pi n'$ are the angular frequencies of the free and frictionless acoustic and electrical circuits, respectively, and K is the coefficient of friction. This may as usual be reduced to proportionalities in the form $y = 1/\sqrt{(1-x^2)^2 + \alpha^2x^2}$ where $x = \omega/\omega'$, $\alpha = K/\omega'$, $y = Y/(E/\omega'^2)$. This y has a crest for $x^2 = 1-\alpha^2/2$.

If $\omega' = 1/LC$ and K is relatively very small, the equation reduces to

$$Y = \frac{ELC}{1-\omega^2LC}\left(1-\left(\frac{K\omega LC}{1-\omega^2LC}\right)^2/2\right)$$

approximately, where ω, K, L are constant and C variable. Hence, even if we neglect the term in K and associate Y with the fringe displacement, s, an equation in this form is not serviceable in identifying $\Delta s \propto \Delta C$ along linear elements, unless ω^2LC is small compared with 1. This would not be the case with the fundamental or any harmonics of the cylindrical pipe. Even if ω refers to the frequency of the spring break taken at pitch a, the equation remains inapplicable.

This suggests a simpler approach through the capacity equation $Q = CV$ whence $\Delta s \propto \Delta i = (dV/dt)\,\Delta C$; or the slopes of the linear elements of the graphs are to be associated with the effective time rate at which the potential of the condenser changes. The value of dV/dt depends on the form of residual wave on which the new impulse is superimposed. Moreover a reason for the broken linear relations of s and C is now apparent; for the fringe displacement s measures the difference of level of the surfaces of mercury in the U-gage. It, therefore, also measures the potential energy localized in the stationary wave at the point of the pinhole probe, though it does this with a coefficient which may be either positive or negative. The stream lines run from the outside to the inside of the pinhole embouchure.

* Advance note from a Report to the Carnegie Inst. of Washington, D. C.

[1] These PROCEEDINGS, **13**, pp. 52–56, 1927.

ATOMIC LATTICES AND ATOMIC DIMENSIONS

BY JARED KIRTLAND MORSE[1]

DEPARTMENT OF PHYSICS, UNIVERSITY OF CHICAGO

Communicated March 4, 1927

By means of the concept of a spherical atom W. L. Bragg[2] and W. P. Davey[3] have independently computed the radii of atomic spheres of influence from the distances of closest approach obtained from X-ray measurements on crystals. In this paper these spherical atoms are specialized and the cubic atom proposed by Lewis and developed by Langmuir is extended to simple polyhedrons inscribable in spheres. It is shown in detail how these simple models can be built up into various types of observed cubic and hexagonal lattices and how the lattice constants are geometrically related to the atomic radii. From these relations *possible atomic radii* are computed and tabulated.

Using cubic models piled together in such a manner that the edges of adjacent cubes are common, a face-centered cubic lattice can be constructed in the following manner. The coördinates of the cube centers and corners are expressed as fractions of the lattice constant a_0 as is customary in space group theory.

FACE-CENTERED CUBIC LATTICE—TYPE I

Cube Centers:	0;	0;	0;	1/2,	0,	1/2;	0,	1/2,	1/2;	1/2,	1/2,	0;
Cube Corners:	1/4,	1/4,	1/4;	1/4,	3/4,	3/4;	3/4,	1/4,	1/4;	3/4,	3/4,	1/4;
	1/4,	1/4,	3/4;	1/4,	3/4,	3/4;	3/4,	1/4,	3/4;	3/4,	3/4,	3/4;

If R is the radius of a sphere circumscribed about any one of these cubes the relation between R and the lattice constant is

$$R = \frac{a_0\sqrt{3}}{4}. \qquad (1)$$

If the cubes are piled so that adjacent corners are common, we can form a second type of face-centered cubic lattice thus:

FACE-CENTERED CUBIC LATTICE—TYPE II

Cube Centers:	0,	0,	0;	1/2,	0,	1/2;	0,	1/2,	1/2;	1/2,	1/2,	0;
Cube Corners:	1/4,	0,	1/4;	3/4,	0,	3/4;	1/4,	0,	3/4;	3/4,	0,	3/4;
	0,	1/4,	1/4;	1/2,	1/4,	1/4;	0,	1/4,	3/4;	1/2,	1/4,	3/4;
	1/4,	1/2,	1/4;	3/4,	1/2,	1/4;	1/4,	1/2,	3/4;	3/4,	1/2,	3/4;
	0,	3/4,	1/4;	1/2,	3/4,	1/4;	0,	3/4,	3/4;	1/2,	3/4,	3/4;

$$R = \frac{a_0\sqrt{2}}{4}. \qquad (2)$$

DIAMOND TYPE CUBIC LATTICE

Cube Centers:	0,	0,	0;	1/2,	1/2,	0;	1/2,	0,	1/2;	0,	1/2,	1/2;
	1/4,	1/4,	1/4;	1/4,	3/4,	3/4;	3/4,	1/4,	3/4;	3/4,	3/4,	1/4;
Cube Corners:	1/8,	1/8,	1/8;	1/8,	1/8,	3/8;	1/8,	1/8,	7/8;	1/8,	3/8,	1/8;
	1/8,	3/8,	3/8;	1/8,	3/8,	5/8;	1/8,	5/8,	3/8;	1/8,	5/8,	5/8;
	1/8,	5/8,	7/8;	1/8,	7/8,	1/8;	1/8,	7/8,	5/8;	1/8,	7/8,	7/8;
	3/8,	1/8,	1/8;	3/8,	1/8,	3/8;	3/8,	1/8,	5/8;	3/8,	3/8,	1/8;
	3/8,	3/8,	3/8;	3/8,	3/8,	7/8;	3/8,	5/8,	1/8;	3/8,	5/8,	5/8;
	3/8,	5/8,	7/8;	3/8,	7/8,	3/8;	3/8,	7/8,	5/8;	3/8,	7/8,	7/8;
	5/8,	1/8,	3/8;	5/8,	1/8,	5/8;	5/8,	1/8,	7/8;	5/8,	3/8,	1/8;
	5/8,	3/8,	5/8;	5/8,	3/8,	7/8;	5/8,	5/8,	1/8;	5/8,	5/8,	3/8;
	5/8,	5/8,	7/8;	5/8,	7/8,	1/8;	5/8,	7/8,	3/8;	5/8,	7/8,	5/8;
	7/8,	1/8,	1/8;	7/8,	1/8,	5/8;	7/8,	1/8,	7/8;	7/8,	3/8,	3/8;
	7/8,	3/8,	5/8;	7/8,	3/8,	7/8;	7/8,	5/8,	1/8;	7/8,	5/8,	3/8;
	7/8,	5/8,	5/8;	7/8,	7/8,	1/8;	7/8,	7/8,	5/8;	7/8,	7/8,	7/8;

$$R = \frac{a_0\sqrt{3}}{8}. \qquad (3)$$

GRAPHITE TYPE HEXAGONAL LATTICE

This lattice can be built up of cubes and for purposes of convenience is considered as a special type of orthorhombic lattice in which $a_0 = b_0\sqrt{3}$ instead of referring it to the hexagonal axes in general use.

Cube Centers:

0, 0, 0; 1/3, 0, 0; 1/2, 1/2, 0; 5/6, 1/2, 0;
1/6, 1/2, 1/2; 0, 0, 1/2; 1/2, 1/2, 1/2; 2/3, 0, 1/2;

Cube Corners:

0, 0, 1/9; 0, 0, 8/9; 0, 0, 7/18; 0, 0, 11/18;
0, 1/2, 1/27; 0, 1/2, 29/54; 1/12, 1/4, 1/27; 1/12, 1/4, 25/54;
1/12, 3/4, 1/27; 1/12, 3/4, 25/54; 1/6, 0, 29/54; 1/6, 0, 26/27;
1/6, 1/2, 7/18; 1/6, 1/2, 11/18; 1/4, 1/4, 1/27; 1/4, 1/4, 29/54;
1/4, 3/4, 1/27; 1/4, 3/4, 29/54; 1/3, 0, 1/9; 1/3, 0, 8/9;
1/3, 1/2, 1/27; 1/3, 1/2, 25/54; 5/12, 1/4, 29/54; 5/12, 1/4, 26/27;
5/12, 3/4, 29/54; 5/12, 3/4, 26/27; 1/2, 0, 1/27; 1/2, 0, 29/54;
7/12, 1/4, 1/27; 7/12, 1/4, 25/54; 7/12, 3/4, 1/27; 7/12, 3/4, 25/54;
2/3, 0, 7/18; 2/3, 0, 11/18; 2/3, 1/2, 29/54; 2/3, 1/2, 26/27;
3/4, 1/4, 1/27; 3/4, 1/4, 29/54; 3/4, 3/4, 1/27; 3/4, 3/4, 29/54;
11/12, 1/4, 29/54; 11/12, 1/4, 26/27; 11/12, 3/4, 29/54; 11/12, 3/4, 26/27;
1/2, 1/2, 1/9; 1/2, 1/2, 8/9; 1/2, 1/2, 7/18; 1/2, 1/2, 11/18;
5/6, 0, 1/27; 5/6, 0, 25/54; 5/6, 1/2, 1/9; 5/6, 1/2, 8/9;

$$R = \frac{a_0}{4\sqrt{2}}; \qquad R = \frac{b_0\sqrt{3}}{4\sqrt{2}}; \qquad R = \frac{c_0}{9}. \tag{4}$$

The axial ratios are $a:c = b_0:c_0 = 1:2.76$.

CLOSE PACKED HEXAGONAL LATTICE

This lattice can be built up of cubes and the following coördinates are also referred to orthorhombic axes for convenience.

Cube Centers: 0, 0, 0; 1/2, 1/2, 0; 1/6, 1/2, 1/2; 2/3, 0, 1/2;

Cube Corners: 0, 0, 3/8; 1/6, 1/2, 1/8; 1/3, 0, 1/8; 1/2, 1/2, 3/8;
5/6, 1/2, 1/8; 2/3, 0, 1/8; 0, 0, 5/8; 1/6, 1/2, 7/8;
1/3, 0, 5/8; 1/2, 1/2, 5/8; 5/6, 1/2, 5/8; 2/3, 0, 7/8;

$$R = \frac{b_0\sqrt{3}}{2\sqrt{2}}; \qquad R = \frac{a_0}{2\sqrt{2}}; \qquad R = \frac{3c_0}{8}. \tag{5}$$

The axial ratios are $a:c = b_0:c_0 = 1:1.633$.

THE BODY-CENTERED CUBIC LATTICE—TYPE I

This lattice can also be built of cubes.

Cube Centers: 0, 0, 0; 1/2, 1/2, 1/2;

Cube Corners: 1/4, 1/4, 1/4; 1/4, 3/4, 1/4; 3/4, 1/4, 1/4; 3/4, 3/4, 1/4;
1/4, 1/4, 3/4; 1/4, 3/4, 3/4; 3/4, 1/4, 3/4; 3/4, 3/4, 3/4;

$$R = \frac{a_0\sqrt{3}}{4} \tag{6}$$

THE BODY-CENTERED CUBIC LATTICE—TYPE II

Another type of body-centered cubic lattice can be formed from rectangular parallelopipeds derived from cubes and circumscribable in spheres.

Centers: 0, 0, 0; 1/2, 1/2, 1/2;
Corners: 0, 1/2, 1/4; 1/2, 0, 1/4; 1/2, 0, 3/4; 0, 1/2, 3/4;

$$R = \frac{a_0\sqrt{5}}{4}. \qquad (7)$$

If the center positions are identified with atomic centers and the corners are considered as possible electron positions the radius R of the circumscribed sphere becomes the radius of the atom and can be defined as the maximum distance between the nucleus and the electron or electrons on the periphery of the atom. Then equations (1)–(7), inclusive, can be used to compute possible atomic radii for such atoms as unite with each other to form lattices by the sharing of electrons. It is considered that the lattices of the elements with the possible exception of argon are formed in this way. It is also possible that these lattices may in some cases be formed by the packing together of spherical atoms in which case the radius of these spheres can be found by halving the distance of closest approach as was pointed out by W. L. Bragg[2] and Wheeler P. Davey.[3,4] The following tables show the values of the atomic radii computed by equations (1)–(7) from the lattice constants together with the radii for spheres. The values of the lattice constants are taken from the International Critical Tables, 1926. For graphite the lattice used is taken from Bernal's[5] investigations.

FACE-CENTERED CUBIC

AT. NO.	ELEMENT	$a_0 \times 10^8$ CM.	$R = a_0\sqrt{3/4}$	$R = a_0\sqrt{2/4}$	SPHERES $R \times 10^8$ CM.
13	Aluminum	4.043	1.751	1.429	1.429
18	Argon	5.43	2.351	1.915	1.915
20	Calcium	5.56	2.408	1.966	1.966
26	Iron γ	3.63	1.572	1.284	1.284
27	Cobalt	3.554	1.539	1.257	1.257
28	Nickel	3.499	1.515	1.237	1.237
29	Copper	3.603	1.560	1.274	1.274
45	Rhodium	3.820	1.654	1.351	1.351
46	Palladium	3.859	1.671	1.364	1.364
47	Silver	4.079	1.766	1.442	1.442
58	Cerium	5.12	2.217	1.810	1.810
77	Iridium	3.823	1.655	1.352	1.352
78	Platinum	3.913	1.694	1.384	1.384
79	Gold	4.06	1.758	1.436	1.436
82	Lead	4.92	2.130	1.736	1.736
90	Thorium	5.04	2.18	1.78	1.78

DIAMOND TYPE CUBIC LATTICE

		$a_0 \times 10^8$ CM.	$R = a_0\sqrt{3/8}$
6	Carbon	3.56	0.77
14	Silicon	5.42	1.173
32	Germanium	5.62	1.217
50	Tin (Grey)	6.46	1.399

BODY-CENTERED CUBIC LATTICE

AT. NO.	ELEMENT	$A_0 \times 10^8$ CM.	$R = a_0\sqrt{3/4}$	$R = a_0\sqrt{5/4}$	SPHERES $R \times 10^8$ CM.
3	Lithium	3.50	1.516	1.957	1.516
11	Sodium	4.30	1.862	2.404	1.862
19	Potassium	5.20	2.252	2.907	2.252
23	Vanadium	3.04	1.316	1.699	1.316
24	Chromium	2.875	1.245	1.607	1.245
26	Iron α	2.855	1.236	1.596	1.236
42	Molybdenum	3.143	1.361	1.757	1.361
73	Tantalum	3.272	1.417	1.829	1.417
74	Tungsten	3.155	1.365	1.764	1.365

HEXAGONAL CLOSE PACKED LATTICE

AT. NO.	ELEMENT	$b_0 \times 10^8$ CM.	$c_0 \times 10^8$ CM.	$R = \frac{b_0\sqrt{3}}{2\sqrt{2}}$	$R = \frac{3C_0}{8}$	SPHERES $R \times 10^8$ CM.
4	Beryllium	2.283	3.607	1.398	1.35	1.14
12	Magnesium	3.22	5.23	1.972	1.961	1.61
22	Titanium	2.92	4.67	1.788	1.751	1.46
27	Cobalt	2.514	4.105	1.539	1.539	1.257
40	Zirconium	3.23	5.14	1.978	1.928	1.615
44	Ruthenium	2.686	4.272	1.645	1.602	1.343
58	Cerium	3.65	5.96	2.235	2.235	1.825
76	Osmium	2.714	4.32	1.662	1.620	1.357

GRAPHITE LATTICE

AT. NO.	ELEMENT	$b_0 \times 10^8$ CM.	$c_0 \times 10^8$ CM.	$a_0 = \frac{B_0\sqrt{3}}{4\sqrt{1}}$	$R = \frac{c_0}{9}$	SPHERES $R \times 10^8$ CM.
6	Graphite	2.46	6.79	0.753	0.754	0.710

One point is worthy of special emphasis. It will be noted that the atomic radius of the carbon atom in diamond is 0.77 Å while that computed from the graphite is 0.75 Å, a difference of only two hundredths of an angstrom. Both of these lattices are built up of cubes having one corner in common. Either this is an astonishing coincidence or it means that a *carbon atom in combination can be treated as a cube, that its radius is approximately constant and equal to 0.76 Å over an extremely wide range of conditions, and that a carbon atom can unite with other carbon atoms by sharing one electron.* The equality of the radii of the cubic hexagonal forms of the iron, cobalt and cerium is not so important as this result would also be obtained if the atoms were spherical.

A consideration of the lattice structures herewith presented indicates

that there are more possible electron positions available than there are valency electrons to fill them, and the question also arises as to which of the radii are to be selected in those cases when two types of lattice are possible. If we knew definitely just how a single electron scatters X-rays these two questions could be easily settled by a quantitative consideration of the intensities of the observed X-ray diffraction patterns. In the present state, however, of our knowledge of scattering, the carrying through of such computations does not seem worthwhile.

In conclusion I wish to express my thanks to Professor Henry G. Gale for his interest in this work.

[1] This investigation was commenced by the author under a NATIONAL RESEARCH FELLOWSHIP.

[2] W. L. Bragg, *Phil. Mag.*, **42**, 169–189, 1920.

[3] W. P. Davey, *Physic. Rev.*, **22**, 211–220, 1923.

[4] W. P. Davey, *Ibid.*, **23**, 218–231, 1924.

[5] T. D. Bernal, *Proc. Roy. Soc.*, **106A**, 749–773, 1924.

THE MAGNETIC DIPOLE IN UNDULATORY MECHANICS

BY PAUL S. EPSTEIN

CALIFORNIA INSTITUTE OF TECHNOLOGY

Communicated March 7, 1927

1. In the following lines we present a method for the computation of the characteristic values of the parameter contained in linear differential equations. This method is applicable in certain cases when the equation cannot be reduced to the hypergeometric type. As the special example with which to illustrate our procedure we select the motion of an electron in the combined fields of a nucleus and of a magnetic dipole attached to this nucleus. This problem has an interesting bearing on the theory of the spinning electron, as will be fully discussed in section 6. The wave equation for this case has been set up by Fock;[1] we prefer, however, to generalize the problem by taking in the effect of relativity neglected by Fock, and so to arrive at an equation which differs from equation (5) of our last paper[2] (to which we shall refer as loc. cit.) only by a term proportional to χ/r^3:

$$\frac{d^2\chi}{dr^2} + \frac{2}{r}\frac{d\chi}{dr} + \left[A + \frac{2B}{r} + \frac{p_0^2 - k(k-1)}{r^2} + \frac{f}{r^3}\right]\chi = 0. \quad (1)$$

The notations are the same as loc. cit., only the constant f is introduced here for the first time and is connected with the moment μ of the dipole by the relation[3]

$$f = 2\mu p_0 j/e, \tag{2}$$

j being a new quantic integer.

The term depending on f is a small correction term. Higher powers than the first of f were neglected in obtaining equation (1). Therefore, we shall restrict ourselves to solutions taking into account f only to the first power. We believe that the method here used will prove of assistance in many other problems of wave dynamics.

2. We use again the substitutions loc. cit. (7), and obtain the equation for M:

$$\frac{d^2M}{dr^2} + 2\left(\alpha + \frac{k}{r}\right)\frac{dM}{dr} + \left(2\,\frac{\alpha k + B}{r} + \frac{p_0^2}{r^2} + \frac{f}{r^3}\right)M = 0. \tag{3}$$

The singular points of this equation are at $r = 0$ and $r = \infty$ and both are indefinite, representing essential singularities. However, in the vicinity of the point $r = \infty$ there exists one integral that can be represented by a descending power series. We can, therefore, start our discussion from this integral, putting

$$M = \sum A_p r^{-p}, \tag{4}$$

and we obtain from (5) the formula connecting the coefficients A_p:

$$fA_{p-2} + (p - k - B/\alpha - \sigma_1 - 1)(p - k - B/\alpha - \sigma_2 - 1)A_{p-1} - 2\alpha(p - k - B/\alpha)A_p = 0, \tag{5}$$

if we denote

$$\sigma_{1,2} = \mp\sqrt{(k - 1/2)^2 - p_0^2} - B/\alpha - 1/2. \tag{6}$$

The exponent of our series is, therefore, $p = k + B/\alpha$, and we arrive at the infinite system of equations:

$$\begin{aligned} -1.2\alpha A_1 \ldots\ldots &= -\sigma_1\sigma_2 A_0 \\ (\sigma_1 - 1)(\sigma_2 - 1)A_1 - 2.2\alpha A_2 \ldots\ldots &= -fA_0 \\ fA_1 + (\sigma_1 - 2)(\sigma_2 - 2)A_2 - 3.2\alpha A_3 \ldots\ldots &= 0 \end{aligned}$$

generally

$$fA_{\tau-2} + (\sigma_1 - \tau + 1)(\sigma_2 - \tau + 1)A_{\tau-1} - \tau.2\alpha A_\tau = 0. \tag{7}$$

3. The choice of A_0 is arbitrary while the rest of the coefficients must

be determined in terms of A_0. If we take the first τ equations of this system, we can determine A_τ as a quotient of two determinants

$$A_\tau = \Delta_\tau / \Delta. \tag{8}$$

The denominator Δ is the determinant of the system and simply reduces to

$$\Delta = \tau!(-2\alpha)^\tau. \tag{9}$$

The numerator Δ_τ is obtained by substituting into Δ the right side of our equations instead of the last column. So we can write

$$\Delta_\tau/\tau!\tau! = (-1)^\tau/\tau!\tau!\cdot$$

$$\begin{vmatrix} \sigma_1.\sigma_2, & -1.2\alpha & , & 0 & ,\ldots. & 0 \\ f & ,(\sigma_1-1)\,(\sigma_2-1), & & -2.2\alpha & ,\ldots. & 0 \\ 0 & , & f & ,(\sigma_1-2)\,(\sigma_2-2), & \ldots. & 0 \\ \ldots & \ldots & \ldots & \ldots & \ldots & \ldots \\ \ldots & \ldots & \ldots & \ldots & \ldots & \ldots \\ 0 & , & 0 & , & 0 & ,\ldots.(\sigma_1-\tau+1)\,(\sigma_2-\tau+1) \end{vmatrix} \tag{10}$$

We have added the factor $1/\tau!\tau!$ in order to secure the convergence of this expression if we should go to the limit $\tau = \infty$.

The integral series (4) is a solution of equation (3) which vanishes for $r = \infty$. Because of this it satisfies one of the physical requirements of finiteness. The second requirement that it be finite for $r = 0$ has still to be satisfied by a suitable choice of α and σ. It is evident that our series (4) will not be convergent unless the coefficients A_p decrease with increasing index, p, so that

$$\lim_{p=\infty} A_p = 0. \tag{11}$$

This is a necessary condition for the finiteness of M in the point $r = 0$. It will be shown in a later publication that this condition is also sufficient. In this note we only wish to point out the numerical possibilities of this method. Since the denominator $\Delta/\tau!\tau!$ does not become infinite in the limit $\tau = \infty$, our condition (11) is equivalent to

$$\lim_{\tau=\infty} (\Delta_\tau/\tau!\tau!) = 0. \tag{12}$$

We have to choose our parameter E on which both α and σ depend, so as to satisfy this condition. In other words E must be a root of the infinite determinant (12).

4. In the present case we wish to find the roots only to the terms of the first order in f. Instead of discussing the infinite determinant we can, therefore, follow a different line of reasoning. We regard quantities of the order f^2 as negligible; if we can determine E in such a way that all the coefficients A_ρ following a certain one of them A_τ be proportional to f^2, we will have solved our problem, since we then obtain what corresponds to a finite series. Let us first consider the case $f = 0$, the determinant Δ_τ then reduces to the product.

$$(\Pi = \sigma_1(\sigma_1 - 1). \ldots .(\sigma_1 - \tau + 1)\sigma_2(\sigma_2 - 1). \ldots .(\sigma_2 - \tau + 1), \quad (13)$$

and the roots of this expression are simply the integral values $\sigma_1 = l$. This is exactly condition loc. cit. (12) since $\sigma_1 = -(\sigma_0 + k + B/\alpha)$, we find, therefore, the same values for our parameters as loc. cit.

Expression (10) differs from Π by terms of the order f; if we substitute into it for E the last root of Π, our purpose will not be accomplished, since the coefficients beginning with A_τ will be of the order f and not smaller. The situation will not be changed, if we take for E the last root of A_τ. This is apparent from the relation

$$\tau.2\alpha A_{\tau+1} = (\sigma_1 - \tau)(\sigma_2 - \tau)A_\tau + fA_{\tau-1}.$$

However, if we take the last but one root of $A\tau$, it is different. This root differs only by a quantity of the order f from the last root of $A_{\tau-1}$, and will make this coefficient itself a small quantity. Therefore, $A_{\tau+1}$ will become quadratic in f, as well as the next coefficient $A_{\tau+2}$. But if two coefficients in succession are of the order f^2, all the following will be small of the same order. It remains to evaluate the last but one root of every coefficient A_τ, or of the corresponding determinant Δ_τ.

5. We take as the index $\tau + 2$ instead of τ and expand $\Delta_{\tau+2}$ with respect to the elements of the first column. If we introduce the notation $\Delta^{(m)}_{\tau+2}$ for the determinant resulting from $\Delta_{\tau+2}$ by crossing off the first m lines and the first m columns, this expansion gives

$$\Delta_{\tau+2} = \sigma_1\sigma_2\Delta^{(1)}_{\tau+2} + 1.2\alpha f\Delta^{(2)}_{\tau+2}.$$

$\Delta^{(2)}_{\tau+2}$ is multiplied by the factor f. Since we wish to determine the roots only to terms of the first order in f, we have to retain only terms of the same order in our equation, and we may substitute 0 for f in the determinant $\Delta^{(2)}_{\tau+2}$

$$\Delta_{\tau+2} = \sigma_1\sigma_2\Delta^{(1)}_{\tau+2} + 2\alpha f\Pi/\sigma_1(\sigma_1 - 1)\sigma_2(\sigma_2 - 1).$$

On the other hand, $\Delta^{(1)}_{\tau+2}$ has the same structure as $\Delta_{\tau+2}$, and we can sub-

ject it to the same expansion. Repeating this procedure $\tau + 1$ times, we obtain

$$\Delta_{\tau+2} = \Pi + 2\alpha f \Pi \cdot \cdot \sum_{1}^{\tau+1 m} m/(\sigma_1 - m + 1)(\sigma_1 - m)(\sigma_2 - m + 1)(\sigma_2 - m).$$

We have to find the last but one root of this expression. The first approximation is obtained by omitting the sum altogether and putting $\Pi = 0$. This case was discussed in the preceding section and the last but one root of $\Pi_{\tau+2}$ is $\sigma_1 = \tau$. The second approximation will differ from this value only by a small correction of the order f. Therefore, Π will contain a small factor and the product $f\Pi$ will be of the second order. This will make all the terms of the sum negligible except the last two containing the same factor in the denominator. Cancelling out all the factors of Π, except the small one, we can write

$$\sigma_1 - \tau + 2\alpha f \left[\frac{\tau}{(\sigma_1 - \tau + 1)(\sigma_2 - \tau)(\sigma_2 - \tau + 1)} + \frac{\tau + 1}{(\sigma_1 - \tau - 1)(\sigma_2 - \tau)(\sigma_2 - \tau - 1)} \right] = 0.$$

Into the correction term we may substitute the approximate value $\sigma_1 = \tau$. At the same time we may neglect in this term p_0^2 which is of the same order of magnitude as f and write[4] $\alpha = \alpha_0 = -me^2/K^2 l$ and $\sigma_2 = \sigma_1 + 2k - 1 = \tau + 2k - 1$, where l is an abbreviation: $l = k + \tau$. We so obtain the second and final approximation[5]

$$\sigma_1 = \tau - me^2 f/2K^2(k - 1/2)k(k - 1). \tag{14}$$

6. It remains to express E in terms of the integers k,τ,l. Going back to equation (6) and comparing it with loc. cit. (12), we see that the only difference is that the integer n is replaced by our expression σ_1. We have, therefore, to substitute σ_1, for n into the energy expression loc. cit. (13). Expanding with respect to p_0^2 and neglecting f in the term of order p_0^4, we obtain

$$E = -\frac{mc^2}{2}\left\{\frac{p_0^2}{(\sigma_1 + k)^2} + \frac{p_0^4}{(k - 1/2)l^3} - \frac{3}{4}\frac{p_0^4}{l^4}\right\}. \tag{15}$$

Substituting for σ_1 its value (14)

$$E = -\frac{mc^2}{2}\left\{\frac{p_0^2}{l^2} + \frac{p_0^4}{(k - 1/2)l^3} - \frac{3}{4}\frac{p_0^4}{l^4} + \frac{me^2 p_0^2 f}{K^2} \cdot \frac{1}{l^3(k - 1/2)k(k - 1)}\right\}. \tag{16}$$

It is known that in the old theory the problem of the magnetic dipole has a close relation to that of the spinning electron: One has only to replace the moment μ by one-half of the spin moment taken with the negative sign

$$\mu = -Ke/4mc, \tag{17}$$

in order to obtain the identical spin formula (including the Thomas correction). It is interesting to see what we obtain by the same procedure in the new theory. Of interest are only the second and fourth terms of our braces, since they are the only ones dependent on k and giving the fine structure. Their sum now becomes

$$p_0^4[1 + j/2k(k-1)]/l^3(k-{}^1/_2). \tag{18}$$

The geometrical significance of j in our problem is the projection of k on the dipole axis. It will be noticed that for the two values $j = k$ and $j = -(k-1)$ our expression reduces to $p_0^4/l^3(k-1)$ and p_0^4/l^3k, which are identical with the levels of the old Sommerfeld theory. *This shows that our formulae (16) and (18) in fact completely represent the effect of the spinning electron as it was suggested by Goudsmit and Uhlenbeck.*

This result must have its cause in a mathematical parallelism of the two problems. When the wave equation for the spinning electron will be set up, it, probably, will prove of the same or a similar type as our equation (1). Taking our formula (18) to be identical with that for the spinning electron, it is easy to see that in this case the absolute value of j must be either k or $k-1$. The procedure of compounding the total momentum vectorially has been worked out by the spectroscopists. According to their normalization the orbital momentum is an integral multiple of K and proportional to $k-1$. The spin momentum of a single electron is $K/2$ and, since this momentum is half integral, the total momentum must be also half integral and proportional to $j-{}^1/_2$. It follows that $k-1+{}^1/_2 \geqslant j-{}^1/_2 \geqslant k-1-{}^1/_2$, whence j is, in absolute value, either k or $k-1$. I.e., the spin axis is either parallel or antiparallel to the orbital momentum $k-{}^1/_2$. This leads to the negative sign of $k-1$ since in the second case spin and orbital momentum have opposite directions.

[1] V. Fock, *Zs. Physik*, **38**, p. 242, 1926.

[2] P. S. Epstein, these PROCEEDINGS, **13**, p. 94, 1927.

[3] For working out this relation I am indebted to Mr. C. F. Richter of the Norman Bridge Laboratory. The magnetic dipole is taken to have a fixed direction in space. However, in the case of a free dipole the reaction of the electron on it would not change the type of equation (1) but only the constant of equation (2).

[4] P. S. Epstein, these PROCEEDINGS, **12**, p. 629, 1926, formula (4).

[5] The case $k = 1$ requires a separate treatment. We have thus to take the last root of every determinant Δ_τ and obtain $\sigma_1 = \tau - me^2f/K^2$.

NUCLEUS AND CYTOPLASM IN RELATION TO DIFFERENTIAL POLLEN-TUBE GROWTH[1]

BY R. A. BRINK AND C. R. BURNHAM

DEPARTMENT OF GENETICS, UNIVERSITY OF WISCONSIN

Communicated March 5, 1927

Differential pollen-tube growth has been assumed to account for certain irregular zygotic ratios in Avena, Datura, Melandrium, Nicotiana, Oenothera, Oryza and Zea.[2] In the flowering plants the two critical stages, meiosis and fertilization, are separated by an entire generation, the gametophyte. Any selective action during this period is of particular interest to the geneticist through the fact that it alters the ratio in which the respective types of spores formed at reduction are represented at fertilization. As has been pointed out elsewhere,[3] if differential pollen-tube growth were a general phenomenon we should have to make important reservations in applying the Mendelian concept to the higher plants.

All the microspores arising from a single individual receive a common cytoplasm from the parent sporophyte. If pollen-tube growth is directly controlled by this extra-nuclear equipment contributed by the diploid plant we should not expect to find any evidence of differential development; on the other hand, if the behavior of the male gametophyte is governed by the nuclear organization of the haploid individual itself selective action is possible. Studies on the effect of the sugary gene in maize on the waxy ratio afford some evidence on the respective parts played by cytoplasm and nucleus in the development of the microgametophyte.

Collins and Kempton[4] first showed that maize plants heterozygous for the waxy gene (*wx*), when self-pollinated or used as pollen parents in combination with the homozygous waxy type give, on the average, a small but significant deficiency of waxy seeds amounting to about 1 per cent and 2 per cent, respectively. This finding has been amply confirmed by later investigators. In the present paper it is demonstrated that the sugary gene which, as Emerson[5] has shown, resides upon a different chromosome from the *Wx wx* pair, exerts a curious modifying action on the waxy ratio. Plants heterozgyous for the waxy gene and homozygous for sugary (*su su Wx wx*) give, when self-pollinated, a significantly lower proportion of waxy seeds than do *Su Su Wx wx* individuals.

In table 1 the net percentages of waxy and non-waxy grains given by comparable non-sugary and sugary plants in three stocks of different origin are presented. It is clear that the sugary individuals show significantly lower proportions of waxy seeds than similar plants carrying the dominant non-sugary gene.

The appropriate crosses have been made to determine if the sugary

gene modifies the waxy ratio through some action in both the pistillate and staminate parents or in one of these only. Twelve ears obtained in the combination *su su wx wx* ♀ × *Su Su Wx wx* ♂, that is, where the pistillate parent only carries the sugary gene, gave 48.61 ± 0.45 per cent waxy seeds. This proportion is not significantly different from the ratio formerly obtained in similar matings not involving the sugary factor.[3]

TABLE 1

PER CENT OF WAXY SEEDS OBTAINED ON SELFING HETEROZYGOUS WAXY PLANTS IN COMPARABLE NON-SUGARY AND SUGARY PROGENIES

PEDIGREE NUMBER OF GROUP	*Su Su Wx wx*		*su su Wx wx*		DIFFERENCES IN PER CENT OF WAXY SEEDS
	NO. OF EARS	PER CENT WAXY SEEDS	NO. OF EARS	PER CENT WAXY SEEDS	
R21–R22	7	23.59 ± 0.53	10	18.37 ± 0.46	5.22 ± 0.73
R23	21	22.92 ± 0.29	18	20.19 ± 0.32	2.73 ± 0.43
R24	13	22.51 ± 0.43	4	10.99 ± 0.87	11.52 ± 0.97

Critical evidence relating to the effect of the sugary gene in the pistillate parent when the pollen comes from a homozygous sugary plant is afforded by a number of matings of the types *Su Su wx wx* ♀ × *su su Wx wx* ♂ and *su su wx wx* ♀ × *su su Wx wx* ♂ in which the same staminate plants were used with the two respective classes of pistillate individuals. Six ears from the first-named combination contained 34.91 ± 0.64 per cent waxy seeds and four ears resulting from the application of samples of the same pollen to double recessive plants (*su su wx wx*) bore 37.76 ± 0.83 per cent waxy grains. Both these values are, of course, far below expectation on the Mendelian basis. The difference between them is not statistically significant.

The sugary gene in homozygous condition in the pistillate member of a pair does not, therefore, lower the waxy ratio. When the pollen parent is homozygous for the sugary factor (*su su Wx wx*) a deficiency of about 15 per cent in the waxy ratio results in back-crosses with waxy plants whether these be sugary or non-sugary. These facts indicate that the sugary gene exerts its disturbing influence on the waxy ratio through some action on the pollen; the composition of the pistillate individual with respect to the *Su, su* pair is apparently not of consequence.

In view of this striking difference in the behavior of non-waxy and waxy pollen from *Su Su Wx wx* and *su su Wx wx* plants, one might expect, if the sugary gene exerts its initial differential action in the pollen grain or in the pollen tube, that the cross *su su wx wx* ♀ × *Su su Wx wx* ♂ would give 48 per cent waxy seeds in the non-sugary class and about 35 per cent in the sugary group. The double heterozygote produces four classes of pollen grains, namely, *Su Wx, Su wx, su Wx* and *su wx*. The first two of these correspond to the types formed by *Su Su Wx wx* plants, which give a minus deviation in the waxy class of about 2 per cent, and the latter

two classes are of the same nuclear composition as the pollen formed by *su su Wx wx* individuals which leads to a 15 per cent deficiency of waxy seeds. If genetic composition of the gametophyte alone is the determining factor the double heterozygote should give markedly different waxy ratios in the sugary and non-sugary classes. The striking fact is that such a difference does not result; the combinations *su su wx wx* ♀ × *Su su Wx wx* ♂ and *Su su Wx wx* selfed give about the same proportion of waxy seeds in the *Su* and *su* classes.

Twenty-one ears from the backcross *su su wx wx* ♀ × *Su su Wx wx* ♂ produced 47.60 per cent waxy seeds in the non-sugary group and 48.41 per cent in the sugary class. The difference is not statistically significant. The distributions on self-pollinated ears from plants of the type *Su su Wx wx* in the three groups mentioned in table 1 reveal, further, that in two of the stocks the differences in the waxy ratio in the sugary and non-sugary classes are small and might well be due to chance. In the case of progeny *R*23 the proportion of waxy seeds in the sugary class proved to be significantly lower but the difference appears to be due, largely at least, to two plants within the group of 21 which behaved irregularly. If these two items are omitted the results conform with the other findings.

These results mean that *su Wx* and *su wx* pollen grains behave differently according to the type of sporophyte which produces them; if the plant is homozygous for the sugary gene (*su su Wx wx*) the two classes of pollen lead to a wide discrepancy in the waxy ratio; on the other hand, if the sporophyte carries the dominant non-sugary gene (*Su su Wx wx*), *su Wx* and *su wx* grains do not behave differently from waxy and non-waxy pollen produced by *Su Su Wx wx* plants.

The marked deficiency of waxy seeds resulting when the pollen of *su su Wx wx* plants is used might be due to a differential rate of growth of waxy and non-waxy pollen tubes. If there were a *constant* difference in this regard throughout the entire period of development in the style we should expect different proportions of waxy seeds at different levels on the ear. The numbers of waxy and non-waxy seeds in the upper and lower halves of 20 ears from a combination of the type *Su Su wx wx* ♀ × *su su Wx wx* ♂ have been recorded separately. The *su su Wx wx* plants used in the crosses were descended from a *su su Wx wx* individual which gave only 8.39 ± 1.63 per cent waxy seeds on self-pollination. The 20 ears produced 7590 seeds of which 20.25 per cent were waxy. This proportion is in defect of the 50 per cent expected in such a backcross by nearly 30 per cent. The upper halves of the ears contained 19.43 per cent waxy grains and the lower portions 21.12 per cent. Student's method of evaluation indicates that the difference is not statistically significant. It is concluded, therefore, that the deficiency in the waxy ratio cannot be

due to a *constant* difference in the rate of growth of waxy and non-waxy pollen tubes.

To account for the modifying effect of the sugary gene on the waxy ratio it is assumed that under the sustained action of the sugary and non-sugary factors, different kinds of cytoplasm are formed in the two respective types of sporophytes. At sporogenesis the cytoplasm of the spore mother cell is partitioned between the microspores so that the young gametophytes are also characterized by the difference existing in the parent diploid individuals. It is further assumed that when waxy and non-waxy nuclei interact with sugary-type cytoplasm the difference in developmental capacity of the two respective classes of male gametophytes is greater than when normal (non-sugary) cytoplasm is present.

We may recognize two stages in the development of the pollen tube in the style; during the first period, which is comparatively short, the gametophyte utilizes the reserves contributed by the pollen grain; thereafter the pollen tube becomes wholly dependent upon food materials supplied by the conducting tissue. The direct cause of the deficiency of waxy seeds is believed to be a differential rate of growth of the two classes of male gametophytes, *su Wx* and *su wx*, arising from sugary homozygotes, during the stage in which the pollen reserves are being used; in their later development it is assumed that the two types of pollen tubes elongate at the same rate.

The mechanism by which the sugary gene operates to depress the waxy ratio is not clear. One might suppose that the deficiency is due to a smaller amount of reserve material in *su wx* pollen, to an alteration in the proportion of the various food substances, or to changes in the rate in which the reserves are utilized during the early stages of pollen-tube growth. Chemical analyses show that pollen from comparable *Su Su Wx Wx*, *Su Su wx wx*, *su su Wx Wx* and *su su wx wx* plants differs in composition but the results do not bear an evident relation to the breeding facts. Information on the effect of the two pairs of genes *Su su* and *Wx wx* on amount of reserves synthesized has been sought through a study of the respective weights of *Su Wx*, *Su wx*, *su Wx* and *su wx* seeds borne on segregating ears. It was found, in both the non-sugary and sugary classes, that waxy seeds are lighter than the non-waxy type but that the difference is not greater in one case than in the other. In other words, the double recessive combination does not occasion a disproportionate decrease.

An experiment has also been carried out to determine rate of sprout development and decrease in amount of endosperm reserves in the four classes of seedlings, *Su Wx*, *Su wx*, *su Wx* and *su wx*. The plants were grown in the dark at 28°C. No significant differences were shown with respect to gain in dry weight of the sprouts. Moreover, estimation of the rate at which the reserves are utilized by following the loss in dry weight

of the seed residue as development of the seedlings progressed did not reveal important variations between the four classes. It is possible, however, that the essential conditions governing rate of growth in the seedling are not comparable to those in the pollen tube.

[1] Papers from the Department of Genetics, Agricultural Experiment Station, University of Wisconsin, No. 76. Published with the approval of the Director of the Station.

[2] For general bibliographies see Brink, R. A., *Genetics*, **10**, 359–394, 1925; and Mangelsdorf, P. C., and D. F. Jones, *Ibid.*, **11**, 423–455, 1926.

[3] Brink, R. A., *Ibid.*, **10**, 359–394, 1925.

[4] Collins, G. N., and J. H. Kempton, *Rept. 4th Confér. Internat. Gén.* (Paris), 347–356, 1911.

[5] Emerson, R. A., *Amer. Nat.*, **58**, 272–277, 1924.

[6] The non-sugary plants in groups *R*23 and *R*24 were of the formula *Su su Wx wx*. As shown later in the text such individuals give the same waxy ratio as *Su Su Wx wx* plants.

ABNORMALITIES IN POLLEN-TUBE GROWTH IN DATURA DUE TO THE GENE "TRICARPEL"[1]

BY J. T. BUCHHOLZ AND A. F. BLAKESLEE

UNIVERSITY OF TEXAS AND CARNEGIE INSTITUTION OF WASHINGTON, DEPARTMENT OF GENETICS, COLD SPRING HARBOR, N. Y.

Communicated March 10, 1927

"Tricarpel" is a recessive gene mutant of *Datura Stramonium*. Since it is described and figured in a paper now in press,[2] its distinctive peculiarities need not be discussed here. The purpose of the present paper is to describe the abnormal behavior of the tricarpel gene (*tc*) in inheritance and to show that an explanation can be found in a study of pollen-tube behavior.

The tricarpel, as well as normal plants described in these experiments, belonged to our Line 1*A* which is a subline derived from a single haploid individual. Barring new mutations, such plants should be homozygous and genetically identical, as has been pointed out in an earlier publication.[3] Our material, therefore, may be considered closely comparable genetically.

In its inheritance, the tricarpel gene is transmitted in a peculiar manner. In the F_2 generation following the cross between tricarpel and normal there is a very marked deficiency in the number of recessive phenotypes obtained. In female back-crosses—*Tctc* × (*tc*)(*tc*)[4]—in which the female is the heterozygote, the ratio obtained is practically 1 : 1; in the male back-crosses—*tctc* × (*Tc*)(*tc*)—in which the pollen parent is the heterozygote, the deficiency in recessives is very pronounced.

The segregation in the offspring from a series of back-crosses grown this

past summer is shown in table 1. Our 11 primary ($2n + 1$) types were rendered heterozygous for *tc* and back-crossed reciprocally to the recessive. In all cases, the male back-crosses (*tctc* × heterozygote) show a deficiency in *tc* individuals (there being 1067*Tc* and 221*tc*, a ratio of about 5:1), while the female back-crosses (heterozygote × *tctc*), except for Reduced, give good 1:1 ratios with no deviation greater than twice the probable error. In addition to the back-crosses shown in the table, seed were sown at the same time from a selfed heterozygous Spinach and from a selfed heterozygous Globe-Echinus. The offspring (including ($2n + 1$) types) gave a total of 236*Tc* and 18*tc* individuals. This is a ratio of 13:1, instead of the 3:1 usually expected in the F_2 generation. The departure from a 3:1 ratio is about what would be expected from the male back-cross ratios given in the table. It is obvious that there is a large elimination of the *tc* element in the (*Tc*)(*tc*) pollen. When and how this elimination takes place will be discussed in later paragraphs.

The data in table 1 were obtained in an attempt to locate the gene for tricarpel in its proper chromosome. It has been earlier shown[5] that, if all the primary ($2n + 1$) types are rendered heterozygous for a given gene, only the type which carries the gene in question in its extra chromosome will give trisomic ratios in its offspring. The trisomic ratio for a female back-cross, when the ($2n + 1$) parent is simplex, is 2 dominants to 1 recessive among the diploid offspring and all dominants among the ($2n + 1$) progeny. From an inspection of the female back-crosses in the table, it will be seen that all the types give normal disomic 1:1 ratios except Reduced which gives a trisomic ratio in its offspring. The complete record for Reduced is 82*Tc*:45*tc* among the diploids and 8*Tc*:0*tc* among the Reduced offspring, a close agreement with the trisomic ratio 2:1:all:0. Data are being secured on the female back-crosses of Globe and Cocklebur but, since a given factor is to be expected in but a single chromosome, we may conclude provisionally that the gene for tricarpel is located in the "Reduced" chromosome.

The elimination of *tc* genes, indicated by the data presented in table 1, may occur at two definite stages and at either may properly be classified under the forms of Developmental Selection[6] which may be designated as gametophytic. The first stage is at the germination of the pollen on the stigma. One class of grains in heterozygous pollen may be incapable of germination or germinates very poorly, while the other class of grains behaves normally. The second stage is during the growth of the pollen tubes. Some kind of elimination or differential growth of pollen tubes may occur as they progress down through the conducting tissue toward the ovary when the pollen is from a heterozygous parent.

All of these possibilities were tested by means of our special technique for the study of pollen tubes.[7,8] A set of slides was prepared by this

dissection method from tests of $2n$ plants in which pollen of the three types —*tctc*, *Tctc* and *TcTc*—were grown on the pistils of the same three types in all nine possible combinations. These preparations were studied statis-

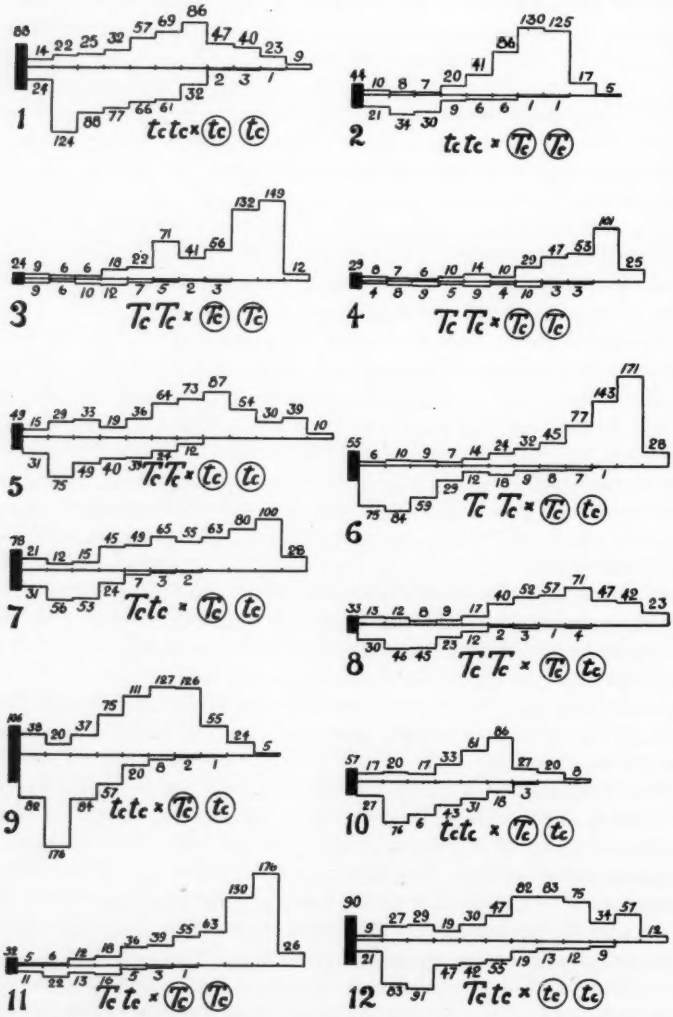
1 tc tc × tc tc
2 tc tc × Tc Tc
3 Tc Tc × Tc Tc
4 Tc Tc × Tc Tc
5 Tc Tc × tc tc
6 Tc Tc × Tc tc
7 Tc tc × Tc tc
8 Tc Tc × Tc tc
9 tc tc × Tc tc
10 tc tc × Tc tc
11 Tc tc × Tc Tc
12 Tc tc × tc tc

tically. The number of tips or ends of pollen tubes observed in each 0.33 mm. wide transect field of the microscope (using mechanical stage) were recorded. These were combined and plotted for 3 mm. intervals in the

distribution curves described here. The flowers were cut with 6 inches of the stems and placed in water at 18.3°C. where the tests were conducted during a period of 12 hours.

All of the pollen types showed a very high proportion of germination, but the *Tc* pollen germinated better than *tc* as will be obvious from a study of these distribution curves. The failure of some of the *tc* class of pollen grains to germinate, or their bursting on the stigma during germination, could account, however, for only a small percentage of the *tc* elimination.

In the distribution curves of the tips of the pollen tubes, certain tubes whose ends appeared very abnormal were plotted below the datum line, the others which appeared normal were plotted above this line. Ungerminated pollen grains and those which burst during germination were plotted as a vertical bar at the left, half above and half below the datum line. They were drawn as if they were all located in the same space interval. Actually, however, the ungerminated and burst pollen grains are found on a convex stigmatic surface extending over a space interval of 3 or 4 mm. on the microscope slide. From a comparison of these distribution curves a fair notion may be gained of some of the processes of gametophytic selection which are at work here.

In crosses between normal plants which are homozygous for the normal allelomorph of the tricarpel gene ($TcTc \times TcTc$), we obtained distribution curves of the pollen tube ends as shown in figures 3 and 4. Figure 4 is from one of the flowers especially pollinated as controls for this experiment and figure 3 is an example from similar tests obtained in a previous year. The pollinations were made at a time when the stigmas were fully receptive. The pollen was evenly distributed over the entire stigma, thus insuring prompt and uniform germination. A very high proportion of the *Tc* pollen grains (93 per cent or more) germinated in each of these instances and the main group of pollen tube ends is near the point reached by the longest. Some abnormal-appearing pollen tubes were found, which are plotted below the datum line. Though these are very conspicuous, they are not numerous in pollen from normal plants. We have obtained distribution curves of this type repeatedly over a period of several years in normal homozygous Daturas whether the flowers were selfed or sibbed, when pollinations were made at the time when capsules were setting favorably. In similar curves previously prepared,[7,8] however, we did not plot the abnormal-appearing pollen tubes separately, but plotted all of the pollen tubes above the datum line in smoothed curves.

In striking contrast with these, are the curves of distribution obtained from tricarpel plants selfed or sibbed. Figure 1 illustrates the distribution curve of the pollen-tube ends in tricarpels—$tctc \times (tc)(tc)$. Here over half of the pollen tubes are abnormal in appearance and the normal-appearing pollen tubes have a much more retarded mode than those in figures 3 and

4. There is only a very slight difference in the germination of the pollen when reduced to percentages.

A critical examination of the pollen tubes which appear abnormal in these tricarpel plants reveals the fact that these are either swollen and beaded in appearance or are actually ruptured. The ruptures occur either at the ends or on the sides near the ends. Much or nearly all of the protoplasm may have been extruded from these burst pollen tubes so that the tubes appear to end in these conspicuous splotches of protoplasm. Other pollen tubes become ensnared in these splotches where they are frequently held in check. The latter may burst sooner or later and sometimes four or five pollen tubes may be observed contributing to a common mass of extruded protoplasm. All stages in the rupture of pollen tubes may be observed. Swollen ends or an irregular contour along their sides are the earliest symptoms of this abnormality, followed by various steps in the extrusion of the protoplasm. The fact that other pollen tubes may become entangled and have their ends remain rounded, apparently intact but imbedded in these areas, had caused us to hesitate for several years in describing similar abnormal pollen tubes previously observed. The pollen-tube populations obtained from certain crosses with tetraploid pollen, in crosses with pollen of $(2n + 1)$ mutants or in those found between normal diploids have some abnormal pollen tubes which may be explained as due largely to bursting. Among the tricarpel pollen tubes, however, there are so many that show this condition in all crosses in which pollen with the *tc* gene is present that, on the basis of quantitative studies as well as of the abundant opportunities afforded for direct observation, there is little room for doubt that these abnormal splotches are masses of protoplasm extruded from pollen tubes which have burst. The structure of the protoplasm in these masses agrees with that in the pollen tubes, and in those which occasionally burst in normal pollen this resemblance in the internal and extruded protoplasm is similarly apparent.

The styles of the tricarpel plants have a looser conducting tissue. Frequently there is an empty stylar canal in tricarpel pistils. This looser condition of these cells of the conducting tissue may have an influence in causing a greater amount of bursting in these pistils. Figure 2 is a tricarpel $\times$ normal in which the pollen came from the same flower as that of figure 4. The proportion of abnormal and ruptured pollen tubes shows a marked increase and the mode of the group is retarded.

On the other hand, when the styles of normal plants are pollinated with tricarpel pollen (Fig. 5), there is a high proportion of bursting or abnormal pollen tubes, amounting to about 37 per cent. In the styles of the heterozygotes (Fig. 12) it is very similar (it is higher in the instance used for figure 12 and slightly lower in another case). All of the tests show that the cause of bursting is largely inherent in the *tc* gametophytes.

Styles of heterozygous plants pollinated with normal pollen (Fig. 11) give essentially the same distribution curves as normal plants. In the styles of heterozygous plants pollinated with heterozygous pollen—*Tctc* × (*Tc*)(*tc*)—the proportion of burst and abnormal pollen tubes is marked. In figure 7 this value is about 25 per cent of the total pollen tube count. In male back-crosses to the dominant—*TcTc* × (*Tc*)(*tc*)—the conditions are very similar; the proportion of burst pollen tubes is about 30 per cent in figure 8 and 37 per cent in figure 6.

In the male back-crosses to the recessive—*tctc* × (*Tc*)(*tc*)—is found the greatest elimination due to bursting of the trials made by the application of heterozygous pollen. Figure 9 shows a proportion of 41 per cent of the pollen tubes abnormal and burst and in figure 10, in which a less vigorous flower and a smaller amount of pollen was used, the abnormal burst portion represents 48 per cent of the pollen tubes. This phenomenon of bursting is, therefore, in itself sufficient to account for the deficiency of recessives in the male back-crosses of table 1.

TABLE 1

MALE AND FEMALE BACK-CROSSES OF (2*n* + 1) TYPES HETEROZYGOUS FOR TRICARPEL (*Tctc*). ONLY 2*n* OFFSPRING SHOWN

(2*n* + 1) TYPES	MALE BACK-CROSSES *tc* × HETEROZYGOUS (2*n* + 1)		FEMALE BACK-CROSSES HETEROZYGOUS (2*n* + 1) × *tc*	
	Tctc	*tctc*	*Tctc*	*tctc*
Globe	63	13		
Poinsettia	72	6	63	58
Cocklebur	76	7		
Ilex	17	2	64	59
Echinus	157	24	57	43
Rolled	92	24	43	40
Buckling	127	65	38	46
Glossy	154	25	17	18
Microcarpic	198	38	54	52
Elongate	111	17	27	27
Totals	1067	221	363	343
Ratios	4.83	1	1.06	1
REDUCED	207	33	82	45

Pollen tubes which carry the gene *tc* are, therefore, subject to a high proportion of bursting within the tissues of the styles, where these styles are those of normal plants, their own styles or those of heterozygotes, as shown consistently from the nine possible combinations described here, which are representative of about three times this number which have been subjected to a similar study.

Other investigators have identified the cause of similar genetic data with differences in pollen-tube growth rate. In a previous report on the Globe,[7] we have given this interpretation on the basis of a bimodal distribution of the pollen tubes, counting the abnormal tubes along with the normals.

Of course the burst pollen tubes may be considered to be out of the race entirely rather than representing a growing element of the population, and those which are still capable of transmitting the character in question are to be found among the normal-appearing pollen tubes.

However, the explanation that the growth rate of the pollen tubes is also involved is fully justified on the basis of these tricarpel data. This is, therefore, an additional factor tending to reduce the proportionate number of pollen tubes which reach the ovary to transmit the *tc* gene, provided that there are fewer ovules to be fertilized than there are pollen tubes, a condition in which the earliest arriving pollen tubes fertilize most of the eggs. For example, if we consider only the normal-appearing fraction of the pollen-tube populations—those plotted above the datum lines in figures 1–12—and compare the rate of growth shown by the average of the (*tc*) pollen-tube group with that of (*Tc*) pollen tubes in each of the styles, then the average of *tc* in figure 1 is at about 93 per cent of the distance of that of *Tc* in figure 2; in figure 5 the average of *tc* is at a distance of 80 per cent of that of *Tc* in figure 4; in fig. 12 the average of *tc* is at a distance of 88 per cent of that of *Tc* in figure 11, all measured from the stigma. Thus the average of the *tc* group of pollen tubes is always retarded when compared to that of *Tc* growing on a style of similar genetic constitution. Very similar results are obtained if the medians or the modes of pollen-tube distribution in these same styles are compared. Likewise the remaining preparations which were not included in figures 1–12 show similar differences between the growth rate of *tc* and *Tc*. The distances reached by the longest pollen tubes in each group are about the same when compared on the same types of styles.

The burst *tc* pollen-tube splotches actually present a different appearance from those of the *Tc*. The extremes of these differences are represented by the burst *tc* pollen tubes in a *tctc* style in comparison with the occasional burst *Tc* pollen tubes in a *TcTc* style. These extreme differences are very striking, but may be explained as due very largely to the mechanical effect of the looseness of the conducting tissue cells of the *tctc* styles in comparison with the compactness of those of the *TcTc* styles. When *Tc* pollen tubes burst in the *tctc* styles, some of them come to resemble the burst splotches from *tc* pollen tubes in similar styles, but most of them are different in shape. Typical *tc* splotches are ovoidal in outline and are often moulded into irregular lobes as the protoplasm flows around the cells of the loose *tctc* tissue. The burst *Tc* pollen tubes are not so regularly ovoidal and have a denser or more deeply staining protoplasm.

In the *TcTc* or *Tctc* styles, the conducting tissue is more compact and the protoplasm from the burst tubes is forced into fusiform or spindle-shaped forms. Pollen tubes of *tc* growing here spread out into less compact and more irregular shapes and are less deeply stained than those of the *Tc*,

but they appear different from *tctc* × (*tc*)(*tc*). These differences in shape, when they grow in the same styles, are doubtless due to differences in the protoplasm but there are also many intergrades in all classes. While it is easily possible to recognize the differences found in the extremes of these combinations we cannot state with assurance that we expect to be able to recognize these differences in the burst pollen tubes from heterozygous pollen when these are growing together on *tctc* styles.

In tricarpel we have a gene which is transmitted with practically no elimination through the female while it suffers under a very pronounced gametophytic selection in the male in passing through the stylar tissue. Such gametophytic selection we believe may have been an important factor in evolution.

[1] Paper presented before the Joint Genetics Section of the Botanical Society of America, December 28, 1926. An abstract is published in *Anat. Rec.*, **34**, 1926, 175. This coöperative investigation was made possible by grants from the JOSEPH HENRY FUND of the NATIONAL ACADEMY OF SCIENCES.

[2] Blakeslee, A. F., Gordon Morrison and A. G. Avery, in press, *J. Heredity*.

[3] Blakeslee, A. F., and John Belling, *J. Heredity*, **15**, 1924, 195–206.

[4] In the text and in the figures, the abbreviations for genes in the pollen are enclosed in parentheses or circles.

[5] Blakeslee, A. F., and M. E. Farnham, *Amer. Nat.*, **57**, 1923, 481–495.

[6] Buchholz, J. T., *Bot. Gaz.*, **73**, April, 1922, 249–286.

[7] Buchholz, J. T., and A. F. Blakeslee, *Science*, **55**, 1922, 597–599.

[8] Buchholz, J. T., and A. F. Blakeslee, in press, *Mem. Hort. Soc. N. Y.*, **3**.

MAGENTA-ALPHA—A THIRD FREQUENTLY MUTATING CHARACTER IN DROSOPHILA VIRILIS

BY M. DEMEREC

CARNEGIE INSTITUTION OF WASHINGTON, DEPARTMENT OF GENETICS, COLD SPRING HARBOR, N. Y.

Communicated February 25, 1927

In the preliminary reports[1,2] on the behavior of reddish and miniature-α evidence was presented which indicated that both of these characters frequently mutate to the wild type. In the case of reddish the mutable condition of the gene was limited to the reduction division of the heterozygous females, and the gene for miniature-α was found to be mutable in all stages of the development, in the germ cells as well as in the somatic cells. Magenta-α eye color character is the third mutable character found in *D. virilis*. Mutations to wild type were observed at the reduction division of homozygous and heterozygous females in males and in a few cases in somatic cells.

Description.—The eye color of magenta-α flies is purplish red when com-

pared with the red color of wild-type flies. It closely resembles magenta,[3,4] of which it is an allelomorph. The character is very distinct in the males but in the females is frequently indistinguishable from the wild type. The viability and fertility of magenta-α males is fairly good, but the homozygous magenta-α females are highly sterile. The magenta-α/magenta females, however, have a good fertility.

Origin.—In June, 1926, two magenta-α males were found among 120 progenies of a pair mating. One of these males was mated to four sisters. In F_1 generation 469 wild-type and 46 magenta-α females, and 365 wild-type, 19 magenta-α and one mosaic male were obtained. That indicated that one or several females used in the experiment were heterozygous for magenta-α. Since the magenta flies could very easily pass unnoticed if not specially looked for, it is not improbable that the magenta-α was present in the cultures for several generations before it was found.

Test for Allelomorphism.—Since it was found that the magenta-α is a sex-linked character, crosses were made between magenta-α and the already known sex-linked eye colors to determine whether it is allelomorphic to any of them. F_1 females from crosses magenta $\times$ magenta-α were of the magenta type, indicating allelomorphism. Since, however, the magenta-α is not always distinct in females, to make the evidence more conclusive, it was crossed with miniature forked, which characters are located close to the magenta, as can be seen from the map of that region of the sex chromosome.

miniature (*mt*)	magenta (*m*)	forked (*f*)
60	67	71

The "map" of the middle part of the X-chromosome.

The data from such a cross would show whether magenta-α is located in approximately the same region as magenta. Very soon after its discovery two lines of magenta-α were separated, viz., a mutable and a constant line. To avoid the irregularities due to mutability of the magenta-α,

TABLE 1

THE SUMMARY OF THE DATA FROM THE CROSSES INVOLVING CONSTANT MAGENTA-α, MINIATURE AND FORKED

F_1 ♀	TOTAL ♀	0		1		2		TOTAL ♂
$\frac{mt\ f}{m\text{-}\alpha}$	1023	318	348	13	15	21	13	728
		+	*mt m-α f*	*mt*	*m-α f*	*mt m-α*	*f*	
$\frac{+}{mt\ m\text{-}\alpha\ f}$	292	110	100	3	1	5	6	225
TOTAL	1315	428	448	16	16	26	19	953

in table 1, the data are presented from the crosses between constant magenta-α and miniature forked. The results of these crosses indicate

that the magenta-α is located between the miniature and forked (3.4 units from miniature and 4.7 units from forked) in approximately the same region as magenta. These data corroborate the F_1 results obtained from crosses between magenta and magenta-α, and lead to the conclusion that these two characters are allelomorphs.

Tests for Mutability.—In F_1 generation of the cross between magenta and magenta-α usually a part of the females are distinctly of the magenta type and the eye color of the other part is either distinctly wild type or intermediate in appearance. The F_2 progeny of the distinct magenta F_1 females is given in table 2, from which it can be seen that in addition to 608 magenta males there were 352 with the wild-type eye color. Since

TABLE 2

THE DATA FROM CROSSES *m f*/*m*-α ♀'s × *m f* ♂'s

F_1 PEDIGREE NUMBER	NO. OF F_1 ♀'S TESTED	F_2 ♀'s	F_2 ♂'s				
			*mf**	*m*-α	+	*f*	TOTAL
4940	7	439	143	69	85	7	304
4953	5	222	99	16	114	1	230
4961	6	220	57	21	77		155
5057	1	41	21	5	22	1	49
5054	1	43	6	1	7	1	15
5413	8	389	74	96	237		407
TOTAL	28	1354	400	208	542	10	1160

* The presence of a lethal factor in *m f* chromosome accounts for the deficiency of *m f* class in some of the crosses.

both of the magentas are allelomorphs, wild-type males from a F_1 magenta female crossed with magenta male could originate only as a result of mutations of one of the magentas to the wild type. The data given in table 3 indicate that the magenta-α is the character which mutates. The wild

TABLE 3

THE DATA FROM CROSSES *mt f*/*m*-α ♀'s × *mt f* ♂'s

F_1 PEDIGREE NUMBER	NO. OF F_1 ♀'S TESTED	F_2 ♀'s	F_2 ♂'s							
			0		1		2			
			mt f	*m*-α	*mt m*-α	*f*	*mt*	*m*-α *f*	+	TOTAL
4941	20	1238	398	451	18	29	19	14	12	941
5031	3	80	41	30	2	2	4	3	5	87
5039	5	220	78	74	2	5	4	3	8	174
5129	11	637	248	263	13	15	11	3	4	557
5160	2	141	67	42		5	3		11	128
5269	5	265	95	94	5	4	4	3	3	208
5286	4	380	162	116	4	12	14	6	22	336
5278	3	198	88	43	1	6	7	2	27	174
TOTAL	53	3159	1177	1113	45	78	66	34	92	2605

class among the F_2 males from crosses miniature forked × magenta-α could result from double cross-overs between miniature and forked or from mutations of the genes for magenta-α to the genes for the wild type. Since the double cross-overs were never observed between factors as close

together as the miniature and forked are (11 units apart) they cannot be expected in this cross, especially since such a high number of wild-type males was observed. Against the double cross-over explanation is also the fact that the miniature magenta-α forked class, which would be reciprocal to the wild-type class, was not observed. The possibility that the poor viability is responsible for the absence of that class is eliminated, because miniature magenta-α forked flies were not only found to be fairly viable but also among the progenies of +/miniature magenta-α forked females miniature forked class (corresponding to the wild-type class) was very numerous (175 individuals) and magenta-α class (corresponding to the miniature magenta-α forked class) was absent. These facts indicate that the mutability of the magenta-α factor is responsible for the unusual results obtained in crosses.

Test of Wild-Type Flies.—Five wild-type males obtained from the F_2 of the cross magenta $\times$ magenta-α, were crossed with magenta females. All (217) F_1 females were distinctly wild type. Among 538 F_2 progenies from a cross between similar males and miniature forked females, no magenta-α flies were observed. The results of these experiments indicate that the change from magenta-α to wild type is not only phenotypic but that it is also genetic.

The Time of Occurrence of Mutations.—The data so far presented indicate that the magenta-α mutates in heterozygous females. Wild males could be obtained from magenta-α/magenta females if magenta-α mutates in the cells from which germ cells are formed, if it mutates at the maturation division or very early after fertilization. If the mutations occur in the cells from which germ cells are formed, it should be expected that they come in groups in the offspring of different females. That was not the case. If wild-type males were results of early somatic mutations, mosaics would be expected more frequently than they were observed. It is very likely that these wild-type males originated, in the majority of cases, from the mutations occurring at maturation, probably during reduction divisions.

Magenta-α mutates also in homozygous females. Nineteen such females gave 656 magenta-α, 110 wild-type and 2 mosaic offsprings.

In crosses between magenta females and magenta-α males wild-type females are obtained very frequently in F_1 generation. Several were tested and they bred as heterozygous for magenta, indicating that the magenta-α mutated in males.

Numerous flies with eyes mosaic for magenta and wild type were observed in experiments with magenta-α, which suggests that magenta-α can mutate in somatic cells. Somatic mutations are rare when compared with the somatic mutations of miniature-α.

The Relation between Crossing-Over and the Occurrence of Mutations.—

In the case of reddish it was observed[5] that the crossing-over in the classes which resulted from mutations of reddish to wild type, was increased in the reddish scute region from 0.7 to 13 per cent, and in the sepia-reddish region was decreased from 2 to 0.2 per cent. From the data given in table 4 a similar increase in the frequency of crossing-over in the magenta-

TABLE 4

THE DATA FROM THE CROSS *m f* × *mt m-α*, INDICATING THE RELATION BETWEEN THE CROSSING-OVER AND THE OCCURRENCE OF MUTATIONS

F_1 PEDIGREE NUMBER	NO. OF F_1 ♀'S TESTED	F_2 ♀'S	0		1–2			MUTATIONS 0	1	2
			m f	*m-α mt*	*mt m f*	*m*		*mt*	+	*mt f*
5745	2	57	19	6	1	1		4	6	.
5795	1	74	22	3	.	1		21	2	.
5755	2	111	42	11	.	2		54	9	.
5853	7	271	84	38	1	7		79	12	2
TOTAL	12	513	167	58	2	11		158	29	2

forked region and decrease in the miniature-magenta region could be observed in the case of mutable magenta-*α*.

Summary.—The results of the experiments indicate that magenta-*α* reverts frequently to wild type. Mutations were observed at the formation of germ cells of heterozygous and homozygous females, in males and in the somatic cells of both females and males.

[1] Demerec, M., these PROCEEDINGS, **12**, 1926 (11–16).

[2] Demerec, M., *Ibid.*, **12**, 1926 (687–690).

[3] Metz, C. W., *Genetics*, **1**, 1916 (591–607).

[4] Metz, C. W., M. S. Moses, and E. D. Mason, *Washington, Carnegie Institution Publ.*, **328**, 1923.

[5] Demerec, M., *Washington, Carnegie Institution Year Book*, **24**, 1925 (30–31).

POLLEN-TUBE GROWTH IN LYTHRUM SALICARIA

BY DONTCHO KOSTOFF

BUSSEY INSTITUTION, HARVARD UNIVERSITY

Communicated March 5, 1927

All investigators who have studied pollen-tube growth in self-sterile plants agree that the immediate cause of the failure to obtain seed after incompatible matings is due to the fact that growth is much slower than it is after compatible matings. The only quantitative investigation of the matter, however, is that of East and Park (1918) on hybrids between *Nicotiana Forgetiana* and *Nicotiana alata*. In this case it was found that pollen-tube growth after an incompatible mating was very nearly linear. The tubes traversed from one-half to two-thirds of the length of the style

in about seven days, at which time the flowers usually fell. Acceleration as growth progressed was slight. Growth curves of pollen tubes after compatible matings, on the other hand, showed remarkable acceleration, and fertilization ensued after about three days.

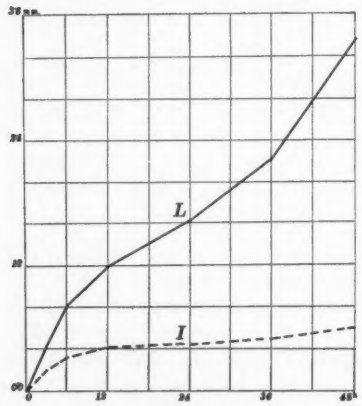

FIGURE 1

Pollen-tube growth in *Lythrum salicaria* after (*L*) legitimate and after (*I*) illegitimate pollination. Mid style × long style.

Since the genetic basis of this self- and cross-incompatibility in Nicotiana is a series of multiple allelomorphs (East and Mangelsdorf, 1925, 1926), and since this interpretation does not appear to fit the phenomenon as exhibited in *Lythrum salicaria*—upon which an extended series of investigations has been carried out in this laboratory—it seemed desirable to determine pollen-tube growth curves for "legitimate" and "illegitimate" unions in this species.

Lythrum salicaria, it will be recalled, is a trimorphic self-sterile species which shows complete fertility only in unions where a given style is pollinated with pollen from stamens of the same tier. Other unions, the "illegitimate" unions, are comparatively infertile, though there is considerable variation among the twelve types of "illegitimate" union.

The material, which consisted of a series of ovaries from a single mid-styled plant pollinated both "legitimately" and "illegitimately" with pollen from a single, long-styled plant, was given to me by Dr. E. M. East. It had been fixed partly in Flemming's medium solution and partly in Bouin's solution and imbedded in paraffin. The styles were fixed separately 3 hours, 6 hours, 12 hours, 24 hours, 36 hours, 48 hours, 60 hours, 72 hours and 85 hours after pollination. Several styles were available for each stated time.

From this material, longitudinal sections 12μ thick were made, and stained with saffranin, Heidenhain's hämatoxilin or saffranin-gentian violet-orange G. The best preparations were those fixed in Flemming's solution and stained with saffranin. The amount of material investigated is shown in table 1.

It was found that the pollen grains germinated as well after an "illegitimate" as after a "legitimate" pollination, but in the former case the growth was far slower. The average length, the major extremes and the variability of the pollen tubes at the various times after pollination are

shown in table 2. The average length of the pollen tubes plotted against time is shown in figure 1. There is a decided difference in the two curves. The curve for a legitimate union appears to be symmetrical with decided

TABLE 1

STYLES OF *Lythrum salicaria* INVESTIGATED

LEGITIMATE UNIONS				ILLEGITIMATE UNIONS			
TIME FIXED AFTER POLLINATION HOURS	NO. OF STYLES INVESTIGATED FLEMMING	BOUIN	TOTAL NO. POLLEN TUBES COUNTED	TIME FIXED AFTER POLLINATION HOURS	NO. OF STYLES INVESTIGATED FLEMMING	BOUIN	TOTAL NO. POLLEN TUBES COUNTED
3	5	4	188	3	5	4	187
6	5	4	148	6	8	5	239
12	6	5	184	12	6	5	173
24	5	5	173	24	8	4	197
36	6	4	203	36	6	3	193
48	8	4	235	48	6	4	168
60	6	5		60	8	5	
72	2	3		72	2	3	
85	2	3		85	2	3	

acceleration during later stages. The curve for an illegitimate union is unsymmetrical. Acceleration is shown in the later stages; but it is very slight.

TABLE 2

VARIABILITY OF POLLEN-TUBE GROWTH IN *Lythrum salicaria*

TIME FIXED AFTER POLLINATION HOURS	MEAN LENGTH MM.	STANDARD DEVIATION	VARIATION AMPLITUDE	TUBE LENGTH IN PER CENT STYLE LENGTH
Leg. 3	0.45	0.35	0.1—1.5	10.0
Leg. 6	0.81	0.45	0.1—1.9	17.3
Leg. 12	1.19	0.60	0.1—3.2	22.7
Leg. 24	1.62	0.70	0.1—3.3	39.8
Leg. 36	2.19	0.95	0.1—3.9	42.8
Leg. 48	3.38	2.20	0.1—7.2	54.5
Leg. 60	The styles begin to fall			
Illeg. 3	0.23	0.07	0.1—0.4	5.1
Illeg. 6	0.34	0.15	0.1—0.7	7.0
Illeg. 12	0.41	0.28	0.1—1.5	8.7
Illeg. 24	0.46	0.35	0.1—2.8	8.5
Illeg. 36	0.48	0.42	0.1—2.9	8.5
Illeg. 48	0.59	0.70	0.1—3.3	10.8
Illeg. 60	The styles begin to fall			

East, E. M., and Park, J. B., "Studies on Self-Sterility II, Pollen Tube Growth," *Genetics*, **3**, 353–366, 1918.

East, E. M., and Mangelsdorf, A. J., "A New Interpretation of the Behavior of Self-Sterile Plants," *Proc. Nat. Acad. Sci.*, **11**, 166–171, 1925; "Studies on Self-Sterility VII, Heredity and Selective Pollen Tube Growth," *Genetics*, **11**, 466–481, 1926.

BENDING OF A QUASI-ELLIPSOIDAL SHELL WITH SPECIAL REFERENCE TO RIGID AIRSHIPS[1]

BY WILLIAM HOVGAARD

MASSACHUSETTS INSTITUTE OF TECHNOLOGY

Communicated February 10, 1927

When a tubular girder with straight axis and with a thin, strongly curved shell is exposed to bending, it will behave quite differently from a plain cylindrical tube and the stress distribution will vary from that which might be expected according to the ordinary theory of bending.

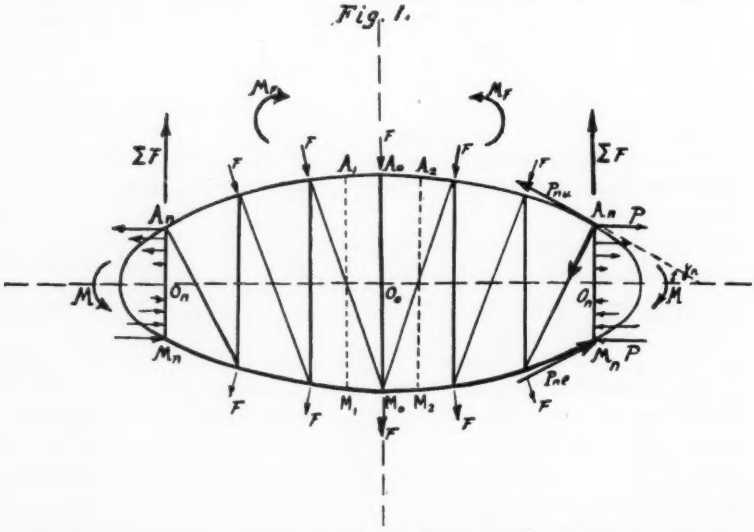

The attention of the author was drawn to this problem in a study of the behavior of curved tubes subject to bending.[2] A similar action, although different in effect, occurs in all tubular girders where the shell is curved in the plane of bending even if the axis is straight, a fact which has not, to the author's knowledge, been previously explained or discussed. In a simple ideal form the problem is that of an ellipsoidal shell, but in principle the solution applies also to plane girders with curved flanges. In the present paper the method is illustrated by application to a rigid airship.

Consider a rigid airship as shown diagrammatically in figure 1. The structure consists of a number of longitudinal girders which perform the function of flanges, while transverse circular or polygonal frames, stiffened by transverse radial and chord wires, and a system of diagonal or shear

wires perform the function of the web. The structure is not unlike a lattice girder, since the transverse frames play the part of vertical posts and the shear wires take the place of the diagonal tie-rods. In order to simplify, it is assumed that the structure is perfectly symmetrical about the axis and the longitudinals are placed at the apices of a regular polygon with the top girder A and the bottom girder M in the center line. For the sake

Fig. 2.

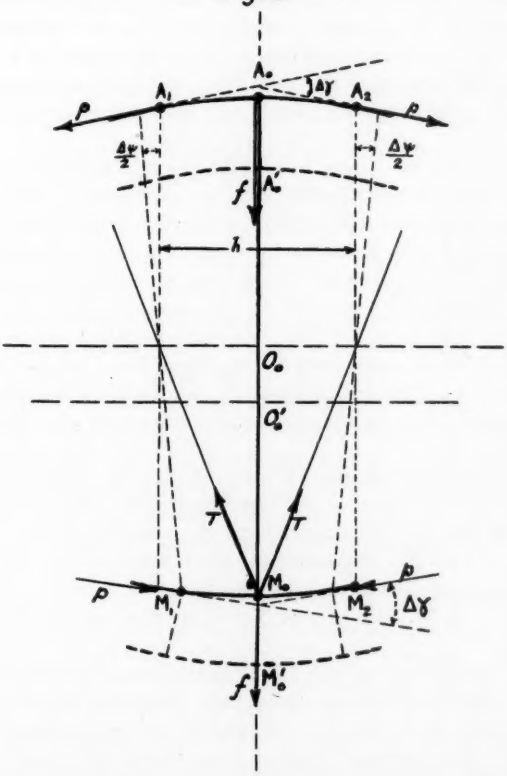

of clearness the longitudinals are omitted in figure 1 except the top and bottom girders, and the shear wires are represented symbolically by diagonal lines. Vertical lines represent the transverse frames. Terminal couples M are assumed to act at certain stations A_nM_n near the ends, produced by a system of horizontal forces, which act on each girder and are proportional to their distance y from the horizontal plane through the axis.

In a straight cylindrical solid bar or tube the transverse stresses are of the second order so long as the strains are within the elastic limit and are usually neglected, but in the case here under consideration they should be taken into account, first because the curvature of the longitudinals, which constitute the flanges, causes the transverse stresses to attain appreciable magnitude and, second, because the resistance of the shear wires, as also of the transverse frames which act as stiffening bulkheads, is relatively small in airships and permit certain peculiar deformations to take place. In a curved tube of cylindrical section, the transverse stresses above and below the axis counteract and balance each other, but in a straight tube with curved shell, we have the remarkable condition that the resultant of the transverse stresses both above and below the axis act in the same direction.

In figure 2 is shown diagrammatically a section amidships of an airship, one frame space in length with a transverse frame in the middle. We assume it to be exposed to a hogging moment, so that the A girder is under a tensile stress p, and due to the curvature the stress forces have a downward directed resultant which we denote by f. Similarly, the lower or M-girder, being under compression, will be subject to an f-force, which likewise acts downward. In fact, all the longitudinals will be subject to f-forces which have a downward component and thus the whole section becomes loaded with a vertical force, F, which causes it to move down until F is counterbalanced by the vertical component of the tension T in the diagonals.

Similar F forces act on every frame and the load so produced is through the diagonals transmitted to the terminal frames where they are counterbalanced by the vertical components P_{nu} and P_{nl} of the longitudinals acting at A_n and M_n, respectively. If it were not for the diagonal at A_n, this point as well as M_n would tend to move upward. The restraining force is equal to ΣF, the sum of the F-forces on one-half of the length of the ship.

We may, therefore, conceive the internal stress system to be equivalent to a distributed load on the longitudinals, everywhere acting in meridional planes, inward directed above the neutral axis and outward below that axis. This load produces vertical shear forces, which, being supported at the terminal stations by the upward forces ΣF, produce internal stress couples M_F acting in a direction contrary to the external couples M. Yet, at any station the resulting bending moment is necessarily M and the bending deflections of the axis may be calculated on this basis without any regard to M_F, but in determining the shearing deflections the f-forces must be taken into account. It is a curious fact that shearing is here produced by pure couples and this shearing, although entirely due to concealed internal reactions, has a very real and tangible effect in that it gives

to the axis a flexure contrary to and superposed on that produced by M. It may be, in fact, so great as to overpower the deflections due to bending.

Shearing flexure will take place even if the transverse frames are absolutely rigid, provided only the diagonals are elastic, but if, as in an airship, also the frames are elastic and of relatively small stiffness, the latter will suffer a peculiar deformation due to the fact that the upper and lower longitudinals are under greater stress and are subject to greater f-forces than those on the sides. Hence the radial or meridional deflection of the longitudinals at and near the top and bottom may be much greater than that of the longitudinals farther from the vertical center plane and nearer to the neutral plane. The consequence is that the top of the frame section will flatten out and the bottom will take on a sharp bulge, giving to the contour a pear-shaped form as indicated in figure 3. The upper girders straighten and the lower girders bulge out, being thus enabled to shirk their duty in opposing the external couples. In order to establish equilibrium these couples must turn through a greater angle than if this action did not exist. The top and bottom girders may not now be the most strained. Longitudinals on the sides nearer the neutral plane may be subject to greater stresses, which may be in excess even of those which the A and M girders should have according to the ordinary theory of bending.

Fig. 3.

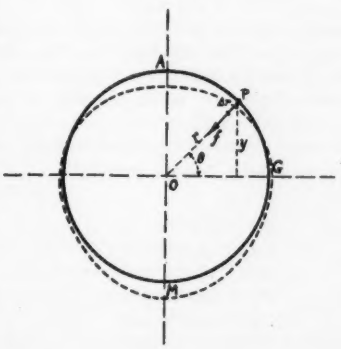

It is seen that we have to deal with two distinctly different deformations besides that due to simple bending. One is a bodily downward movement of the frames due to shearing deflections of the whole ship. The other is a deformation of the transverse frames due to unequal loading. The magnitude of the former deformation depends on shearing stiffness in the longitudinal plane, the latter on stiffness in the transverse plane.

The effects here pointed out are most marked in short airships of full form and show the necessity for a good stiffness of the transverse frames.

In non-rigids, where the stiffening element provided by transverse frames is absent, the effects are probably much greater than in rigid airships.

Appendix.—The displacement of a longitudinal normal to the surface is denoted by Δn, the radial transverse displacement by Δr and the transverse tangential displacement by Δt. Let γ be the inclination of the tangent to the axis at any point P, then $\Delta r =$

$\Delta n \cos \gamma$. The relation between Δr and Δt is found under the assumption of inextensibility of the transverse frame.

Referring to the midship frame section, figure 2, each of the longitudinals is subject to a stress p, which causes it to stretch or contract as in an ordinary girder, producing an angular deflection $\Delta\psi$ of the boundary planes relative to each other, but at the same time, due to the curvature of the girders, the f-forces will cause the longitudinals to move down to the points A_0' and M_0' whereby the strain is reduced. The movement of the transverse frame consists of two parts; first, its form is changed from circular to pear-shaped without any displacement of the center; second, it moves bodily downward, without change of form, a distance Δy_o, as allowed by the tension in the diagonals. Due to the latter deflection the longitudinals above the axis straighten out and those below the axis bulge down, thus relieving the stresses, but the bending couples at once turn the bounding planes through an additional angle $\Delta\psi_o$ until equilibrium is established, when the stress distribution will be the same as before the shearing deflection took place.

It is first assumed that the diagonals are rigid while the frames are elastic and we consider in particular the deformation of the midship frame in its own plane, when exposed to a hogging moment.

Let

h = frame spacing

ρ = radius of curvature of the longitudinals

r = radius of the transverse frame

y = vertical ordinate at any point P of the frame referred to a horizontal plane through the axis

s = length of a longitudinal, within the frame space considered. Amidships we reckon $s = h$

$\Delta\gamma = \frac{s}{\rho}$ = angle subtended by s. For the midship frame $\Delta\gamma = \frac{h}{\rho}$ approximately.

$\Delta\psi$ = angular deflection of a transverse plane due to bending, i.e., the angle between the two bounding transverse planes of the section in the strained condition.

θ = angle between the radius OP and the horizontal radius OG. Figure 3.

The elongation due to longitudinal strains, assuming that the bounding planes remain plane, is $y\Delta\psi$ and that due to the radial displacement of P is approximately $\Delta r \Delta\gamma$. Thus the total elongation of A_1A_2 is $\epsilon = y\Delta\psi + \Delta r \Delta\gamma$ and this expression holds for any girder both above and below the axis.

Following Ritz's method the unknown deflection Δr was expressed in a series of trigonometrical or exponential terms with a corresponding number of constants.

It was found that the expression which best fulfilled the limiting conditions was:

$$\Delta r = \zeta r \sin\theta - \beta r \sin^3\theta \qquad (1)$$

where ζ is a coefficient to be determined so that the downward parallel displacement due to shear is zero, and β, which characterizes the deformation of the frame, is determined so as to make the internal elastic work a minimum, not including the work done on the diagonals.

The assumed inextensibility of the frame leads to:

$$\Delta t = r(\zeta - \beta)\cos\theta + \frac{1}{3} r\beta \cos^3\theta \qquad (2)$$

which for $\theta = 0$ gives the downward displacement of the center:

$$\Delta t_o = r\zeta - \frac{2}{3} r\beta$$

Since this is to be zero we must have: $\zeta = \frac{2}{3}\beta$.

Substituting and dividing the total elongation by $s = h = \rho\Delta\gamma$ we find the unit elongation

$$e = r\left(\left(\frac{\Delta\psi}{h} + \frac{2}{3}\frac{\beta}{\rho}\right)\sin\theta - \frac{\beta}{\rho}\sin^3\theta\right) \tag{3}$$

and the longitudinal stress

$$p = Er\left(\left(\frac{\Delta\psi}{h} + \frac{2}{3}\frac{\beta}{\rho}\right)\sin\theta - \frac{\beta}{\rho}\sin^3\theta\right). \tag{4}$$

Let ω be the area of the longitudinals per unit length of the contour of the transverse section, imagining their area to be distributed uniformly along the circumference. We can then determine the f-forces which result from the curvature of the longitudinals. For the midship frame space we have:

$$f = p\omega r d\theta d\gamma = \frac{\omega s r^2 E}{\rho}\left(\left(\frac{\Delta\psi}{h} + \frac{2}{3}\frac{\beta}{\rho}\right)\sin\theta - \frac{\beta}{\rho}\sin^3\theta\right)d\theta \tag{5}$$

so that the total vertical force acting on this section is:

$$F = \int_0^{2\pi} f\sin\theta = \frac{hEI}{\rho r}\left(\frac{\Delta\psi}{h} - \frac{1}{12}\frac{\beta}{\rho}\right) \tag{6}$$

where $I = \pi\omega r^3$ is the moment of inertia of the ship about the neutral axis.

This downward force will be resisted by the shear wires so that by equating F to the sum of the vertical components of the tensions T in the shear wires all round the section we can find these tensions.

We may now proceed to determine the elastic work done by the internal stresses in the various parts of the structure.

This work includes first the straining of the longitudinals under the stress p, which work we denote by W_1, second, W_2, the work done in deformation of the frame ring against its inherent stiffness and third, W_3, that done against the tension of the transverse wires. The work done against the tension of the shear wires, W_s is considered separately as it is independent of β. We have thus the internal work: $W_i = W_1 + W_2 + W_3$.

This equation takes the form:

$$W_i = \frac{\beta^2}{144\rho^2}(5\delta + 144(\mu + \lambda)) - \frac{1}{12}\frac{\delta}{h\rho}\beta\Delta\psi + \frac{\delta}{2h^2}\overline{\Delta\psi}^2. \tag{7}$$

where μ is quantity which depends on the transverse stiffness of the frame itself and λ depends on the transverse wires in the plane of the frame ring. The quantity δ is equal to hEI which expresses the stiffness of the whole section multiplied by the frame space.

In order to determine β it is argued that it must be such as to make the internal elastic work a minimum. Hence the angular deflection $\Delta\psi$ is regarded as constant and β, which determines the displacement of the longitudinals, is supposed to vary and is adjusted so as to make:

$$\frac{\partial W_i}{\partial\beta} = 0. \tag{8}$$

This is an equation of the first degree in β and gives

$$\beta = \frac{6\rho\delta}{h(5\delta + 144(\mu + \lambda))}\Delta\psi. \tag{9}$$

We next substitute the value of β so determined in the expression for the bending moment M:

$$M = \int_0^{2\pi} py\omega r d\theta = EI\left(\frac{\Delta\psi}{h} - \frac{1}{12}\frac{\beta}{\rho}\right) \tag{10}$$

and find $\Delta\psi$ in terms of M

$$\Delta\psi = \frac{h^2M}{\delta}\frac{(10\delta + 288(\mu + \lambda))}{(9\delta + 288(\mu + \lambda))} = A\frac{hM}{EI} \tag{11}$$

where A is a factor which is always greater than one, showing that the angular deflection of a girder of this type will be greater than that found by the ordinary formula. It appears that A is not much greater than unity in rigid airships if the frames are well stiffened, but it will probably attain higher values in non-rigids.

If we now substitute the value of $\Delta\psi$ in (9) we obtain

$$\beta = \frac{12\rho hM}{9\delta + 288(\mu + \lambda)} \tag{12}$$

which gives β in terms of the bending moment.

The solution here obtained satisfies the condition that the internal and external work shall be equal, $W_i = \frac{1}{2} M\Delta\psi$.

It remains to show that W_s, the work done against the shear wires, has its equivalent in work done by M turning through the additional angle $\Delta\psi_s$.

Assume that the frames are rigid but the longitudinals and diagonals elastic, then the shearing deflection calculated by the method ordinarily used in rigid airships is found:

$$\Delta y_s = 2Kr\rho\delta\frac{\Delta\psi_1}{h} \tag{13}$$

where K is a factor depending on the resistance to shear and $\Delta\psi_1$ is the angular deflection caused by the strains in the longitudinals as in ordinary bending.

$$\Delta\psi_1 = \frac{Mh}{EI} = \frac{Mh^2}{\delta} = \frac{\Delta\psi}{A}. \tag{14}$$

The work done is: $W_s = Kh^2M^2$ which is equal to $\frac{1}{2} F\Delta y_s$ and is seen to be independent of the deformation of the frame.

As explained above, the shearing deflection causes the bounding plane to rotate through an angle $\Delta\psi_s$ taking up, so to speak, the slack in the longitudinals. It can be shown geometrically that

$$\Delta\psi_s = 2K\delta\Delta\psi_1 = 2K\delta\frac{\Delta\psi}{A}. \tag{15}$$

Hence the external work is $\frac{1}{2} M\Delta\psi_s = K\delta M\Delta\psi_1 = Kh^2M^2 = W_s$ and we have complete equality between the external and the total internal work:

$$W_e = W_i + W_s = \frac{1}{2} M\Delta\psi + \frac{1}{2} M\Delta\psi_s = \frac{1}{2} M\Delta\psi_1(A + 2K\delta) \tag{16}$$

The total angle through which M turns is seen to be greater than that in ordinary bending in the ratio $(A + 2K\delta)$.

The formulas for other frame sections where the hull is tapering gives analogous formulas differing from the above only in the occurrence of $\cos\gamma$ and $\sec\gamma$ in the expressions for β and $\Delta\psi$.

The total downward shear deflection of the amidship frame and the total rotation of the end frames in the ship are the sum of the respective deflections of all the frame sections on one side of amidships.

[1] A more detailed account will probably appear in *Trans. Institution of Naval Architects*, London, 1927.

[2] *Proc. Nat. Acad. Sci.*, **12**, No. 6, June, 1926.

INFLUENCE OF IRON CONTENT ON MORTAR STRENGTH

BY H. WALTER LEAVITT AND JOHN W. GOWEN

UNIVERSITY OF MAINE, ORONO

Communicated February 23, 1927

Those most intimately concerned with the use of concrete for bridges, highways or other work freely admit that the most important problem is the variation in mortar strength developed by mixtures of different kinds of sands. This variation in actual test conditions lies between 100 and 600 pounds per square inch in the 28-day tension test. In the attempt to find the cause for some of this variation and, therefore, its control the authors have been investigating several different elements of sand and mortar structure, chemical content, etc., which might lead to or influence mortar strength. One of the elements which has come under consideration is that of the iron found in the native sand. This element is usually present as an oxide, due to the weathering or disintegration of some of the component materials found in the sand aggregate. The iron may be present as a disintegration of several of the common component minerals or due to the leaching of ferruginous material from other sources into the sand. It should be noticed that the makeup of the sand aggregate with regard to iron is quite different under these two methods of allocating the iron in the aggregate. It is, however, difficult to differentiate between iron derived from one source as contrasted with that derived from the other. The material will, therefore, be treated as though the iron content came from the same source.

After some experiment a delicate test for determining the presence and the approximate amount of iron was developed in this laboratory.[1] Through the use of this test it is possible to arrange sands on the basis of the amount of iron present in them and to contrast this with the strength developed by these sands in the ordinary mortar test. While the amount of the iron detected in this manner is extremely small in total amount the data show that its effect on strength is significant for the 284 native Maine sands involved. The percentages of the sand's iron content are arranged on a geometric basis.

Table 1 shows that there is a slight but consistent increase in the strength developed by mortars on the 28-day test as the content of the iron found in

TABLE 1

AVERAGE 28-DAY TENSILE STRENGTH OF MORTARS IN RELATION TO THE IRON CONTENT OF THE SAND

RELATIVE IRON CONTENT	NUMBER OF SANDS	MEAN MORTAR STRENGTH (1:3 MIX)
Trace	18	282
0.00022%	55	284
0.00044%	81	306
0.00088%	65	298
0.00176%	28	322
0.00352%	11	332
0.00704%	26	388

the native sand increases. This increase amounts to about 100 pounds over the whole range, an increase well worthy of consideration.

Attention may now be turned to the variations in the strength for any given iron class. These variations are shown in the correlation tables

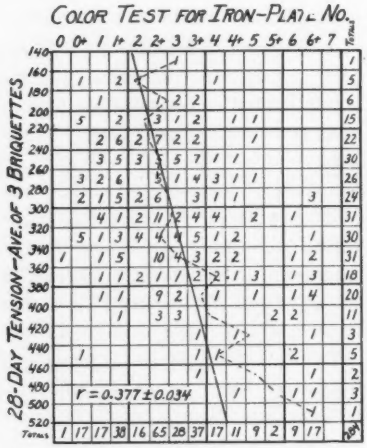

TABLE 2

Correlation Table showing the relation between iron content and 28-day tensile strength.

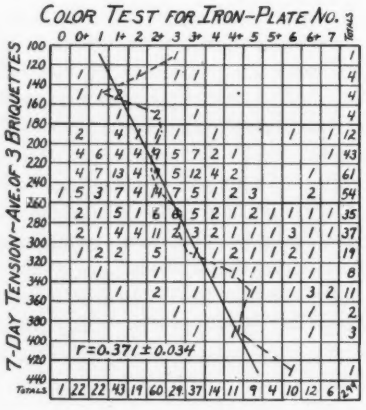

TABLE 3

Correlation Table showing the relation between iron content and 7-day tensile strength.

2 and 3. Table 2 for 28-day tensile strength and table 3 for 7-day tensile strength.

It will be noticed from tables 2 and 3 that the tensile strength increases as the iron content of the sand increases. This increase when the iron is

plotted in the geometric manner is linear. The correlation coefficients for these relationships are 28-day tensile strength 0.377 ± 0.034, 7-day tensile strength 0.371 ± 0.034. The correlations are, therefore, significant. There is, as will be noticed, a considerable range of breaking strength for any given iron content class. Thus while the iron content significantly increases the strength, it does not account for all of the variability in tensile strength by any manner of means. The amount of the variation which is controlled by limiting the iron content to one given class is equivalent to about 7% of the total variation. The iron content of a sand, therefore, is an important consideration in bringing about a control of the variation in the sand strength but is by no means the only cause of this variation.

The fact that the correlation coefficients are the same for the 7-day and 28-day periods indicates that the effect of iron on a mortar strength is essentially the same for each period.

In an earlier paper[2] the authors showed that the tension test and the compression test measured different attributes of the strength-giving properties of mortar mixtures. Comparison of the iron content in the sand shows that apparently this element is one of the properties of the sand measured by the tension test which does not influence the compressive strength of the mortar. Thus while the correlation between iron content and 28-day tensile strength is 0.377 ± 0.034, a very significant correlation, that for compressive strength is 0.084 ± 0.040, not a significant correlation. The important fact coming from this relationship is that iron content is important to tensile strength and unimportant to compressive strength. This further substantiates our earlier conclusion that both the tensile and compressive strength tests should be performed on the mortar as they show different properties of the sand.

Summary.—The evidence presented indicate that the chemical constituent of the sand, iron, is an important factor in influencing the tensile strength of mortar; the larger the amount of iron the greater the average tensile strength.

[1] This test utilizes ammonium thiocyanate as the reagent. A description will appear elsewhere.

[2] "The Significance of the Common Test Method for Determining the Strength of Mortars," by John W. Gowen and H. Walter Leavitt, *Proc. Amer. Soc. Testing Materials*, **25**, Part II, 218–227, 1925.